Fast Order-Recursive Hermitian Toeplitz Eigenspace Techniques for Array Processing

by

Monique P. Fargues

Dissertation submitted to the Faculty of the

Virginia Polytechnic Institute and State University

in partial fulfillment of the requirements for the degree of

Doctor of Philosophy

in

Electrical Engineering

APPROVED:

A.A. (Louis) Beex, Chairman

C.A. Beattie

I.M. Besieris

R.L. Moose

K.B. Yu

August 1988

Blacksburg, Virginia

Fast Order-Recursive Hermitian Toeplitz Eigenspace Techniques for Array Processing

by

Monique P. Fargues

A.A. (Louis) Beex, Chairman

Electrical Engineering

(ABSTRACT)

Eigenstructure based techniques have been studied extensively in the last decade to estimate the number and locations of incoming radiating sources using a passive sensor array. One of the early limitations was the computational load involved in arriving at the eigendecompositions. The introduction of VLSI circuits and parallel processors however, has reduced the cost of computation tremendously. As a consequence, we study eigendecomposition algorithms with highly parallel and localized data flow, in order to take advantage of VLSI capabilities.

This dissertation presents a fast Recursive/Iterative Toeplitz (Hermitian) Eigenspace (RITE) algorithm, and its extension to the generalized strongly regular eigendecomposition situation (C-RITE). Both procedures exhibit highly parallel structures, and their applicability to fast passive array processing is emphasized. The algorithms compute recursively in increasing order, the complete (generalized) eigendecompositions of the successive subproblems contained in the maximum size one. At each order, a number of independent, structurally identical, non-linear problems is solved in parallel. The (generalized) eigenvalues are found by quadratically convergent iterative search techniques. Two different search methods, a restricted Newton approach and a rational approximation based technique are considered. The eigenvectors are found by solving Toeplitz systems efficiently. The multiple minimum (generalized) eigenvalue case and the case of a cluster of small (generalized) eigenvalues are treated also. Eigenpair residual norms and orthonormality norms in comparison with IMSL library routines, indicate good performance and stability behavior for increasing dimensions for both the RITE and C-RITE algorithms.

Application of the procedures to the Direction Of Arrival (DOA) identification problem, using the MUSIC algorithm, is presented. The order-recursive properties of RITE and C-RITE permit estimation of angles for all intermediate orders imbedded in the original problem, facilitating the

earliest possible estimation of the number and location of radiating sources. The detection algorithm based on RITE or C-RITE can then stop, thereby minimizing the overall computational load to that corresponding to the smallest order for which angle of arrival estimation is indicated to be reliable.

Some extensions of the RITE procedure to Hermitian (non-Toeplitz) matrices are presented. This corresponds in the array processing context to correlation matrices estimated from non-linear arrays or incoming signals with non-stationary characteristics. A first-order perturbation approach and two Subspace Iteration (SI) methods are investigated. The RITE decomposition of the Toeplitzsized (diagonally averaged) matrix is used as a starting point. Results show that the SI based techniques lead to good approximation of the eigen-information, with the rate of convergence depending upon the SNR and the angle difference between incoming sources, the convergence being faster than starting the SI method from an arbitrary initial matrix.

Acknowledgements

I would like to especially thank Dr. A.A. (Louis) Beex for his help and readiness in discussing the questions I had while doing the research for this dissertation. In addition, Dr. Beex's guidance and technical insight were invaluable during the years I spent in graduate school. I am indebted to Dr. C.A. Beattie for his assistance and for numerous enthusiastic discussions of the research material. His suggestions were always helpful, and his careful approach to numerical implementations was a source of inspiration for me. I also am grateful to Dr. I.M. Besieris, Dr. R.L. Moose, Dr. K.B. Yu, and Dr. W.T. Baumann for their advice and their critiques of this dissertation.

My parents have always encouraged me to do my best in all aspects of life. I would like to thank them here for their encouragement and support during this lengthy process.

Finally, I wish to thank five close friends who shared the ups and downs of the dissertation process, and have contributed to make these years so much more enjoyable for me. A thousand thanks to

This work was supported in part by UNISYS Corporation under grant number V120483, and in part by the Center for Innovative Technology under grant numbers INF-85-020 and INF-86-018.

Table of Contents

List of Illustrations

List of Tables

1.0 Introduction

1.1 Formulation of the Problem

In many applications such as radar, sonar, seismology, medical imaging, one is faced with the problem of resolving an unknown number of incoming sources, possibly closely spaced, in a noisy environment. Different categories of spectral techniques have been developed along the years [KAY], the oldest ones based on direct Fourier transforms of the data. The last decade has seen the extensive development of new array processing methods called *high resolution methods.* These techniques are based on the earlier work of Pisarenko [PIS] in the early seventies and the more recent ones of Schmidt [SCH] or Bienvenu [BIE]. Basically, these techniques use the eigenstructure of the received signal correlation matrix and the concept of signal and/or noise vector spaces to determine the number of incoming sources along with their characteristic parameters such as directions and intensities. One of their early limitations used to be in the computational load involved with the eigenstructure decompositions. However, the introduction of VLSI circuits has tremendously reduced the cost of computations and recent hardware implementations. Parallel processors have provided the tools to implement these improved performance estimators. As a

consequence, algorithms with highly parallel and localized data flow are presently studied to take advantage of VLSI capabilities.

Numerous procedures based on Hermitian eigendecompositions for array processing have been studied. Each of these have advantages and drawbacks, depending upon the user's requirements (computational speed, in/off line applications, small storage requirements or not, precision of the results, etc...). For equi-spaced linear sensor arrays the signal and noise correlation often have Hermitian Toeplitz structure. Therefore, it seems natural to try to exploit that special structure to reduce the computation time of the Direction-Of-Arrival (DOA) estimation process for the earliest possible detection.

This dissertation presents a fast Recursive/Iterative Toeplitz (Hermitian) Eigenspace (**RITE**), algorithm based on an idea presented earlier by Beex et al [BX1,BF1,BF3], and its extension to the generalized strongly regular[1] eigendecomposition situation (Colored-RITE[2], or **C-RITE**) [BF2,FA1,FA2]. The procedures modify and extend an algorithm proposed earlier by Gueguen [GUE] which was not insured to converge, and are applied to the linear sensor array processing situation.

The basic idea implemented for the RITE and C-RITE algorithms is to use the Hermitian Toeplitz structure of the matrix, or the pencil, to compute recursively in increasing order the eigendecompositions of submatrices, or subpencils, imbedded in the original problem. At each order a number of independent, structurally identical non-linear problems is solved in parallel, facilitating fast implementation. The eigenvalues can be found by quadratically convergent iterative search methods [FA2,BFB], and the eigenvectors are obtained by solving Toeplitz systems efficiently. The multiple (generalized) eigenvalue case is treated also, using information already found at the rank before to directly identify all but one of the eigenvectors associated with the multiple (generalized) eigenvalue, thereby reducing the overall computational load of the algorithm.

---

[1] i.e. the matrices constituting the pencil have all regular minors.

[2] because, in the array processing application context, the generalized eigendecomposition case appears when dealing with incoming signals in a colored noise environment.

The RITE and C-RITE techniques are restricted to Hermitian Toeplitz matrices. In the array processing context, this corresponds to correlation matrices estimated from incoming signals with stationary characteristics. However, there are situations where this assumption is not satisfactory, such as those corresponding to time-varying or exponentially damped incoming signals. In such cases, correlation matrices lose their Toeplitz characteristics and the proposed recursive procedures cannot be applied directly. Nevertheless, for nearly stationary processes, leading to Hermitian structures, underlying stationary behavior may still be present and could potentially be used to extend the technique. Thus, this dissertation proposes extensions of the RITE procedure (i.e. the regular eigenproblem) to the Hermitian case and presents applications to the array processing situation.

1.2 Previous Results

Determining the number and location of radiating sources using a passive array of sensors is an important problem in radar, sonar, seismology, and even medical imaging. In all these areas the problem is to identify an unknown number of sources, possibly closely spaced, in a noisy environment. Essentially, this can be viewed as a spectral estimation problem. Different categories of estimation techniques exist. The oldest ones are based on direct Fourier transformations of the time series. Methods using windowing, periodograms, etc., became extremely popular in the sixties with the development of the Fast Fourier Transform. These conventional methods assume that the data covariance sequence is zero outside the segment under study. However, this assumption is usually incorrect in practice and it then degrades estimator performance.

Model-based methods belong to a different category. Here, the techniques extend the covariance sequence outside the segment under study by using the chosen model parameters. Hence, they completely specify the infinite covariance sequence and the problem becomes a

parameter estimation problem. Numerous techniques such as the Burg method, the Capon method and ARMA modelling can be found in the literature [KAY].

Modelling methods achieve high resolution when the models chosen are appropriate, especially when the amount of data is small. However, these modelling techniques are based on convolutive models (i.e. noise is assumed present at the input of the model). If measurement noise is present (i.e. uncertainty or inaccuracy in the observations is present), then these methods mismodel the data and the performances are not as good.

The above spectral estimation techniques may be applied to array processing. However much higher performance techniques have been developed in the past decade. These *high resolution methods* use the eigenstructure of the signal correlation matrix and concepts of signal and/or noise vector spaces to determine the number of incoming signals along with their characteristic parameters such as directions-of-arrival and intensities. The early seventies pioneering work of Pisarenko was restricted to the case of a one-dimensional signal nullspace and a linear array [PIS]. Schmidt [SCH] and Bienvenu and Kopp [BIE] later independently improved on the idea, and extended it to the general array case. Schmidt developed the MUltiple SIgnal Characterization (MUSIC) algorithm based on the complete eigenstructure of the correlation matrix. Independently, Bienvenu and Kopp developed a frequency domain technique based on the eigenstructure of the spectral density matrix of the received signals. Improved linear prediction methods, to estimate damped sines in noise, have been proposed by Kumaresan and Tufts [KUM] and Reddy [RED]. Other eigen-based techniques have since been introduced by Johnson and DeGraaf [JOH], Bronez and Cadzow [BRO] and Roy et al [RPK] among others. Roy et al's technique, Estimation of Signal Parameters via Rotational Invariance Technique (ESPRIT), is restricted to sensor arrays with displacement invariance but is computationally less expensive than MUSIC and appears to be more robust to array imperfections. More recently, Roy et al have presented an improved ESPRIT method which uses a total least squares criterion [RPK]. The authors show that the TLS criterion used cancels the bias affecting the regular ESPRIT technique at low SNR's. All the eigen-based techniques mentioned above are computationally expensive as they involve the full eigen-decomposition of the correlation matrix, and a search procedure to recover the DOA

information. Therefore, several researchers, such as Tufts et al [TUM] or Fuhrmann et al [FUL], have tried to decrease the computational load by approximating the information needed to recover the DOA parameters.

The high-resolution techniques mentioned above yield asympotically unbiased estimates even in the case where the sources are partially correlated. However, difficulties arise when the sources are *coherent*. In such cases, the covariance matrix of the sources becomes singular and the eigenstructure techniques cannot be used directly any more. Several methods have been proposed in order to overcome this difficulty [SWK,KLF,FOK,HWK,WK2,BRK]. Shan et al [SWK] for instance, applied a *spatial smoothing* scheme, introduced earlier by Evans, to the DOA estimation problem. Basically, the idea is to construct averages of overlapping submatrices contained in the original correlation matrix in order to destroy the cross-correlation between the coherent sources. The Toeplitz Approximation Method (TAM), proposed by Kung et al [KLF], considered the spatial data as the output of an ARMA process, and proposed a state space formulation approach to recover the DOA information.

The eigenstructure methods mentioned so far usually require that the additive noise be spatially white. When the noise is colored and the algorithms designed for white noise are still used, Martin shows that bias and poor resolution result [MAT]. The *colored noise case* with known correlation structure can still be solved by prewhitening the data [BIE] or by solving a generalized eigenvalue problem [ZOL]. Difficulties increase when the noise characteristics are not completely known. However, when the noise is isotropic, the *Covariance Difference Technique* can be applied to solve the DOA problem [PAK, TR1, TR2, PWM]. Here, small rotations of the array are used to form the covariance difference matrix. This matrix is then used to solve the eigen-decomposition problem.

Note that all the techniques mentioned so far estimate the correlation matrices first, followed by computation of the eigen-decompositions. *Adaptive algorithms* which can update the eigenstructure information are often very useful because they can track slowly time-varying processes. Karhunen [KAR], Vaccaro [VAC], Wilkes and Hayes [WIH] and Sharman [SHA] among others have proposed adaptive implementations of eigen-based methods. More recently,

Shan and Kailath have introduced a new adaptive array estimator which does not require any *a-priori* information [SHK], such as an approximate range of directions of arrival of the desired signals or SNR values.

The growing interest in these eigen-based techniques has motivated the numerous performance analyses published recently. Wang and Kaveh [WK1], Spielman and Kailath [SPK], Sibul and Burke [SIB], and Johnson and Miner [JOM] among others have performed analyses and studied performance. Note that the nonlinearities involved have actually prohibited the derivation of general analytical performance results. Most of the results are obtained from simulations or first-order perturbation analyses. Kaveh and Barabell [KAB] however, have recently proposed an approximate statistical performance analysis of the MUSIC and the Minimum-Norm algorithms. They derived approximate expressions for bias and variance of the null spectra. The analysis appears very appealing from a theoretical viewpoint but the complexity of the derivations makes it difficult to readily interpret the expressions. Nevertheless, their approach could open the path to more complete performance analysis.

Computing the eigen-decomposition of the correlation matrix is only the first step of the DOA identification problem. The correct number of incoming signals and the parameters still have to be identified. Methods used for this can be globally divided into two categories. The first approach is to extract the information by plotting the projections of the mode vectors onto signal and/or noise subspaces. Direct estimation of the DOA parameters may be difficult for low SNR. In such cases, the applied information criteria, developed by Wax and Kailath [WAK], can be used for the decision process that determines the number of sources. Unlike other statistical techniques, the Minimum Description Length (MDL) criterion and the Akaike Information Criterion (AIC) do not require any threshold settings; the number of signals is determined by minimization of the criterion expressions. A first consistency analysis, proposed by Wax and Kailath, showed that the MDL criterion yields a consistent estimate of the number of signals while the AIC criterion tends to overestimate the number of signals asymptotically. The absence of threshold settings makes these criteria extremely appealing and several performance studies have since been performed. For instance, Wang and Kaveh show that the performance of the decision criteria depends on the

quality of the covariance estimates[3] [WK1, WK2]. The recent article of Zhao et al [ZKB] shows that theoretical work is still in progress in this area. Those authors point out an incorrect assumption made by Wax and Kailath, question the validity of their consistency analysis, and use different arguments to derive the MDL consistency property.

The second approach to identifying the DOA parameters involves looking at the roots of the eigenfilters. This method is sometimes referred to as the *Root-Music Algorithm.* It is shown to exhibit better resolution than the regular MUSIC algorithm [WAL]. For low SNR and/or estimated correlation sequences, the degeneracy of the noise subspace creates spurious peaks in MUSIC, and the zeroes tend to fall far away from their true locations on the unit circle [KUM] in ROOT-MUSIC. In such cases, the separation of spurious and true peaks (or extraneous and true zeroes) becomes difficult. Additional processing may then become necessary for the identification process [BAR, OR1, OR2].

One of the early limitations of eigen-based techniques used to be the computational load involved in the eigenstructure decompositions, and numerous procedures aimed at minimizing the computational cost have been proposed; [FUH,KUM] among others. For equi-spaced linear sensor arrays the signal and noise correlation matrices often have the Hermitian Toeplitz structure. It seems natural then, to try to exploit that special structure to achieve gains in the throughput of the resulting algorithm. Interest in Toeplitz matrices spreads spreads far beyond the array processing context and a lot of research concerning these special structured matrices has been conducted.

A Look at Toeplitz Matrices

Toeplitz matrices are of great interest in many areas. In estimation problems for instance, they appear as covariance matrices of stationary processes. They are commonly found in time series analysis, image and signal processing, control theory, statistics, etc... Numerous researchers have exploited the specific Toeplitz structure in an attempt to decrease the overall computational load

---

[3] i.e. the number of snapshots used to compute the covariance sequence.

of algorithm implementations. Conventionally, solving a n-dimensional linear system of equations requires $O(n^3)$ operations. Levinson [LEV] introduced in 1947 a recursive algorithm reducing the computational load to $O(n^2)$ for the Hermitian case. A restriction of the Levinson algorithm to autoregressive models was presented by Durbin [DUR]. Trench [ZO1] and Zohar [ZO2] later proposed a new recursive inversion algorithm applied to nonsymmetric, Hermitian Toeplitz systems. This algorithm was then generalized to solving Toeplitz systems by Zohar [ZO2]. See also the algorithms introduced by Bareiss [BAE] and Jain [JAI]. Trench, Zohar, Bareiss and Jain take advantage of the specific structure of the system to be solved by doing an upper and lower triangular factorization and simultaneously exploiting the Toeplitz structure.

More recently, very diverse, asymptotically fast algorithms solving Toeplitz systems in $O(n\log^2 n)$ have been proposed [BGY,BIA,HOO,MOR]. Brent et al [BGY] use the fact that solving a Toeplitz system is closely related to finding a rational approximation to a specific power series known as Pade Approximation. The works of Morf [MOR] or Bitmead and Anderson [BIA], independently published in the same period, are conceptually much easier. Their algorithms are based on the notion of displacement rank[4] and doubling techniques[5] to achieve efficiency. De Hoog [HOO] uses the derivations of Trench and Bareiss and doubling techniques to reduce the computational load of his algorithm.

Most of the techniques mentioned above are arranged in a recursive fashion. They perform, at least implicitly, the computation of the inverse of imbedded sub-Toeplitz systems and are restricted to matrices with all non-zero principal minors. Unfortunately, the degenerate case often occurs, for example in estimation. This difficulty has directed some new attention to the Levinson algorithm. Gueguen and Sidahmed [GUS] proposed an extension of the Levinson algorithm when one of the minors of the matrix studied is singular. More recently, Delsarte et al [DEK] have presented a generalization of the Levinson algorithm for solving Hermitian Toeplitz systems without any restriction on the nested ranks.

---

[4] defined, for any matrix R, as the smallest integer α such that $R = \sum_{1}^{\alpha} L_i U_i$, where L_i and U_i are lower and upper triangular Toeplitz matrices [KKM].

[5] meaning that the problem under consideration is divided into subproblems of half size.

The development of parallel processors has reduced tremendously the cost of computations, and parallel implementations of Toeplitz solvers which require O(n) time have been proposed [BRL,KU1]. Furthermore, the efficiency of fast Toeplitz solvers makes them prime candidates for practical implementations, and several numerical stability analyses have been proposed [BU1,BU2,BU3,CY1]. Stability studies are difficult to conduct especially when the algorithms are recursive. Furthermore, these algorithms are often used in applications which are ill-conditioned by nature, which complicates the analyses; in such cases one has to separate the inherent stability behavior of the procedure from the ill-conditioning characteristics of the underlying problem the algorithm is applied to. Some preliminary results have been given, yet stability questions are still unanswered, especially for general Toeplitz solvers. Cybenko [CY1], for instance, addressed the numerical stability question of the Levinson-Durbin algorithm. Using a first order error analysis, he showed that the computed solution of a Yule-Walker equation has small residual norm when the Toeplitz matrix is positive definite. However, he could not draw any conclusion when the positive definiteness restriction was dropped. Bunch [BU1,BU2,BU3] extended the notion of stability to weak[6] and strong stability[7] in order to study the stability of recursive techniques, such as the Levinson or Trench algorithms, and some of the asymptotically fast algorithms. His analysis showed that the Levinson or Trench-Zohar type algorithms are weakly stable if the associated Toeplitz matrix is positive definite.

Stability problems occurring with fast Toeplitz solvers are often linked to the positive definiteness property of the matrix studied. Recall that a Positive Definite (PD) matrix is strongly regular (i.e. with all regular minors). This property is extremely appealing because methods based on partitioning, such as the Trench, Levinson, Zohar or Bitmead and Anderson algorithms, fail if one of the submatrices contained in the original one is singular. Worse, they may give incorrect

---

[6] "...An algorithm for solving linear equations in finite precision arithmetic is weakly stable for a class of matrices $\mathcal{L}$ if, for each well-conditioned A in $\mathcal{L}$ and for each b, the computed solution x_c to $Ax = b$ is close to x" [BU2].

[7] "...An algorithm for solving linear equations in finite precision arithmetic is strongly stable for a class of matrices $\mathcal{L}$ if, for all A in $\mathcal{L}$ and for all b, the computed solution x_c to $Ax = b$ is the exact solution to a nearby system belonging to the same class $A_c x_c = b_c$, where A_c is in $\mathcal{L}$, and is close to A, and b_c is close to b" [BU2].

results if one of the submatrices is close to singular. Most of the methods mentioned above however, still perform well when the positive definiteness requirement is dropped, provided that the matrix is strongly regular. Therefore, checking the potential accuracy of a computed solution using a PD Toeplitz matrix can be done by checking the conditioning of the matrix. When the positive definiteness restriction is dropped the conditioning of the entire matrix is no longer representative (a well-conditioned non-PD matrix can have singular minors). Stability questions dealing with partitioning algorithms for general Toeplitz matrices are thus more difficult to study, and answers depend very much upon the specific structure of the particular matrix used (i.e. whether it is strongly regular or not).

Whereas a lot of effort has been devoted to linear Toeplitz systems, less is known about the finite Toeplitz eigenproblem which is difficult and still under study [MAK,RE2,DEG]. The inverse Toeplitz eigenproblem, for example, is unsolved [DEG,LAU]. Note that a lot of attention has been given indirectly to the symmetric Toeplitz eigenproblem, as symmetric Toeplitz matrices belong to the extensively studied class of symmetric, or Hermitian, centrosymmetric matrices (i.e. matrices which are symmetric about their diagonal and cross diagonal) [AN1,AN2,CAB,CAD]. The recent interest in the finite Toeplitz eigenproblem, especially in engineering applications, has motivated researchers to try to exploit the specific Toeplitz structure to reduce the computational cost of the algorithms. Some work in this direction has been proposed [KU2,CYV,HAC,WIK], in which researchers have been taking advantage of the properties of the Levinson algorithm. For instance, Cybenko and Van Loan [CYV], Hayes and Clements [HAC] developed algorithms for finding the minimum eigenvalue of a positive definite Toeplitz matrix based on the Levinson algorithm. Wilkes and Hayes [WIH] have proposed a recursive algorithm for finding the eigenvalues of a Toeplitz matrix from the eigenvalues of the submatrices imbedded in the original one. Finally, Hu and Kung [KU2] have proposed an algorithm for computing the minimum eigenpair of a Toeplitz matrix, where they take advantage of the fast Toeplitz solver they developed earlier [KU1] to solve the minimum eigenproblem. The TESS algorithm proposed by Hu and Kung is an iterative procedure based on the shifted inverse power iteration. Its performance depends upon the number of iterations required to obtain a good approximation of the minimum eigenpair.

1.3 *Present Contributions*

Chapter 2 presents the derivation of the order-recursive regular eigendecomposition (RITE) procedure, which exhibits highly parallel computation capabilities. Two quadratically convergent eigenvalue search techniques are considered, and their advantages and drawbacks are discussed. The eigenvector task is presented including the minimum multiple eigenvalue case and the case for a minimal eigenvalue cluster, both as being of practical interest in array processing. This chapter also includes performance analyses of the procedure. The extension of RITE to the generalized problem, denoted C-RITE, and performance analyses of that algorithm are given in Chapter 4. It is of practical importance that no factorization of the matrix pencil is required here. Application of the RITE and C-RITE algorithms to passive bearing estimation is described in Chapter 5. In this application, no a-priori knowledge on the number of sources is needed; the procedures (RITE for the white noise case, or C-RITE for the colored noise situation) use the successive (generalized) eigendecompositions to first estimate the number of sources, and subsequently their locations. The detection algorithm based on RITE or C-RITE (the MUSIC algorithm [SCH] and the information criteria proposed by Wax and Kailath [WAK] are used) can then stop, minimizing the overall computational load, at the smallest subproblem for which the DOA parameters are indicated to be reliable. Chapter 6 presents some extensions of RITE to the non-stationary Hermitian environment. This corresponds in the array processing context to correlation matrices estimated from non-linear arrays or incoming signals with non-stationary characteristics. The RITE decomposition of the Toeplitzsized (diagonally averaged) matrix is used as a starting point. Two different approaches are considered; a first-order perturbation and a subspace iteration approach are investigated and their performances compared. Results show that the SI based techniques lead to good approximation of the eigen-information, with the rate of convergence depending upon the SNR and the angle difference between sources. Finally, Chapter 7 presents conclusions and gives recommendations for future research.

2.0 The Recursive/Iterative Toeplitz Eigenspace (RITE) Decomposition Approach

2.1 Introduction

The derivation of the RITE algorithm is presented in Section 2.2. The eigenvalue problem is examined in Section 2.3. Two different eigenvalue updating techniques, a restricted Newton approach and a rational approximation based scheme, are considered and advantages and drawbacks of each are presented. Section 2.4 studies the eigenvector problem, and three different cases are considered to identify the eigenvectors associated with distinct or clustered eigenvalues or a multiple minimal eigenvalue. Section 2.5 presents some algorithmic implementation considerations. Finally, performance analyses of the RITE procedure compared with an IMSL subroutine are given in Section 2.6.

2.2 *Order Recursive Eigendecomposition*

Eigenspace Relations of Hermitian matrices

Any Hermitian Toeplitz p-dimensional matrix R_p can be written in the form of its spectral decomposition according to Golub and Van Loan [GVL]

$$\begin{aligned} R_p &= \sum_{n=1}^{p} \lambda_n^{(p)} \underline{u}_n^{(p)} \underline{u}_n^{(p)*} \\ &= U_p \Lambda_p U_p^* \end{aligned} \tag{1}$$

The n^{th} column of U_p is the normalized (unit norm) eigenvector $\underline{u}_n^{(p)}$ of the Hermitian Toeplitz matrix R_p with first column $[r_0, r_1, \ldots r_{p-1}]^t$. The matrix Λ_p is diagonal, and has as its elements the eigenvalues $\lambda_n^{(p)}$, arranged in non-decreasing order. This formulation results in a simple corresponding expression for the inverse

$$R_p^{-1} = U_p \Lambda_p^{-1} U_p^* \tag{2}$$

Recursive Procedure

The question we like to answer is the following: *Suppose we know the eigendecomposition* (U_{p-1}, Λ_{p-1}) *for* R_{p-1}, *can we find from it the eigendecomposition* (U_p, Λ_p) *for* R_p *?* That is, find all eigenvalues and eigenvectors recursively in order. In the array processing application, the eigen-information found for a subsystem imbedded in the original one can then be used to recover the DOA parameters. The order-recursive **RITE** algorithm stops as soon as the information contained in an intermediate eigendecomposition is sufficient for the estimation procedure, thereby reducing the overall computational load of the algorithm.

To this end the following equation needs to be solved.

$$(R_p - \lambda I)\underline{a} = \underline{0} \tag{3}$$

Since we know the eigendecomposition for R_{p-1}, equation (3) is rewritten as

$$\begin{bmatrix} r_0 - \lambda & \underline{r}^* \\ \underline{r} & R_{p-1} - \lambda I \end{bmatrix} \begin{bmatrix} 1 \\ \hat{\underline{a}} \end{bmatrix} = \underline{0} \tag{4}$$

where $\underline{r} = [r_1, \ldots, r_{p-1}]^t$. Consequently, the solutions $(\lambda, \hat{\underline{a}})$ should be found to

$$r_0 - \lambda + \underline{r}^* \hat{\underline{a}} = 0 \tag{5a}$$

$$(R_{p-1} - \lambda I)\hat{\underline{a}} = -\underline{r} \tag{5b}$$

Defining $\underline{u}_n^{(p)}$ as the normalization of $\underline{a} = [1, \hat{\underline{a}}^t]^t$ then gives a new order updated eigenpair $(\lambda_n^{(p)}, \underline{u}_n^{(p)})$.

First note that the matrix in (5b) is Toeplitz Hermitian. Thus for any given λ, the solution $\hat{\underline{a}}$ can be found efficiently, as shown later. The remaining problem then is to solve for all possible eigenvalues $\lambda_n^{(p)}$ from (5a). To that end, substitute (5b) into (5a) to eliminate $\hat{\underline{a}}$.

$$r_0 - \lambda - \underline{r}^* (R_{p-1} - \lambda I)^{-1} \underline{r} = 0 \tag{6}$$

Using the known eigendecomposition of R_{p-1} leads to the equality

$$\begin{aligned} r_0 - \lambda &= \underline{r}^* U_{p-1} (\Lambda_{p-1} - \lambda I)^{-1} U_{p-1}^* \underline{r} \\ &= \sum_{n=1}^{p-1} \frac{|\beta_n|^2}{\lambda_n^{(p-1)} - \lambda} \end{aligned} \tag{7}$$

where

$$\beta_n = \underline{r}^* \mathrm{col}_n(U_{p-1})$$

Therefore, the resulting system to be solved becomes:

$$r_0 - \lambda = \sum_{n=1}^{p-1} \frac{|\beta_n|^2}{\lambda_n^{(p-1)} - \lambda} \tag{8a}$$

$$(R_{p-1} - \lambda I)\hat{\underline{a}} = -\underline{r} \tag{8b}$$

2.3 *The Eigenvalue Problem*

2.3.1 The Restricted Newton Scheme

Recall that the correlation matrix R is Hermitian, hence the eigenvalues satisfy the following interlace property [GVL]:

$$\lambda_{i-1}^{(p)} \leq \lambda_{i-1}^{(p-1)} \leq \lambda_i^{(p)} \leq \lambda_i^{(p-1)} \leq \lambda_{i+1}^{(p)} \leq \lambda_{i+1}^{(p-1)}$$

where $\lambda_i^{(p)}$ represents the i^{th} eigenvalue associated with the p-dimensional matrix R_p.

Let us define :

$$h(\lambda) = -r_0 + \lambda + \sum_{n=1}^{p-1} \frac{|\beta_n|^2}{\lambda_n^{(p-1)} - \lambda} \tag{9}$$

thus,

$$h'(\lambda) = 1 + \sum_{n=1}^{p-1} \frac{|\beta_n|^2}{(\lambda_n^{(p-1)} - \lambda)^2} \tag{10}$$

The function $h(\lambda)$ is monotone between its singular points $\lambda_i^{(p-1)}$ for i = 1, ... , p-1, because $h'(\lambda) \geq 1$ from (10). Using the interlace property mentioned above, the search intervals for each $\lambda_i^{(p)}$ can be restricted to $I_i^p = [\lambda_{i-1}^{(p-1)}, \lambda_i^{(p-1)}]$ for all i = 2, ..., p-1, $I_1^p = [K_1, \lambda_1^{(p-1)}]$ and $I_p^p = [\lambda_{p-1}^{(p-1)}, K_2]$, where K_1 and K_2 are constants defined such that $K_1 < \lambda_1^{(p)}$ and $\lambda_p^{(p)} < K_2$. Note that the procedure needs to be used only for distinct eigenvalues, i.e. when $\lambda_i^{(p-1)} - \lambda \neq 0$. Multiple eigenvalues can be identified directly as shown later in Section 2.4. As shown below (10), $h(\lambda)$ is monotone in each interval I_i^p. Hence, the restricted Newton algorithm designed to achieve up to quadratic convergence in the iterative search, is used to identify the updated eigenvalue $\lambda_n^{(p)}$ in the interval I_n^p

$$y_{k+1} = \lambda_k - \frac{h(\lambda_k)}{h'(\lambda_k)} \tag{11}$$

$$\lambda_{k+1} = \begin{cases} y_{k+1} \quad \text{if } y_{k+1} \in I_n^p \\ (\lambda_k + \lambda_n^{(p-1)})/2 \text{ if } y_{k+1} > \lambda_n^{(p-1)} \\ \quad \lambda_k \text{ replaces } \lambda_{n-1}^{(p-1)} \end{cases} \tag{*}$$

$$\lambda_{k+1} = \begin{cases} (\lambda_k + \lambda_{n-1}^{(p-1)})/2 \text{ if } \lambda_{k+1} < \lambda_{n-1}^{(p-1)} \\ \quad \lambda_k \text{ replaces } \lambda_n^{(p-1)} \end{cases} \tag{*}$$

$$\text{if } \operatorname{sign}(h(\lambda_k)) \neq \operatorname{sign}(h(\lambda_{k+1})) \text{ then } \lambda_{k+1} = \frac{\lambda_k + \lambda_{k+1}}{2} \tag{**}$$

$$\text{stop if } |\lambda_{k+1} - \lambda_k| < \varepsilon_1 \lambda_{k+1}$$

where ε_1 is the convergence threshold chosen by the user. Note that when an iteration goes outside the restricted interval, since the gradient is larger than one, this indicates the direction in which the solution is to be found. Consequently the search interval for the next iteration can be further restricted as indicated (*). To prevent the iterate from potentially bouncing between the same two points at either side of the solution (**) is introduced. Newton's method is hereby guaranteed to converge, and near the solution this convergence is quadratic. Note that the eigenvalue search

procedure is valid for general Hermitian matrices, since no specifically Toeplitz matrix property was used in its construction.

Initial bracketing for the extreme eigenvalues

As mentioned earlier, the search intervals for the extreme eigenvalues are $I_1^p = [K_1, \lambda_1^{(p-1)}]$ and $I_p^p = [\lambda_{p-1}^{(p-1)}, K_2]$. Several bounds on extreme eigenvalues of Hermitian matrices have been proposed in the literature [CYV,DEM]. Dembo [DEM] has presented easily computable bounds for positive semidefinite Hermitian matrices H which are given in terms of the extreme eigenvalues of the principal submatrix. For a p-dimensional Hermitian matrix H with elements denoted by h_{ij}, the bounds derived by Dembo are

$$\frac{h_{11}+\lambda_1^{(p-1)}}{2} - \sqrt{(h_{11}-\lambda_1^{(p-1)})^2/4} \le \lambda_1^{(p)} \le \frac{h_{11}+\lambda_{p-1}^{(p-1)}}{2} - \sqrt{(h_{11}-\lambda_{p-1}^{(p-1)})^2/4 + \underline{b}^*\underline{b}} \tag{12a}$$

$$\frac{h_{11}+\lambda_1^{(p-1)}}{2} + \sqrt{(h_{11}-\lambda_1^{(p-1)})^2/4} \le \lambda_p^{(p)} \le \frac{h_{11}+\lambda_{p-1}^{(p-1)}}{2} + \sqrt{(h_{11}-\lambda_{p-1}^{(p-1)})^2/4 + \underline{b}^*\underline{b}} \tag{12b}$$

where $\underline{b} = [h_{12}, \ldots, h_{1p}]^t$. Therefore, using (12), the extreme bounds defined for positive definite Hermitian matrices may be chosen as

$$\begin{aligned} K_1 &= \min\left(0, \frac{h_{11}+\lambda_1^{(p-1)}}{2} - \sqrt{(h_{11}-\lambda_1^{(p-1)})^2/4 + \underline{b}^*\underline{b}}\right) \\ K_2 &= \frac{h_{11}+\lambda_{p-1}^{(p-1)}}{2} + \sqrt{(h_{11}-\lambda_{p-1}^{(p-1)})^2/4 + \underline{b}^*\underline{b}} \end{aligned} \tag{13}$$

2.3.2 The Rational Approximation Based Approach

An alternative to the restricted Newton scheme, based on an idea presented earlier by Bunch et al [BNS], is proposed next. Bunch et al studied the rank-one modification eigenproblem, and derived an iterative technique to update the eigenvalues. They pointed out that the Newton method

is based on a local linear approximation of the rational eigenvalue search function, and noted that a method based on rational approximations of the search function would potentially converge faster to the updated eigenvalues (at least in terms of the number of iterations needed). This idea has since been used and modified by DeGroat and Roberts [DER] who simplified the approach of Bunch et al [BNS] for the rank-one modification problem and applied it to the study of slowly time varying signals.

The RITE procedure can be viewed as a specific rank-one extension problem [BEA] designed for Hermitian Toeplitz matrices, and the associated eigenvalue search function differs only slightly from the search function associated with the rank-one modification problem. Not surprinsingly then, similar ideas to those presented by Bunch et al can be followed to derive rational approximations to the RITE eigenvalue search function.

Rational Approximation Particulars

Recall that the eigenvalue search function is given by

$$h(\lambda) = -r_0 + \lambda + \sum_{n=1}^{p-1} \frac{|\beta_n|^2}{\lambda_n^{(p-1)} - \lambda} \tag{14}$$

where $|\beta_n|^2 = \underline{r}^* \mathrm{col}_n(U_{p-1})$ and $\underline{r} = [r_1, \ldots, r_{p-1}]^t$. Let us first assume that we are looking for the updated eigenvalue $\lambda_k^{(p)}$ contained in $[\lambda_k^{(p-1)}, \lambda_{k+1}^{(p-1)}]$ for $k = 2, \ldots, p-1$. The cases $k = 1$ and $k = p$ are treated separately afterwards. Let

$$\psi(\lambda) \triangleq \lambda + \sum_{n=k}^{p-1} \frac{|\beta_n|^2}{\lambda_n^{(p-1)} - \lambda} \tag{15}$$

and

$$\phi(\lambda) \triangleq r_0 + \sum_{n=1}^{k-1} \frac{|\beta_n|^2}{\lambda - \lambda_n^{(p-1)}} \tag{16}$$

Then, the updated eigenvalue $\lambda_k^{(p)}$ is such that

$$\phi(\lambda_k^{(p)}) - \psi(\lambda_k^{(p)}) = 0 \tag{17}$$

where $\phi(\lambda)$ is a positive decreasing convex function in the interval $[\lambda_k^{(p-1)}, \lambda_{k+1}^{(p-1)}]$, as illustrated in Figure 1 on page 25. Similarly, $\psi(\lambda)$ is a positive increasing convex function on the same interval. Hence, following the approach of Bunch et al, the idea is to obtain successive approximations λ_i to $\lambda_k^{(p)}$ by successively approximating ϕ and ψ with rational approximations. Let us define v and u as respectively the following rational approximations to ϕ and ψ

$$v(\lambda) = t + \frac{q}{\lambda - \lambda_k^{(p-1)}} \quad \text{and} \quad u(\lambda) = r + \frac{s}{\lambda_{k+1}^{(p-1)} - \lambda} \tag{18}$$

We then require the approximations to have the same functional values and derivatives as the approximations, leading to the following set of constraints

$$\begin{aligned} \psi(\lambda_i) &= u(\lambda_i) \triangleq \psi_1 \\ \phi(\lambda_i) &= v(\lambda_i) \triangleq \phi_1 \\ \psi'(\lambda_i) &= u'(\lambda_i) \triangleq \psi'_1 \\ \phi'(\lambda_i) &= v'(\lambda_i) \triangleq \phi'_1 \end{aligned} \tag{19}$$

The rational approximations u and v are respectively located above ψ and ϕ, as shown in Appendix C. Hence, there exists λ_{i+1}, intersection of v and u, in the search interval. Local convergence of λ_{i+1} to the solution of (17) is quadratic, as shown in Appendix D.

Identification of $\lambda_k^{(p)}$ for $k = 2, \ldots, p-1$

The rational approximation coefficients can be found from (19) as

$$
\begin{aligned}
r &= \psi_1 - \psi'_1(\lambda_{k+1}^{(p-1)} - \lambda_i) \\
s &= \psi'_1(\lambda_{k+1}^{(p-1)} - \lambda_i)^2 \\
t &= \phi_1 + \phi'_1(\lambda_i - \lambda_k^{(p-1)}) \\
q &= -\phi'_1(\lambda_i - \lambda_k^{(p-1)})^2
\end{aligned}
\tag{20}
$$

Therefore, given the i^{th} approximation, denoted λ_i to the root $\lambda_k^{(p)}$, the $(i+1)^{th}$ approximation to the root, denoted λ_{i+1}, is obtained by solving

$$
r + \frac{s}{\lambda_{k+1}^{(p-1)} - \lambda_{i+1}} = t + \frac{q}{\lambda_{i+1} - \lambda_k^{(p-1)}} \tag{21}
$$

which leads to the quadratic equation:

$$
\begin{aligned}
\lambda_{i+1}^2[t-r] + \lambda_{i+1}\left[q + s - (t-r)(\lambda_k^{(p-1)} + \lambda_{k+1}^{(p-1)})\right] + (t-r)\lambda_k^{(p-1)}\lambda_{k+1}^{(p-1)} \\
- q\lambda_{k+1}^{(p-1)} - s\lambda_k^{(p-1)} = 0
\end{aligned}
\tag{22}
$$

Closed form solutions to (22) can then be used to identify the new iterate. Note that if the leading coefficient of (22) is zero (i.e. $t - r = 0$), then the quadratic equation degenerates to a first order linear equation with solution

$$
\lambda_{i+1} = \frac{q\lambda_{k+1}^{(p-1)} + s\lambda_k^{(p-1)}}{q+s} \tag{23}
$$

Equations (22) or (23) are used to compute the updated roots $\lambda_i^{(p)}$, for $i = 2, \ldots, p-1$. For the extreme roots, the rational approximation expressions are modified as follows

Identification of $\lambda_p^{(p)}$

For $k = p$, $\phi(\lambda)$ and $\psi(\lambda)$ become

$$\phi(\lambda) = r_0 + \sum_{n=1}^{p-1} \frac{|\beta_n|^2}{\lambda - \lambda_n^{(p-1)}}$$
$$\psi(\lambda) = \lambda \tag{24}$$

and the rational approximations chosen are

$$v(\lambda) = t + \frac{q}{\lambda - \lambda_{p-1}^{(p-1)}}$$
$$u(\lambda) = \lambda \tag{25}$$

Hence, the corresponding quadratic equation to be solved is

$$-\lambda_{l+1}^2 + \lambda_{l+1}(t + \lambda_{p-1}^{(p-1)}) - t\lambda_{p-1}^{(p-1)} + q = 0 \tag{26}$$

where t and q are defined as before.

Identification of $\lambda_1^{(p)}$

For $k = 1$, $\phi(\lambda)$ and $\psi(\lambda)$ become

$$\phi(\lambda) = r_0$$
$$\psi(\lambda) = \lambda + \sum_{n=1}^{p-1} \frac{|\beta_n|^2}{\lambda_n^{(p-1)} - \lambda} \tag{27}$$

and the rational approximations chosen are

$$v(\lambda) = t$$
$$u(\lambda) = r + \frac{s}{\lambda_1^{(p-1)} - \lambda} \tag{28}$$

where t, r and s are defined as before. Hence, the equation to be solved becomes

$$t - r - \frac{s}{\lambda_1^{(p-1)} - \lambda_{l+1}} = 0 \tag{29}$$

Note that equation (29) is linear. Therefore, the updated root can be directly identified and is given by

$$\lambda_{l+1} = \frac{-s}{t-r} + \lambda_1^{(p-1)} \tag{30}$$

Performance Comparisons

The performances of the rational approximation based approach and the restricted Newton method, in terms of the number of iterations needed to compute $\lambda_k^{(p)}$, were compared on a range of 20 positive definite symmetric 6-dimensional matrices (recall that the eigenvalue task portion of the algorithm is not restricted to Toeplitz matrices). The stopping criterion defined earlier by

$$\frac{|\lambda_{k+1} - \lambda_k|}{|\lambda_k|} < \varepsilon_1 \quad \text{where} \quad \varepsilon_1 = 5.10^{-8}$$

was used for the simulations. The results, given in Table 1 on page 24, show that on the average 35% fewer iterations were needed to compute the updated eigenvalues when using the rational approximation based approach as opposed to when using the restricted Newton method. We note however that the computational cost per step is somewhat higher for the rational approximation approach. Recall that only the eigenvalue function and its derivative are needed for the Newton method. In addition to those two evaluations, the rational approximation requires the computation of the four coefficients r,s,t,q in (20) and the closed form solutions of a quadratic equation in (22) (which involves a square root computation). Thus, the Newton technique appears more appropriate for small dimensional problems, while the rational approximation may be more advantageous for larger size problems. Definite conclusions regarding the computational speeds of both approaches are difficult to draw, as they will depend upon the type of hardware implementation chosen, which is beyond the scope of this work.

Note that a recent comparison of the above upper quadrant rational approximation with the more familiar existing left quadrant monotone technique of Bunch et al [BNS] for the rank-one

modification problem was conducted by Beattie [BE2], who reported a 25-30% reduction in iteration count when using the upper quadrant approximation scheme proposed here.

2.4 *The Eigenvector Problem*

When the updated eigenvalues $\lambda_i^{(p)}$ are distinct, the matrix $(R_{p-1} - \lambda_i^{(p)} I)$ is strongly regular. Hence, the eigenvectors $\underline{u}_i^{(p)}$ can be found by substituting the order updated eigenvalues $\lambda_i^{(p)}$ in equation (8b) and solving for $\hat{\underline{a}}$. The normalization of $\underline{a} = [1, \hat{\underline{a}}^t]^t$ then results in the new eigenpair $(\lambda_n^{(p)}, \underline{u}_n^{(p)})$. Basically, the main questions raised during the first implementations were linked to the technique chosen to solve the Toeplitz system in (8b):

a) How can the Toeplitz system (8b) be solved efficiently?

b) How do we handle the singular case (occurring with multiple eigenvalues)?

c) How do we handle the close-to-singular case (occurring with clustered eigenvalues)?

The Toeplitz Solver

The Toeplitz solver used in this implementation is the complex version of the Zohar algorithm [ZO2], and its implementation is presented in Appendix A. This algorithm was chosen because its only restriction is that the matrix under study be strongly regular (i.e. with all regular submatrices). This specific version was chosen because it minimizes storage requirements, has optimized performance and is easy to implement. Furthermore, checking numerical stability of the algorithm is easily done[8] . Recall that the Zohar algorithm can be used with non positive definite strongly regular Toeplitz matrices. Note that $(R_{p-1} - \lambda_i^{(p)} I)$ is not positive definite for $i = 2, \ldots, p$. Nevertheless, it is strongly regular, provided that R_p has distinct eigenvalues only. When R_p has a

[8] The strongly non-singular property of the Toeplitz matrix used is checked by the magnitude of the parameter FLAMDA(λ) (see Appendix A).

Table 1. Number of iterations required for Newton and Rational Approximations

Run	1	2	3	4	5	6	7	8	9	10	11	12	13	14	15	16	17	18	19	20
Newton	32	38	33	32	38	35	34	38	44	44	41	42	35	37	44	39	46	41	42	36
Rational	24	25	26	23	26	25	25	24	26	25	27	25	29	26	21	28	26	29	23	26

Averaged number of iterations per run

Newton (N)	Rational (R)	Ratio R/N
39.40	25.45	0.646

multiple eigenvalue, i.e. there is an index i such that $\lambda_i^{(p)} = \lambda_i^{(p-1)} = \lambda_{i+1}^{(p)}$, then the resulting $(R_{p-1} - \lambda_i^{(p)} I)$ is singular and the Zohar algorithm cannot be used any longer. In practice, we have to deal carefully with nearly singular systems because of the convergence threshold imposed on the iterative search for the eigenvalues and the rounding errors resulting from the numerical implementations. In such cases, a different 2-step procedure is followed, as presented next.

Treatment of Multiple and/or Clustered Eigenvalues

The design of the RITE algorithm is closely related to the array processing application of interest. For this application, theoretically when the incoming sources have high SNR, a p-dimensional Toeplitz Hermitian correlation matrix is shown to have m large and distinct eigenvalues, and p-m smaller and clustered eigenvalues (when dealing with estimated correlation sequence information) or one smaller eigenvalue of multiplicity p-m (when dealing with true correlation sequence information). The large eigenvalues represent the m incoherent incoming signals, while the other ones represent the noise contribution. Therefore, the recursive algorithm was designed for matrices with only one multiple minimum eigenvalue or one set of clustered small eigenvalues. Thus, when the minimum eigenvalue has multiplicity $k > 1$ the system (8b) is singular for $\lambda = \lambda_{\min}$ and the Zohar algorithm cannot be used. For estimated correlation sequences, we get a set of eigenvalues clustered near the true minimum eigenvalue, which in turn produces a loss of

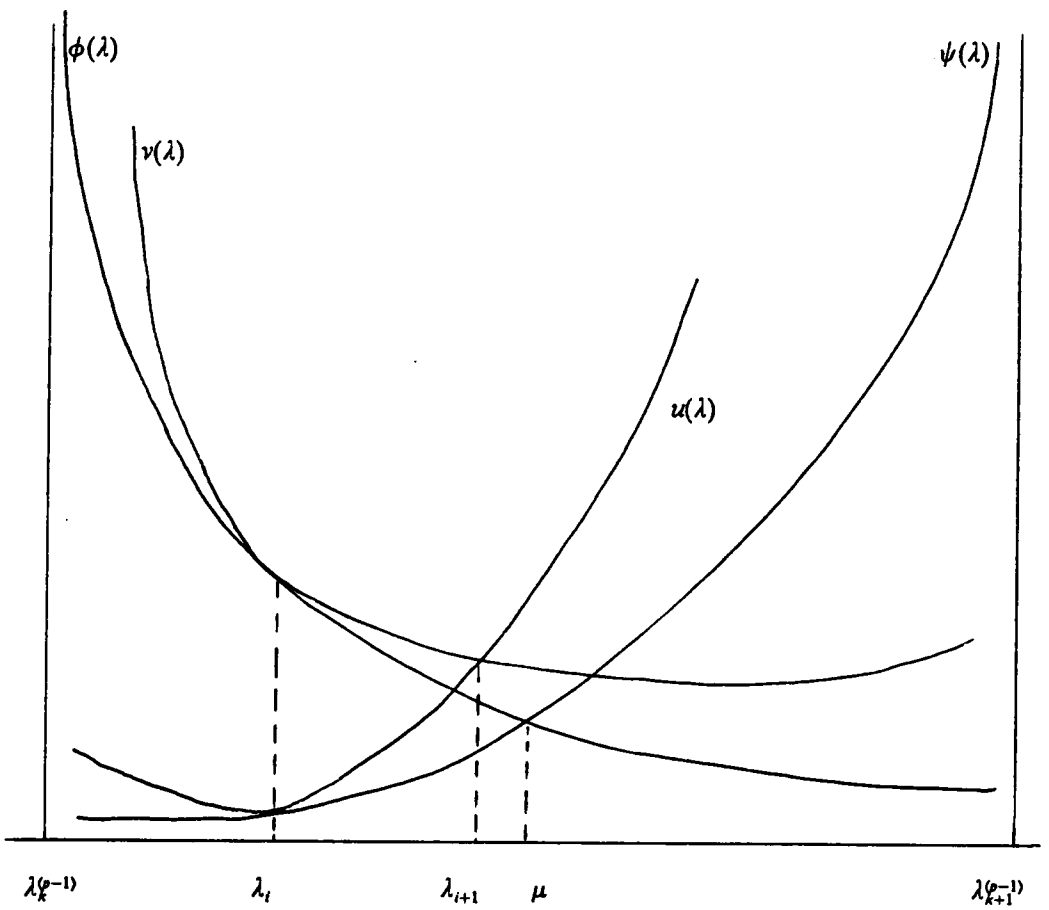

Figure 1. Plot of the functions ϕ, ψ, and their respective rational approximations v and u

orthogonality between the estimated eigenvectors[9]. Recall that the updated eigenvectors are identified by using the updated eigenvalues and solving (8b). However, no direct information on the previously computed vectors is used there, and therefore, clustered eigenvalues will produce nearly dependent eigenvectors. Therefore, a different 2-step approach is followed to insure accurate determination of the clustered or multiple eigenvectors[10]. The procedure uses the fact that $\text{Rank}(R_p - \lambda I) = p - k$, for λ of multiplicity k, to first compute initial eigenvector estimates associated with the set of clustered eigenvalues. These initial estimates are then refined in the second step.

The first step uses the specific Toeplitz structure of the correlation matrix to build recursively k-1 of the k clustered eigenvectors (note that this approach was proposed earlier by Delsarte and Genin [DEG]). Let us describe this procedure with an example. Assume that the following system of order 4 has an eigenvalue of multiplicity 2. Let us denote the set of clustered eigenvectors by $(\underline{u}_1^{(4)}, \underline{u}_2^{(4)})$.

$$(R_4 - \lambda I)\begin{bmatrix} C \\ a_1 \\ a_2 \\ a_3 \end{bmatrix} = \underline{0} \tag{31}$$

If λ has multiplicity 2, then $\text{Rank}(R_4 - \lambda I) = 2$. Thus a solution vector, if it exists, has two free elements which can be fixed. Taking $C = 0$ in (31) leads to

$$(R_3 - \lambda I)\hat{\underline{a}} = \underline{0} \tag{32}$$

Recognize that $(R_3 - \lambda I)$ is still singular, and of rank 2; therefore, one more unknown element of the vector $\hat{\underline{a}}$ can be fixed. For $a_1 = 1$, (32) becomes

$$(R_2 - \lambda I)\begin{bmatrix} a_2 \\ a_3 \end{bmatrix} = -\begin{bmatrix} r_1 \\ r_2 \end{bmatrix} \tag{33}$$

---

[9] i.e. the eigenvectors associated with the set of clustered eigenvalues.

[10] i.e. the eigenvectors associated with the multiple eigenvalue.

Note that we solved this problem already at the previous iteration step. Thus, the updated eigenvector $\underline{u}_2^{(4)}$ is built up by using the eigenvector defined at order 3 associated with the smaller eigenvalue, i.e. $\underline{u}_2^{(4)} = (0, \underline{u}_1^{(3)t})^t$. Then, the last clustered eigenvector $\underline{u}_1^{(4)}$ can be identified by deflation on $(\underline{u}_2^{(4)}, \ldots, \underline{u}_4^{(4)})$, using a Gram-Schmidt orthogonalization type procedure.

In general, the initial eigenvectors of dimension p associated with the set of k clustered eigenvalues may be identified by the following procedure:

1. Build up the first k-1 vectors of the set by using the vectors of length (p-1) defined for the set of k-1 clustered eigenvalues at the previous order and fix their first components to 0, i.e.

$$\hat{\underline{u}}_n^{(p)} = \begin{bmatrix} 0 \\ \underline{u}_{n-1}^{(p-1)} \end{bmatrix} \quad \text{for all } n = 2, \ldots, k \tag{34}$$

where $\underline{u}_{n-1}^{(p-1)}$ represents the $(n-1)^{st}$ eigenvector of the (p-1)-dimensional matrix,

2. Compute the last vector $\hat{\underline{u}}_1^{(p)}$ associated with the set of clustered eigenvalues by deflating a fixed vector of unit length, chosen arbitrarily as $(1,1, \ldots, 1)^t/p$, to the set of p already known eigenvectors. (35)

Note that the procedure described above is based on the fact that we have a unique eigenvalue with multiplicity k. In the estimated correlation case however, we have a set of k clustered eigenvalues. Therefore, a single iteration of the following Shifted Inverse Power (SIP) Method [GVL] using the fast Toeplitz solver, with shift equal to the estimated eigenvalue, is applied to the approximate eigenvectors $\hat{\underline{u}}_n^{(p)}$ to correct the original assumption of a single multiple eigenvalue. Numerical properties of the SIP method are examined in [PAR].

$$(R_p - \lambda_n^{(p)} I)\underline{u}_n^{(p)} = \hat{\underline{u}}_n^{(p)} \quad \text{for all } n = 1, \ldots, k \tag{36}$$

This extra step will insure the production of an adequate eigenvector estimate as the shifts are chosen very close to the true eigenvalues.

Theoretically, the SIP iteration needs to be used only for the eigenvectors associated with the set of clustered eigenvalues. We have noted slight improvement in the eigenvector orthonormality performance however, when the SIP iteration is used on all estimated eigenvectors. This is due to the fact that the eigenvector problem is ill-conditioned for Hermitian matrices [GVL]. Recall that the eigenvalues, estimated by an iterative process, are used in the computation of the eigenvectors. This introduces numerical perturbations in the eigenvector estimate which are then corrected by the SIP step.

Deflation Procedure

The deflation technique used to compute the last of the set of multiple or clustered eigenvectors is known as a *deflation by subtraction procedure.* The basic idea is to suppress the influence of particular eigenvectors as soon as the vectors have been identified [PAR,WIL]. In our specific application, only the smallest eigenvalues (corresponding to the noise eigenvalues) are clustered. Therefore, the idea is to suppress the dominant eigenvectors and (k-1) multiple (clustered) eigenvectors already found in order to identify the last k^{th} eigenvector $\underline{u}_1$ associated with the set of multiple (clustered) vectors. The deflation method is an iterative procedure and is defined by [WIL]:

$$\underline{v}_{n+1} = R_p \underline{v}_n \tag{37a}$$

$$\underline{w}_{n+1} = \underline{v}_{n+1} - \sum_{i=2}^{p} (\underline{v}_{n+1} \underline{u}_i^*) \underline{u}_i \tag{37b}$$

$$\underline{v}_{n+1} = \underline{w}_{n+1} / \|\underline{w}_{n+1}\|_2 \tag{37c}$$

where $\underline{v}_0$ represents the initial vector chosen for the iteration, and $\| \|_2$ is the Euclidian norm. Note that equation (37b) suppresses the components of $(\underline{u}_2, \ldots, \underline{u}_p)$ in the vector $\underline{w}_{n+1}$, while it seems that equation (37a) tends to increase the unwanted components from already known vectors. However, Wilkinson [WIL] has shown that (37b) can be rewritten as

$$\begin{aligned} \underline{w}_{n+1} &= \underline{v}_{n+1} - \sum_{i=2}^{p} (\underline{v}_{n+1}\underline{u}_i^*)\underline{u}_i \\ &= \left(R_p - \sum_{i=2}^{p} \lambda_i \underline{u}_i \underline{u}_i^* \right) \underline{v}_{n+1} \end{aligned} \tag{38}$$

Therefore, the deflation method can be viewed as a power method applied to $\hat{R}_p = R_p - \sum_{i=2}^{p} \lambda_i \underline{u}_i \underline{u}_i^*$, which has eigenvalues $\hat{\lambda}_2 = \cdots = \hat{\lambda}_n = 0$, and $\hat{\lambda}_1 = \lambda_1$. Furthermore, Parlett [PAR, Chapter 5], has shown that roundoff errors, present in any numerical implementation, do not degrade the performance of this orthogonalization technique. Practically, convergence of the orthogonalization technique is usually obtained in less than 4-5 iterations, and the vectors obtained have good eigenproperties[11].

Simulations showed that better eigen-performance[12] is obtained by this orthogonalization technique than by reorthogonalizing against the other eigenvectors with a regular single step of the Gram-Schmidt (GS) procedure. However, improvement in the eigen-performance for this process can be obtained by using the GS procedure with reorthogonalization. Recall that the GS algorithm has poor numerical properties, in that a loss of orthogonality can occur between the "orthogonalized" vectors when they are almost parallel to begin with. In this case, the resulting eigenvector found after applying the GS procedure is very small with a large relative error [PAR,DGK]. Reorthogonalization can then be used to enforce numerical stability. The idea is to apply the GS process iteratively, and the process stops when the iterate has converged. Performance similar to that obtained with the deflation technique is reached after 2 to 3 iterations. Note that the deflation technique was used in the implementation of the regular eigendecomposition algorithm RITE. In the generalized eigendecomposition algorithm C-RITE,

---

[11] i.e. the vector obtained is "strongly" orthonormal to the rest of the set, and the associated residual norm is small.

[12] defined for an eigenpair $(\lambda, \underline{u})$ in terms of the residual norm of the eigenpair, and the orthonormal behavior of the eigenvector $\underline{u}$ with the other eigenvectors of the matrix studied.

the eigenvectors are not orthonormal in the Euclidian norm any longer[13], and the GS procedure with reorthogonalization is used, as explained further in Section 3.4. The performance of RITE is illustrated in Section 2.6.

2.5 *Algorithmic Implementation Considerations*

A summary of the RITE algorithm is given in Table 2 on page 34. In this implementation, the correlation sequence is normalized before the eigen-decomposition such that $r(0) = 1$, which re-scales the eigenvalues. Four threshold quantities are introduced in the procedure.

1. ε_1: the convergence threshold defined for the iterative eigenvalue search method, chosen as 5.10^{-8}.

2. ε_2: represents the minimum distance that separates two consecutive eigenvalues for them to be considered as not clustered. When the eigenvalue separation is less than 5.10^{-4}, the fast Toeplitz solver is not used as this would lead to linearly dependent eigenvectors.

3. ε_3: defines the minimum distance, chosen as 1.10^{-6}, between two consecutive eigenvalues for them to be considered not multiple. Only the single inverse iteration step is applied to the eigenvectors associated with the non-multiple eigenvalues.

4. ε_4: is the convergence threshold used for the deflation procedure. The iterative process is considered to have converged to the eigenvector $\underline{u}_{i,k}^{(p)}$ when $\|\underline{u}_{i,k}^{(p)} - \underline{u}_{i,k+1}^{(p)}\|_2 \leq \varepsilon_4$, where $\varepsilon_4 = 10^{-3}$.

---

[13] however, note that the eigenvectors of the pencil (R,B) are still orthonormal in the B-inner product, i.e. $U^*BU = I$, where U is defined as the generalized eigenvector matrix.

Note that a similar block decomposition of the original eigen-equation is used by Cybenko and Van Loan [CYV] to compute the minimum eigenpair of a symmetric positive definite Toeplitz matrix. They compute the minimum eigenvalue by using an iterative search function and present several methods to identify the initial minimum eigenvalue search interval. The RITE algorithm is more general in the sense that it leads to the complete eigendecomposition of a Toeplitz matrix, which does not have to be positive definite, and it can handle the situation where the minimum eigenvalue has multiplicity greater than one. Recall furthermore, that the eigenvalue search functions can easily be evaluated using the eigendecomposition obtained at the previous order. Therefore, the RITE algorithm seems more adapted for applications, such as high-resolution eigen-techniques, where complete eigenspace information is needed to estimate frequencies or direction of arrival of incoming signals.

2.6 Performance Measures

A drawback of recursive procedures is the potential error accumulation from one order to the next. In this specific case, accuracy of the eigenpairs has to be as good as possible to avoid excessive degradation of the next decomposition. The sensitivity of the procedure is expected to depend on the order, and the specific structure, of the matrix (i.e. on the separation of the eigenvalues). It might be expected to be more sensitive for matrices with closely clustered eigenvalues, i.e. for matrices as generated later in Chapter 4, from signals with high SNR. In such a case however, correct identification of the DOA information is obtained for eigendecompositions of relatively low dimensions, and the recursive procedure could be stopped there. Stability and sensitivity tests have been conducted for our algorithm and comparisons of the performance of the recursive algorithm with those of the IMSL (version 9.2) subroutine EIGCH are presented in Figure 2 on page 35 to Figure 6 on page 39. Note that the restricted Newton scheme was used for the eigenvalue identification task. The IMSL routine is not specifically designed for Toeplitz Hermitian matrices.

To the author's knowledge however, no optimized procedures for performing Toeplitz eigendecompositions are readily available. The subroutine EIGCH was chosen as it is highly optimized for Hermitian matrices and widely available. The algorithm used in the eigendecomposition routine EIGCH is as follows [IMS] :

1. The matrix is reduced to a real symmetric tridiagonal matrix.

2. The eigenvalues and (optionally) the eigenvectors of this new matrix are computed.

3. The eigenvectors (if needed) are backtransformed to retrieve the eigenvectors of the original Hermitian matrix.

The tests used to check the performance of the Recursive Iterative Toeplitz Eigenspace (RITE) algorithm versus EIGCH are the Averaged Residual (Frobenius) NORM squared defined as

$$\mathbf{ARNORM} = \frac{1}{p} \| R_p U_p - U_p \Lambda_p \|_F^2$$

and the Averaged ORTHOnormality (Frobenius) norm squared

$$\mathbf{AORTHO} = \frac{1}{p} \| U_p^* U_p - I_p \|_F^2$$

where p represents the dimension. The results represent the values obtained for 10 trial runs on different correlation matrices. The matrices R_p were built from the estimated correlation sequences generated by two sources of variable angle locations with different SNR in a white noise environment. A complete list of the parameters used to generate the correlation sequences can be found in Figure 2 on page 35, where Nest represents the number of snapshots used to estimate the correlation sequences. Figure 2 to Figure 5 show that the RITE algorithm yields larger variations of the Averaged Residual NORM (ARNORM) and the Averaged ORTHOnormality norm (AORTHO) than the IMSL subroutine. This indicates a higher sensitivity of the recursive algorithm. Recall that the RITE algorithm uses estimated eigenvalues to solve for the eigenvectors,

so that errors in the eigenvalues are expected to introduce errors in the determination of the corresponding eigenvectors. Nevertheless, the average magnitude of the two norms is well behaved with increasing dimension and they seem to stabilize for the RITE algorithm around the respectable values of 10^{-24} for ARNORM and 10^{-19} for AORTHO. Realizing that a difference of 10 orders of magnitude for AORTHO between RITE and IMSL appears large, a measure of angle difference between IMSL and RITE eigenvectors for corresponding eigenvalues was also evaluated. This measure is defined as

$$\text{ANGLE} = \frac{1}{p}\sum_{i=1}^{p} \cos^{-1}(|\underline{u}^{*}_{i,RITE}\underline{u}_{i,IMSL}|) \cdot 180/\pi$$

The results, plotted in Figure 6 on page 39, represent the values obtained for the ten trial runs presented in Figure 2 on page 35. They show that the actual eigenvector directions, obtained with the two different techniques, are very close. Note in Figure 2 and Figure 3 that the algorithm, at higher dimensions, actually recovers from outlying errors at previous dimensions. The test sequences were computed from two incoming sources in white noise, thereby generating matrices with two large and distinct eigenvalues, while the others were small and clustered (especially for matrices of high dimension). If the algorithm is sensitive to the multiple eigenvalue situation, it is certainly being tested here. Recall that the purpose of the array processing application will be to identify the DOA information as early as possible, and to then stop, or continue and confirm. In the case of two incoming sources, correct identification of the parameters will be obtained for orders much smaller than 50. Thus, these tests can be considered as lower performance bounds on the procedure; they show that potential propagation errors, present in any recursive process, do not accumulate fast enough to cause a marked degradation of the proposed algorithm for orders up to 50.

Table 2. RITE algorithm implementation

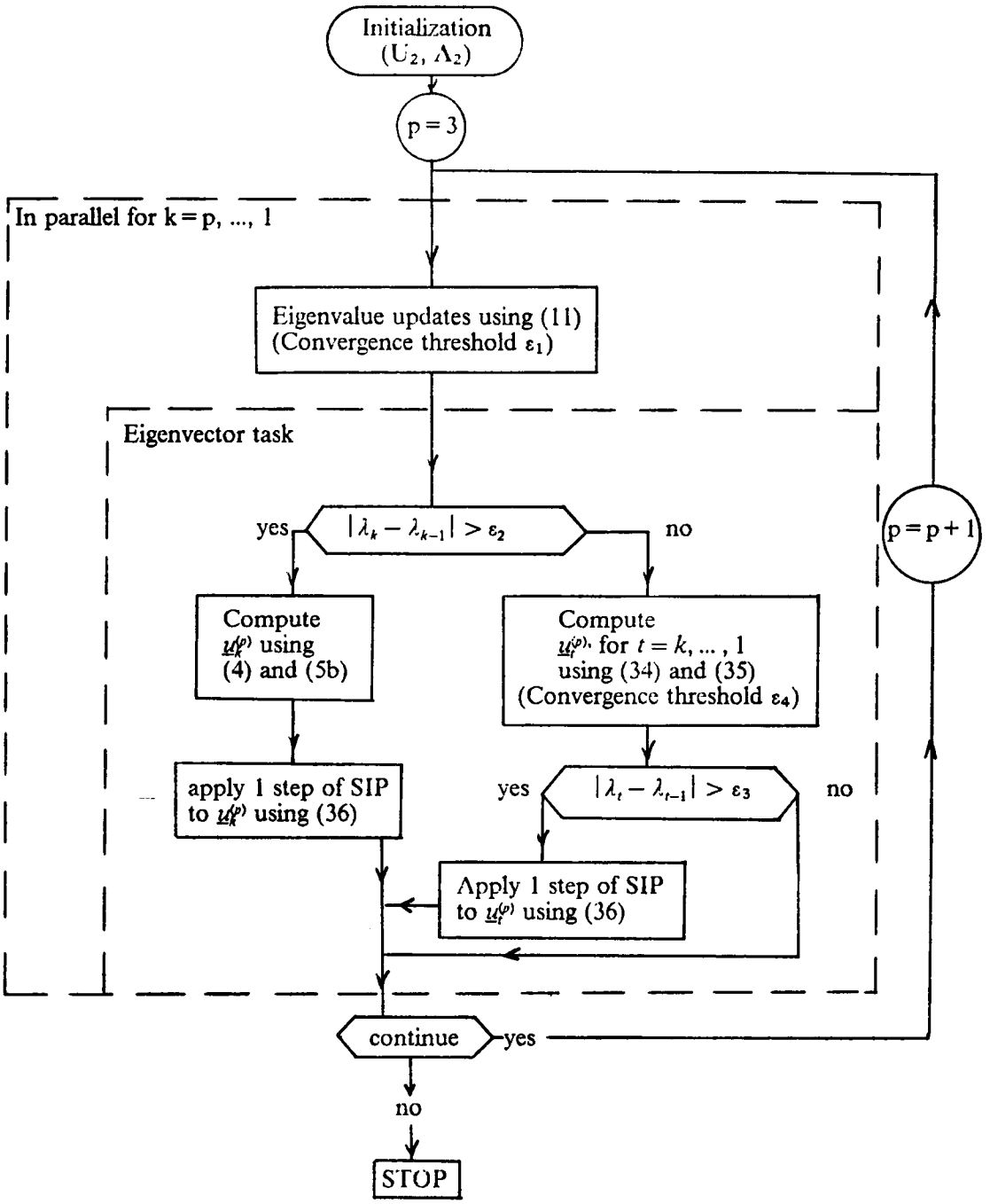

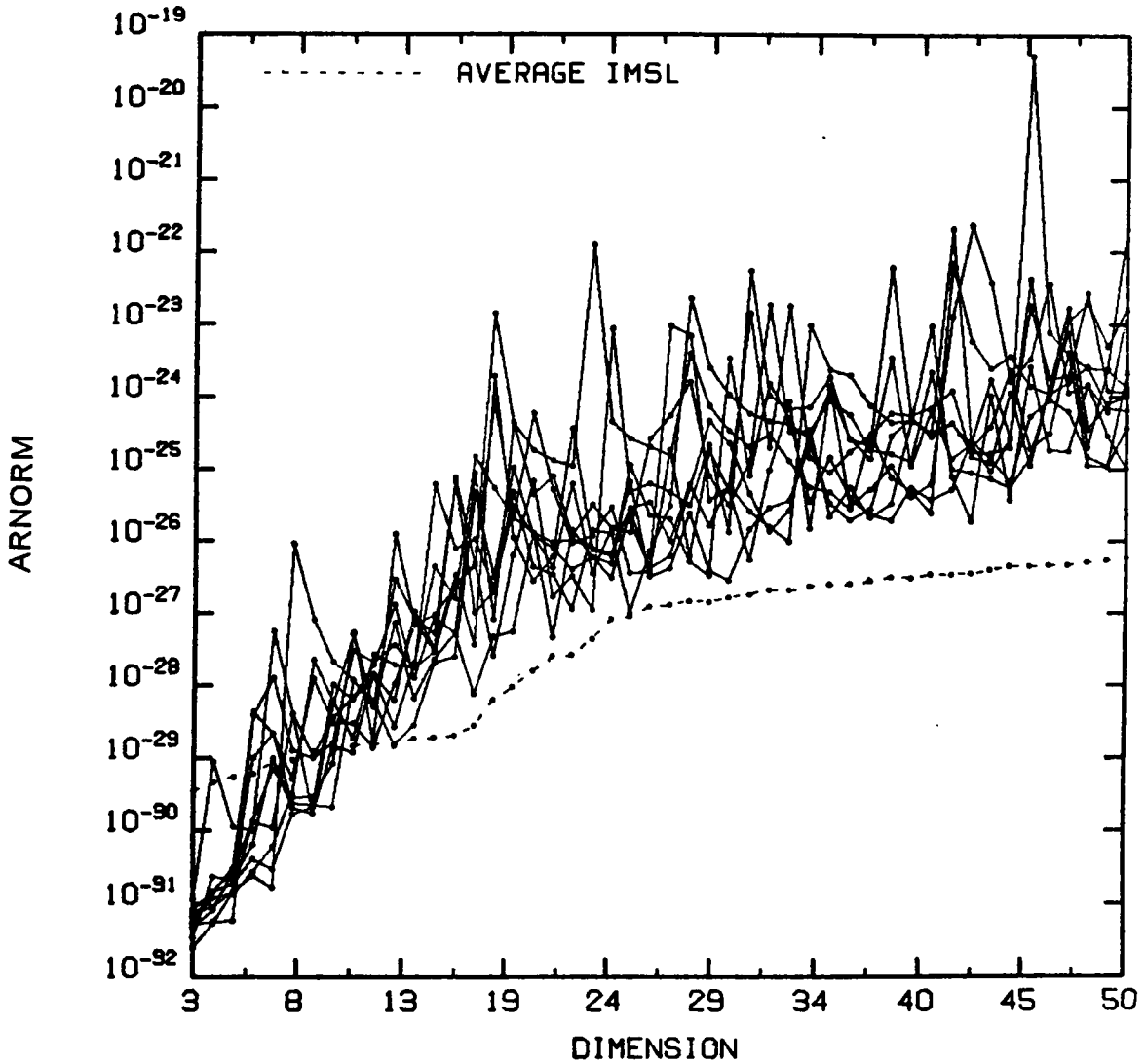

Trial Run Parameters										
θ_1 (Deg)	30	18	60	20	40	05	70	10	08	80
θ_2 (Deg)	35	22	65	25	45	25	75	30	15	82
SNR (dB)	10	05	02	10	0	05	02	05	0	03
Nest	300	200	100	400	200	100	100	100	200	100

Figure 2. Averaged residual norms squared for the RITE algorithm: 10 trial runs.

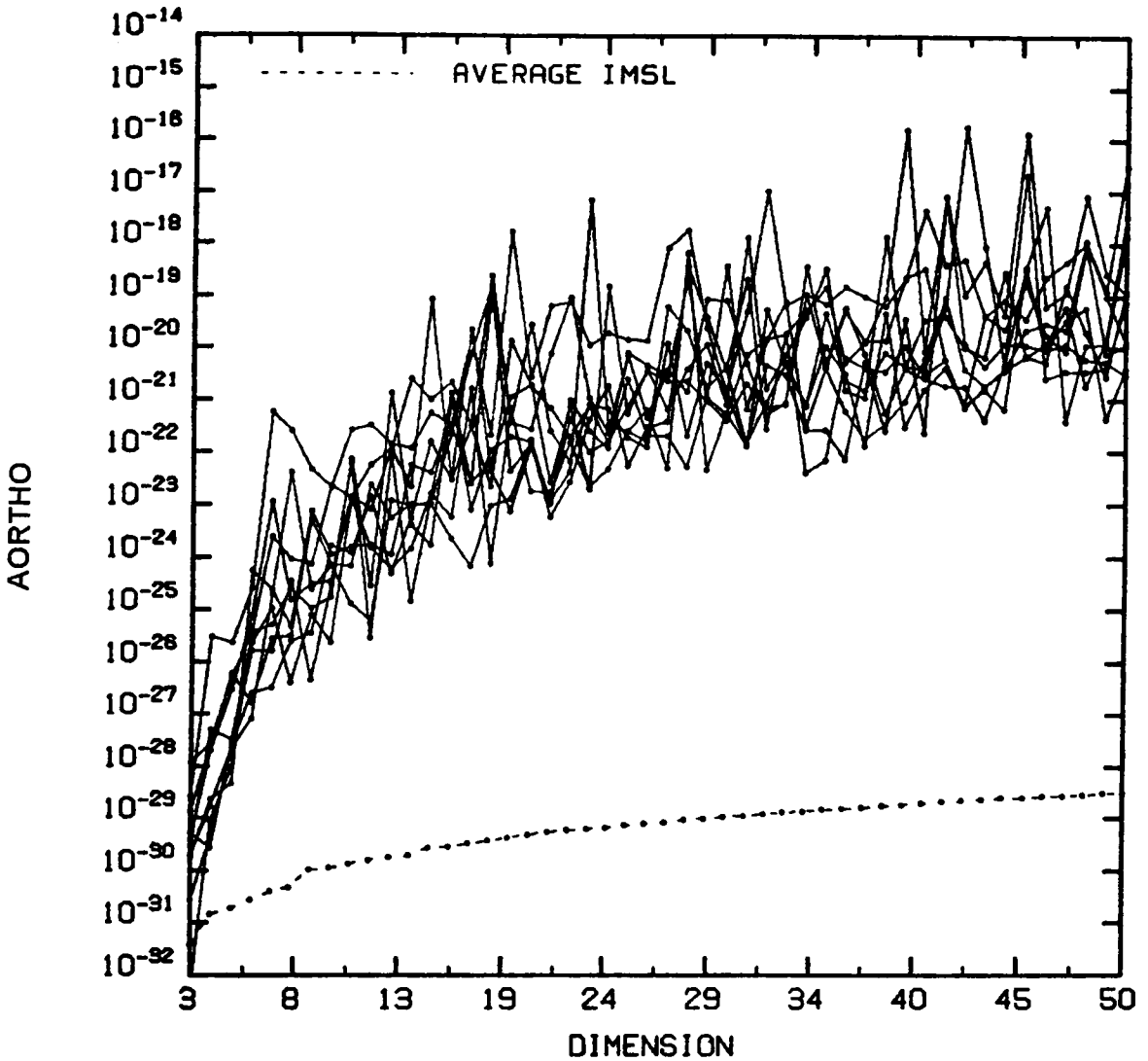

Figure 3. Averaged orthonormality norms squared for the RITE algorithm: 10 trial runs.

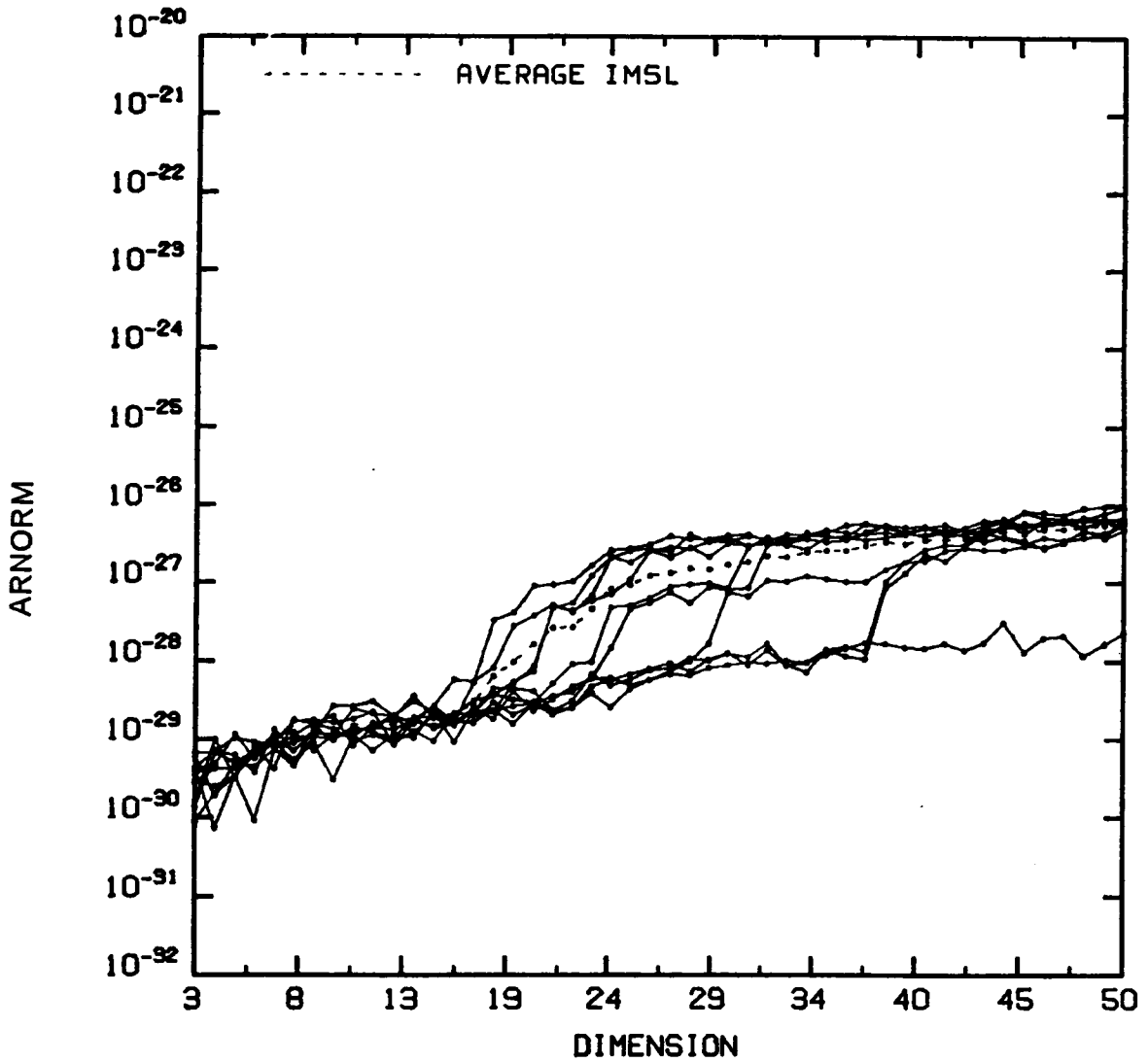

Figure 4. Averaged residual norms squared for the IMSL routine EIGCH: 10 trial runs.

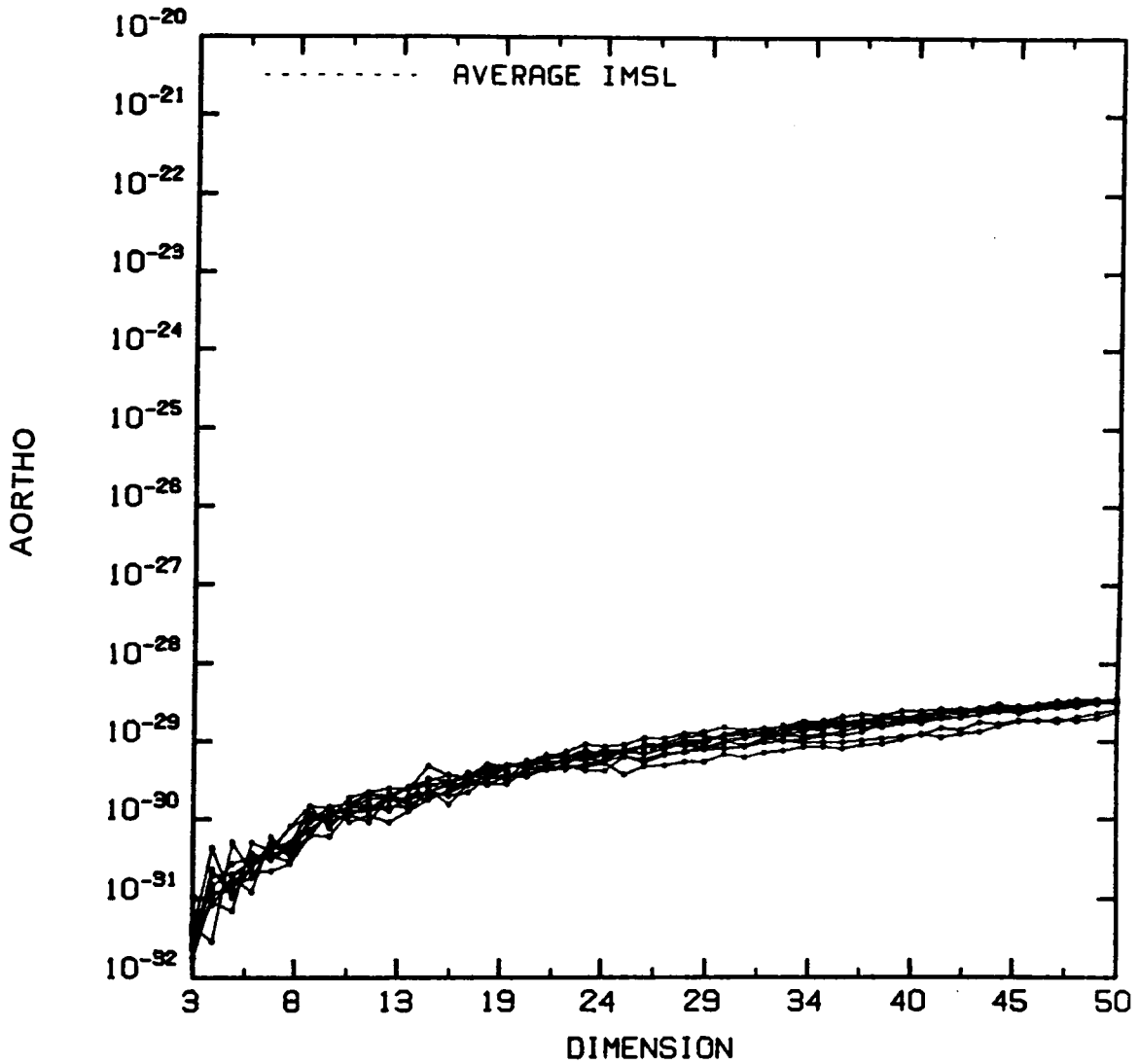

Figure 5. Averaged orthonormality norms squared for the IMSL routine EIGCH: 10 trial runs.

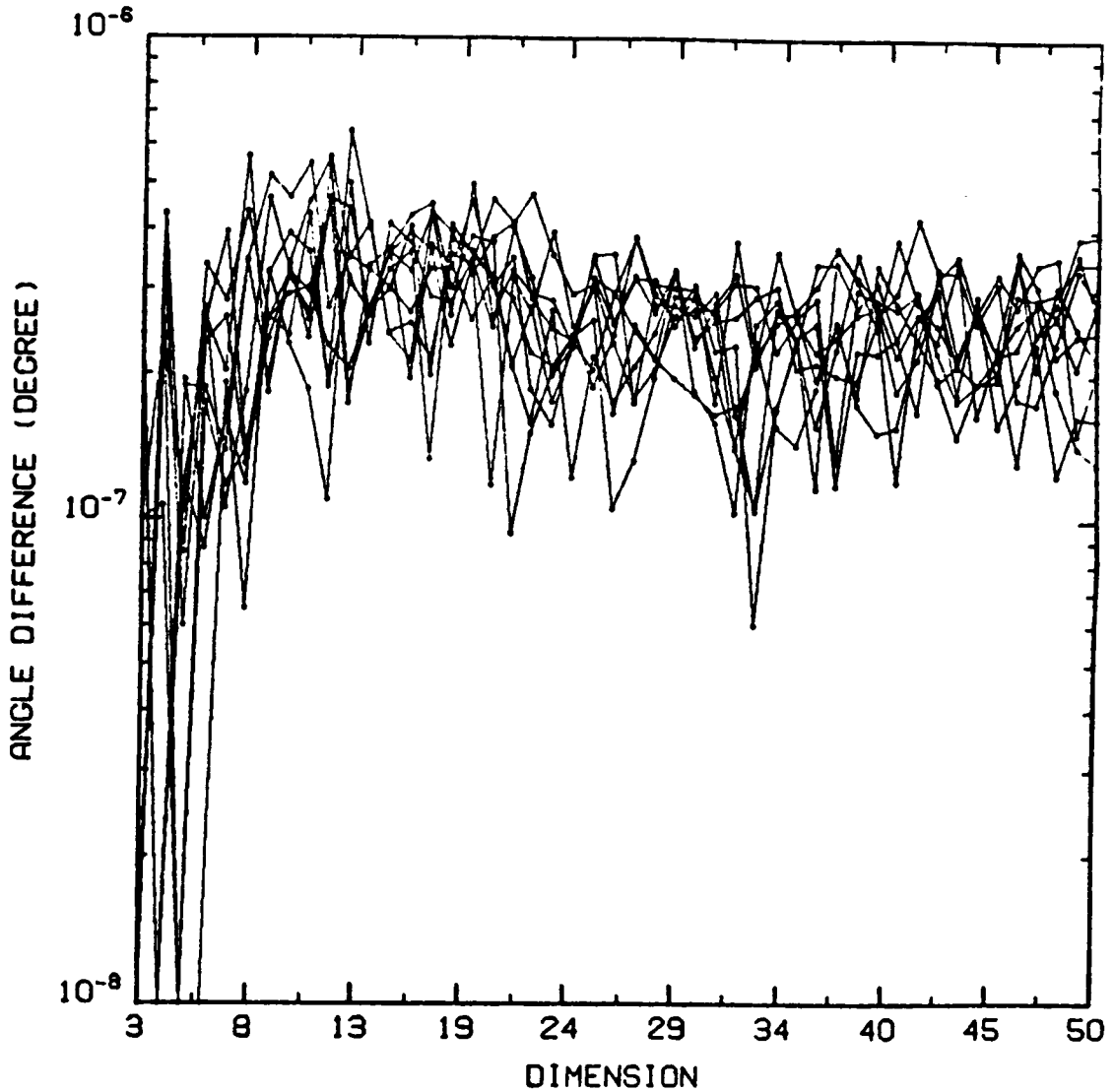

Figure 6. Averaged angle difference between RITE and IMSL eigenvectors for corresponding eigenvalues: 10 trial runs.

3.0 The Generalized Eigenspace Decomposition Extension

3.1 Presentation

The RITE technique can be extended to the generalized eigendecomposition of strongly regular[14] Toeplitz Hermitian pencils (R,B). The modifications needed for this extension, defined as the Colored-RITE (C-RITE)[15], turn out to be easy to implement, and in fact no factorization of the matrix B is required for the procedure. The main differences with the regular case lie in the definition of the (generalized) eigenvalue search functions, and the (generalized) inner product needed for the multiple eigenvalue case. The successive decompositions are computed recursively for pencils of increasing dimension, and optimization of the computational speed can be obtained by taking advantage in the parallel executable steps of the algorithm, as introduced earlier in Chapter 2 for the RITE implementation.

---

[14] i.e. with all regular submatrices.

[15] because, in the array processing context, a generalized eigendecomposition is needed in order to recover the signal information when the noise is colored.

3.2 *Order-Recursive Generalized Eigendecomposition*

As for the RITE derivation, the question to answer is the following: *Suppose we know the eigendecomposition* (U_{p-1}, Λ_{p-1}) *of the (p-1)-dimensional pencil* (R_{p-1}, B_{p-1}), *can we use it to find the eigendecomposition* (U_p, Λ_p) *for the p-dimensional pencil* (R_p, B_p)? In other words: can we find the eigenstructure of the Hermitian Toeplitz pencil recursively in order.

Note that the order-recursive nature of such an algorithm can then be used to estimate the DOA parameters using the eigen-information obtained from potentialy still low-dimensional subsystems imbedded in the maximum size one in the array processing application considered.

To this end the following equation needs to be solved.

$$(R_p - \lambda B_p)\underline{a} = \underline{0} \tag{39}$$

where R_p and B_p are Hermitian Toeplitz matrices of dimension p. Since we know the eigendecomposition for (R_p, B_p), equation (39) is rewritten as

$$\begin{bmatrix} r_0 - \lambda b_0 & \underline{r}^* - \lambda \underline{b}^* \\ \underline{r} - \lambda \underline{b} & R_{p-1} - \lambda B_{p-1} \end{bmatrix} \begin{bmatrix} 1 \\ \hat{\underline{a}} \end{bmatrix} = \underline{0} \tag{40}$$

where $\underline{r} = [r_1, \ldots, r_{p-1}]^t$ and $\underline{b} = [b_1, \ldots, b_{p-1}]^t$. Therefore, the generalized eigenpair solutions satisfy the following system

$$r_0 - \lambda b_0 + (\underline{r}^* - \lambda \underline{b}^*)\hat{\underline{a}} = 0 \tag{41a}$$

$$(R_{p-1} - \lambda B_{p-1})\hat{\underline{a}} = -(\underline{r} - \lambda \underline{b}) \tag{41b}$$

First note that the matrix in (41b) is Hermitian Toeplitz, so that for any given λ the solution $\hat{\underline{a}}$ can be found, as in the RITE procedure, and under the same strongly regular conditions, by using the Toeplitz system solver proposed by Zohar [ZO2]. Thus, as before, the remaining problem is

to solve for all possible eigenvalues $\lambda_n^{(p)}$, for $n = 1, \ldots, p$, from (41a). To that end, substitute (41b) into (41a) to eliminate $\hat{\underline{a}}$.

$$r_0 - \lambda b_0 - (\underline{r}^* - \lambda \underline{b}^*)(R_{p-1} - \lambda B_{p-1})^{-1}(\underline{r} - \lambda \underline{b}) = 0 \tag{42}$$

Substituting for B_{p-1} its Choleski factorization, and *restricting the analysis to the case of strongly regular matrices B,* we have:

$$R_{p-1} - \lambda B_{p-1} = C_{p-1}^*\left[C_{p-1}^{-*} R_{p-1} C_{p-1}^{-1} - \lambda I\right] C_{p-1} \tag{43}$$

where C^{-*} denotes the inverse of the conjugate transpose of the matrix C. Note that S_{p-1}, defined as $S_{p-1} = C_{p-1}^{-*} R_{p-1} C_{p-1}^{-1}$, is Hermitian. Hence, its eigenvector matrix V_{p-1} may be chosen to be unitary, i.e.

$$V^* V = V V^* = I \quad \text{and} \quad V^* = V^{-1} \tag{44}$$

Furthermore, for regular pencils (R,B) we have the following generalized eigen-relationships

$$\lambda(R, B) = \lambda(R, C^* C) = \lambda(C^{-*} R C^{-1}, I) \tag{45a}$$

$$S_{p-1} = V_{p-1} \Lambda_{p-1} V_{p-1}^* \tag{45b}$$

Therefore, using properties (44) and (45) in (43) above leads to

$$(R_{p-1} - \lambda B_{p-1}) = C_{p-1}^*\left[\mathrm{V}_{p-1} \Lambda_{p-1} V_{p-1}^* - \lambda V_{p-1} V_{p-1}^*\right] C_{p-1} \tag{46}$$

and as a result

$$(R_{p-1} - \lambda B_{p-1})^{-1} = C_{p-1}^{-1} V_{p-1}^{-*} (\Lambda_{p-1} - \lambda \mathrm{I})^{-1} V_{p-1}^{-1} C_{p-1}^{-*} \tag{47}$$

where Λ_{p-1} is the diagonal generalized eigenvalue matrix with $\lambda_n^{(p-1)}$, $n = 1, \ldots, p-1$, as elements. Substituting (47) into (42), yields

$$r_0 - \lambda b_0 = (\underline{r} - \lambda \underline{b})^* C_{p-1}^{-1} V_{p-1}^{-*} (\Lambda_{p-1} - \lambda I)^{-1} V_{p-1}^{-1} C_{p-1}^{-*} (\underline{r} - \lambda \underline{b}) \tag{48}$$

Using the fact that $C_{p-1}U_{p-1} = V_{p-1}$, as shown in Appendix B, where U_{p-1} is the B-normalized generalized eigenvector matrix associated with the pencil (R_{p-1}, B_{p-1}), equation (48) becomes

$$r_0 - \lambda b_0 = (\underline{r} - \lambda \underline{b})^* U_{p-1}(\Lambda_{p-1} - \lambda I)^{-1} U_{p-1}^*(\underline{r} - \lambda \underline{b}) \tag{49}$$

Note that the matrix $(\Lambda_{p-1} - \lambda I)$ is diagonal. Therefore, its inverse can easily be computed, and equation (49) may be rewritten as

$$(r_0 - \lambda b_0) = \sum_{k=1}^{p-1} \frac{|\beta_k|^2}{\lambda_k^{(p-1)} - \lambda} \tag{50}$$

where

$$\beta_k = (\underline{r} - \lambda \underline{b})^* \mathrm{col}_k(U_{p-1})$$

Therefore, using the generalized eigen-decomposition (U_{p-1}, Λ_{p-1}) at order p-1, the new system of equations to be solved becomes:

$$-(r_0 - \lambda b_0) + \sum_{k=1}^{p-1} \frac{|\beta_k|^2}{\lambda_k^{(p-1)} - \lambda} = 0 \tag{51}$$

$$(R_{p-1} - \lambda B_{p-1})\hat{\underline{a}} = -(\underline{r} - \lambda \underline{b}) \tag{52}$$

3.3 *The Eigenvalue Problem*

3.3.1 Introduction

Let us define the generalized eigenvalue search function as

$$h(\lambda) = -r_0 + \lambda b_0 + \sum_{k=1}^{p-1} \frac{|\beta_k|^2}{\lambda_k^{(p-1)} - \lambda} \tag{53}$$

Recall that R and B are Hermitian and strongly regular. Hence, using property (45a), we know that the generalized eigenvalues still satisfy the following interlacing property :

$$\lambda_{n-1}^{(p)} \leq \lambda_{n-1}^{(p-1)} \leq \lambda_n^{(p)} \leq \lambda_n^{(p-1)} \leq \lambda_{n+1}^{(p)} \leq \lambda_{n+1}^{(p-1)}$$

Therefore, the search intervals for each updated eigenvalue $\lambda_n^{(p)}$ can be restricted to $I_n^p = [\lambda_{n-1}^{(p-1)}, \lambda_n^{(p-1)}]$ for all $n = 2, \ldots, p-1$, $I_1^p = [K_1, \lambda_1^{(p-1)}]$ and $I_p^p = [\lambda_{p-1}^{(p-1)}, K_2]$, where K_1 and K_2 are constants defined such that $K_1 < \lambda_1^{(p)}$ and $\lambda_p^{(p)} < K_2$. Recall that, in the RITE derivation, the eigenvalue search function was easily shown to be monotone between its singular points, which in turn allowed the use of quadratically convergent iterative search techniques. Monotonicity of the generalized search function is proved in the next section.

3.3.2 Monotone Behavior of the Generalized Search Function

The key behind the proof is to note that the set of eigenvalues associated with the matrix $C^{-*}RC^{-1}$ is identical to the set of generalized eigenvalues associated with the pencil (R, C^*C), when C^*C is strongly regular. First, we show that the eigenvalue search function for the

eigen-decomposition of a Hermitian matrix is monotone between its poles. This result is then used to prove that the eigenvalue search function for the generalized eigen-decomposition of the Hermitian pencil (R,B) is monotone between its poles also. For purposes of clarity, the eigenvalue search function for a regular (white noise) eigen-decomposition is denoted $h_w(\lambda)$, and the eigenvalue search function for the general case (colored noise) is denoted $h_c(\lambda)$. Note that the proof is restricted to the case of distinct eigenvalues. There is no need to use a search technique to identify the multiple eigenvalues as they are directly identified from the eigenvalues obtained at the previous order.

The generalized eigenvalue search function $h_c(\lambda)$ for the pencil (R_p, B_p) is defined as:

$$h_c(\lambda) = -r_0 + \lambda b_0 + \sum_{n=1}^{p-1} \frac{|\beta_n|^2}{\lambda_n^{(p-1)} - \lambda} \tag{54}$$

where $\beta_n = (\underline{r} - \lambda \underline{b})^* \mathrm{col}_n(U_{p-1})$. From (54)

$$h'_c(\lambda) = b_0 + \sum_{n=1}^{p-1} \left[\frac{-2\mathrm{Real}\left[\beta_n^* (\underline{b}^* \mathrm{col}_n(U_{p-1}))\right]}{\lambda_n^{(p-1)} - \lambda} + \frac{|\beta_n|^2}{(\lambda_n^{(p-1)} - \lambda)^2} \right] \tag{55}$$

White Noise Case - Monotone Behavior of h

In the white noise case $b_0 \equiv 1, \underline{b} \equiv \underline{0}$ and the above nonlinear equations degenerate to

$$h_w(\lambda) = -r_0 + \lambda + \sum_{l=1}^{p-1} \frac{|\beta_l|^2}{\lambda_l^{(p-1)} - \lambda} \tag{56}$$

where $\beta_l = \underline{r}^* \mathrm{col}_l(U_{p-1})$, and

$$h'_w(\lambda) = 1 + \sum_{l=1}^{p-1} \frac{|\beta_l|^2}{(\lambda_l^{(p-1)} - \lambda)^2} \tag{57}$$

It is easy to see that $h_w(\lambda)$ is monotone between its singular points $\lambda_i^{(p-1)}$ for $i = 1, \ldots, p-1$, because $h'_w(\lambda) \geq 1$. Note that this monotonicity property is not restricted to Toeplitz Hermitian matrices; it is valid for all Hermitian matrices.

Colored Noise Case - Monotone Behavior of h

Using the fact that C^*C is strongly regular, we have

$$\begin{aligned} |R_p - \lambda B_p| &= |B_p|\,|C_p^{-*} R_p C_p^{-1} - \lambda I| \\ &= |B_p|\,|\hat{R}_p - \lambda I| \end{aligned} \tag{58}$$

where $\hat{R}_p = C_p^{-*} R_p C_p^{-1}$. The Gauss Algorithm [GAT] provides alternative expressions for the determinants. Recall that this algorithm shows that

$$\begin{aligned} \mathrm{DET}\begin{bmatrix} A & B \\ C & D \end{bmatrix} &= |A|\,|D - CA^{-1}B| \quad \text{if } A^{-1} \text{ exists} \\ &= |D|\,|A - BD^{-1}C| \quad \text{if } D^{-1} \text{ exists} \end{aligned} \tag{59}$$

Therefore, using the above Gauss property for the matrix $(\hat{R}_p - \lambda I)$, leads to

$$\begin{aligned} |\hat{R}_p - \lambda I| &= |\hat{R}_{p-1} - \lambda I|\,|\hat{r}_0 - \lambda - \hat{\underline{t}}^*(\hat{R}_{p-1} - \lambda I)^{-1}\hat{\underline{t}}| \\ &= |\hat{R}_{p-1} - \lambda I|\, h_w(\lambda) \end{aligned} \tag{60}$$

where $\hat{R}_{p-1}$ is defined as the upper left (p-1)-dimensional matrix contained in $C_p^{-*} R_p C_p^{-1}$ denoted $(C_p^{-*} R_p C_p^{-1})_{p-1}$, and $h_w(\lambda)$ is the regular eigenvalue search function for the Hermitian matrix $\hat{R}_p$. Substituting (60) into (58) leads to

$$|R_p - \lambda B_p| = |B_p|\,|\hat{R}_{p-1} - \lambda I|\, h_w(\lambda) \tag{61}$$

Similarly, applying (59) to the matrix $(R_p - \lambda B_p)$ yields

$$\begin{aligned} |R_p - \lambda B_p| &= |R_{p-1} - \lambda B_{p-1}|\,|r_0 - \lambda b_0 - (\underline{r} - \lambda \underline{b})^*(R_{p-1} - \lambda B_{p-1})^{-1}(\underline{r} - \lambda \underline{b})| \\ &= |R_{p-1} - \lambda B_{p-1}|\, h_c(\lambda) \end{aligned} \tag{62}$$

Note that $(\hat{R}_{p-1} - \lambda I)^{-1}$ and $(R_{p-1} - \lambda B_{p-1})^{-1}$ exist because the proof is only considering the distinct eigenvalue case. Recall furthermore, that the C-RITE algorithm is restricted to strongly regular matrices B. Therefore, B_{p-1} is non-singular and applying the Gauss property (59) to $|B_p|$ leads to

$$|B_p| = \left|\begin{bmatrix} B_{p-1} & \underline{b} \\ \underline{b}^* & b_0 \end{bmatrix}\right| = |B_{p-1}|\,|b_0 - \underline{b}^* B_{p-1}^{-1}\underline{b}| \tag{63}$$

Substituting (63) into (61), we get

$$\begin{aligned} |R_p - \lambda B_p| &= |b_0 - \underline{b}^* B_{p-1}^{-1}\underline{b}|\,|C_{p-1}^* C_{p-1}|\,|\hat{R}_{p-1} - \lambda I|\,h_w(\lambda) \\ &= K|C_{p-1}^*|\,|\hat{R}_{p-1} - \lambda I|\,|C_{p-1}|\,h_w(\lambda) \\ &= K|C_{p-1}^*(C_p^{-*} R_p C_p^{-1})_{p-1} C_{p-1} - \lambda B_{p-1}|\,h_w(\lambda) \end{aligned} \tag{64}$$

Now, using the fact that $(C_p^{-*} R_p C_p^{-1})_{p-1} = C_{p-1}^{-*} R_{p-1} C_{p-1}^{-1}$, as shown below in lemma 1, equation (64) becomes

$$|R_p - \lambda B_p| = K|R_{p-1} - \lambda B_{p-1}|\,h_w(\lambda) \tag{65}$$

Equating (65) and (62) leads to

$$K|R_{p-1} - \lambda B_{p-1}|\,h_w(\lambda) = |R_{p-1} - \lambda B_{p-1}|\,h_c(\lambda) \tag{66}$$

Recall that for distinct eigenvalues $|R_{p-1} - \lambda B_{p-1}| \neq 0$, so that (66) becomes

$$h_c(\lambda) = K h_w(\lambda) \tag{67}$$

where $K = b_0 - \underline{b}^* B_{p-1}^{-1}\underline{b}$ from (64). Hence, using the fact that $h_w(\lambda)$ (associated with the matrix $\hat{R}_p$) is monotone between its poles $\lambda_i^{(p-1)}$ as shown earlier, we get the property that $h_c(\lambda)$ (associated with the pencil (R_p, B_p)) is monotone between the same singular points also.

Lemma 1: Let (R_p,B_p) be a p-dimensional Hermitian positive definite pencil. Let C_{p-1} and C_p be defined respectively as the upper triangular Choleski decompositions for the matrices B_{p-1} and B_p. Then the (p-1)-dimensional upper left submatrix imbedded in the matrix $C_p^{-*}R_pC_p^{-1}$ is such that

$$(C_p^{-*}R_pC_p^{-1})_{p-1} = C_{p-1}^{-*}R_{p-1}C_{p-1}^{-1} \tag{68}$$

Proof:

Using the matrix definitions above, we have

$$C_p = \begin{bmatrix} C_{p-1} & \underline{c} \\ \underline{0} & c \end{bmatrix} \tag{69}$$

where $\underline{c}$ is a p-dimensional vector and c is a one-dimensional constant. Using the fact that the original B_p is strongly regular by assumption, C_p^{-1} and C_{p-1}^{-1} exist, and therefore

$$C_p^{-1} = \begin{bmatrix} C_{p-1}^{-1} & -C_{p-1}^{-1}c^{-1}\underline{c} \\ \underline{0} & c^{-1} \end{bmatrix} \tag{70}$$

Hence,

$$\begin{aligned} R_pC_p^{-1} &= \begin{bmatrix} R_{p-1} & \underline{r} \\ \underline{r}^* & r_0 \end{bmatrix}\begin{bmatrix} C_{p-1}^{-1} & -C_{p-1}^{-1}\underline{c}c^{-1} \\ \underline{0} & c^{-1} \end{bmatrix} \\ &= \begin{bmatrix} R_{p-1}C_{p-1}^{-1} & -R_{p-1}C_{p-1}^{-1}\underline{c}c^{-1} + \underline{r}c^{-1} \\ \underline{r}^*C_{p-1}^{-1} & -\underline{r}^*C_{p-1}^{-1}\underline{c}c^{-1} + r_0c^{-1} \end{bmatrix} \end{aligned} \tag{71}$$

Therefore, with $\underline{x}$, x denoting *don't care* entries, we have

$$\begin{aligned} C_p^{-*}R_pC_p^{-1} &= \begin{bmatrix} C_{p-1}^{-*} & \underline{0} \\ \underline{x}^t & x \end{bmatrix}\begin{bmatrix} R_{p-1}C_{p-1}^{-1} & \underline{x} \\ \underline{x}^t & x \end{bmatrix} \\ &= \begin{bmatrix} C_{p-1}^{-*}R_{p-1}C_{p-1}^{-1} & \underline{x} \\ \underline{x}^t & x \end{bmatrix} \end{aligned} \tag{72}$$

■

Example:

The monotone behavior of $h_w(\lambda)$ and $h_c(\lambda)$ described above is illustrated in the following example generated from the 3-dimensional positive definite symmetric Toeplitz pencil (R_3, B_3). The matrices R and B are generated from their first rows

$$\text{Row}_1(R) = [5,3,1]$$
$$\text{Row}_1(B) = [4,1,-1]$$

The singular points of the two eigenvalue search functions are located at 0.66 and 1.60. The updated eigenvalues of the third-dimensional pencil are located at 0.561, 0.799, and 2.139. The functions $g_c(\lambda) = -h_c(\lambda)$ and $g_w(\lambda) = -h_w(\lambda)$ are plotted in Figure 7 on page 50. As expected, the two functions are monotone between their singular points, and the constant factor K is 3.33.

3.3.3 Generalized Eigenvalue Search Implementation

As shown above, the function $h(\lambda)$ is monotone between its singular points $\lambda_n^{(p-1)}$. Thus, quadratically convergent iterative techniques, similar to those presented for RITE, can be used. The restricted Newton algorithm presented in Chapter 2, equation (11), can be applied directly to the generalized problem. Recall that $h_c(\lambda) = Kh_w(\lambda)$, as shown in Section 3.3.2, where h_c and h_w are the search functions associated respectively with the pencil (R_p, B_p) and the matrix $C_p^{-*}R_pC_p^{-1}$, and $K = b_0 - \underline{b}^*B_{p-1}^{-1}\underline{b}$. Therefore, rational approximations similar to those presented for RITE can be used for C-RITE, and the properties presented in Appendix C and D still hold for the generalized eigenproblem.

Note that the restricted Newton technique, which was developed first, is used for the algorithm implementations because it appears to be more competitive for small size problems than the rational approximation based approach.

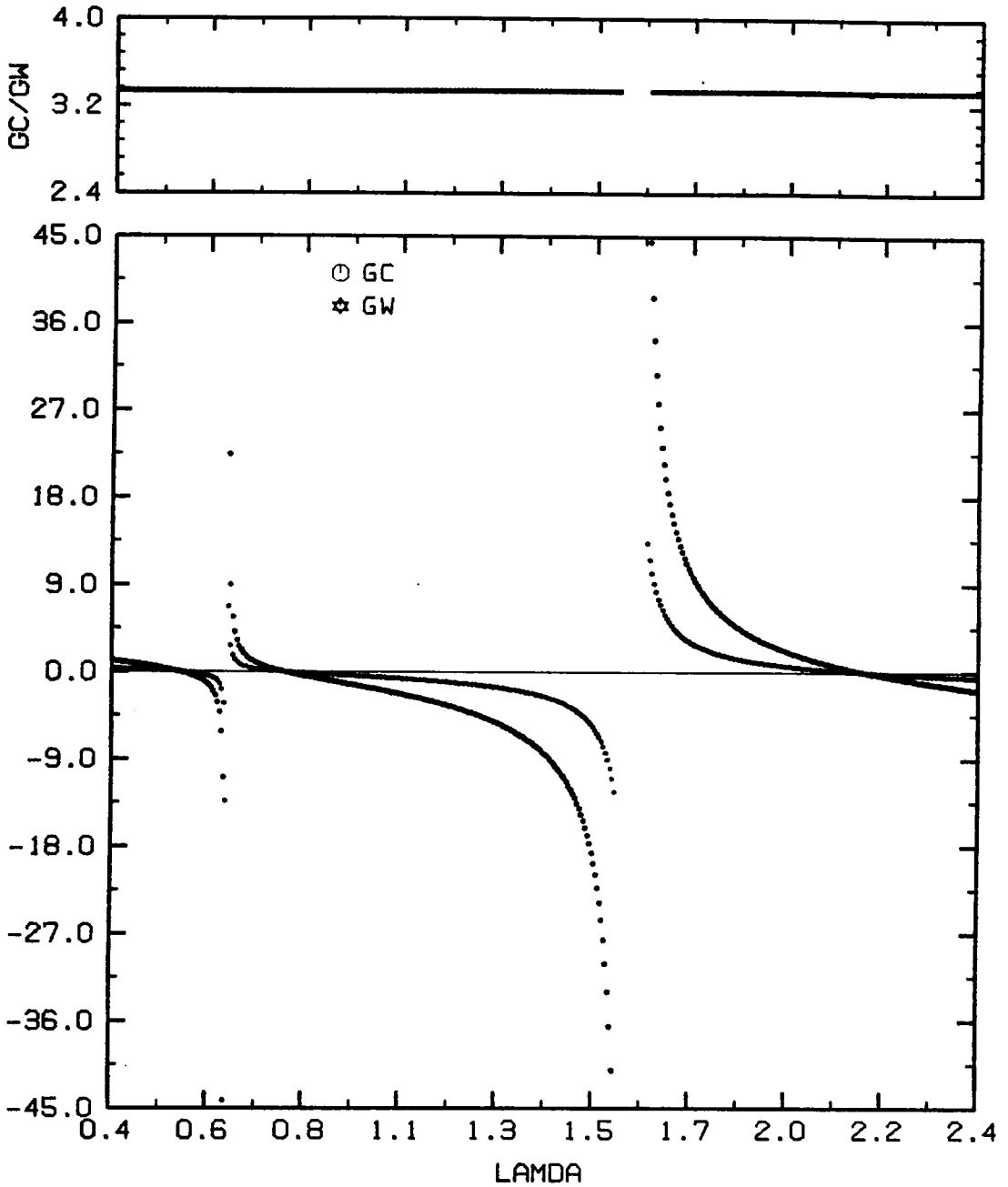

Figure 7. **Monotone behavior of the eigenvalue search functions h_c and h_w:** Symmetric Toeplitz positive definite pencil of dimension 3

3.4 The Eigenvector Problem

A procedure similar to that presented for the RITE derivation is followed to solve for the eigenvectors. The generalized eigenvectors associated with distinct generalized eigenvalues are computed using (40) and (41b) with the efficient Toeplitz solver. The multiple and/or clustered eigenvectors are then computed following a similar 2-step procedure as for RITE. Note that the changes in this new 2-step procedure, are the deflation technique used to identify the last eigenvector and the generalized version of the shifted inverse power (SIP) method.

Thus, the eigenvectors of dimension p associated with the set of k clustered eigenvalues are identified by the following procedure:

1. Build up the first k-1 vectors of the set by using the vectors of length p-1 defined for the clustered set of k-1 eigenvalues at the previous order and fix their first components to 0, i.e.

$$\hat{\underline{u}}_n^{(p)} = \begin{bmatrix} 0 \\ \underline{u}_{n-1}^{(p-1)} \end{bmatrix} \quad \text{for all } n = 2, \ldots, k \tag{73}$$

where $\underline{u}_{n-1}^{(p-1)}$ represents the $(n-1)^{st}$ generalized eigenvector of the (p-1)-dimensional pencil;

2. Compute the k^{th} generalized eigenvector $\hat{u}^{(p)}$ by orthogonalizing in the B-inner product[16] a fixed vector of unit length, chosen arbitrarily as $\underline{u} = [1,1, \ldots, 1]^t/p$, to the set of already known eigenvectors. (74)

Then, as for the RITE derivation, a single iteration of the generalized SIP method using the fast Toeplitz solver, with shift equal to the estimated generalized eigenvalue, is applied to the approximate eigenvectors $\hat{\underline{u}}_n^{(p)}$ to correct the original assumption of a single multiple eigenvalue.

---

[16] The B-inner product of vectors $\underline{x}$ and $\underline{y}$ is defined by: $\underline{x}^* B \underline{y}$

$$(R_p - \lambda_n^{(p)} B_p)\underline{u}_n^{(p)} = B_p \underline{\hat{u}}_n^p \quad \text{for all } n = 1, \ldots, k \tag{75}$$

A summary of the algorithm is given in Table 3 on page 56. The four threshold quantities, as defined earlier for the RITE implementation are used again. For the simulations presented, $\varepsilon_1 = 5.10^{-8}$, $\varepsilon_2 = 10^{-4}$, $\varepsilon_3 = 10^{-6}$, and $\varepsilon_4 = 10^{-3}$.

3.5 *Performance Measures*

Sensitivity of the recursive algorithm to potential accumulation errors and separation of the generalized eigenvalues is studied in the following. The performance of C-RITE compared with the IMSL (Version 9.2) subroutine -EIGZC- is presented in Figure 7 on page 50 to Figure 10 on page 59. The tests used generalized versions of the previous ones, and are defined as the Averaged Residual (Frobenius) NORM squared

$$\textbf{ARNORM} = \frac{1}{p} \| R_p U_p - B_p U_p \Lambda_p \|_F^2$$

and the Averaged ORTHOnormality (Frobenius) norm squared

$$\textbf{AORTHO} = \frac{1}{p} \| U_p^* B_p U_p - I_p \|_F^2$$

where p represents the dimension. The results represent the values obtained for 10 trial runs on different correlation matrices. The matrices R_p were built from the estimated correlation sequences generated by two sources of variable angle locations with different SNR in a colored noise environment. The real and imaginary parts of the colored noise sequences are respectively generated by AR(2) systems, and the real and imaginary noise part characteristics are given in terms of their pole locations. The noise correlation matrices are then estimated from these complex noise

sequences. A complete list of the parameters used to generate the correlation sequences can be found in Figure 8 on page 57, where Nest represents the number of snapshots used to estimate the correlation sequences. Figure 8 to Figure 11 show that the C-RITE and IMSL algorithms yield similar variations of the Averaged Residual NORM (ARNORM) and the Averaged ORTHOnormality norm (AORTHO). A higher sensitivity is apparent when the pencils to be solved are ill-conditioned, i.e. when the noise matrix B is close to singular. This situation may occur for example when a small number of snapshots is used to estimate the correlation sequences. However, these tests show that the algorithm performance is satisfactory for positive definite pencils of orders up to at least 30.

3.6 Recursive Eigendecomposition Timing Aspects

The computational load of RITE and C-RITE is divided into two different contributions, the eigenvalue and eigenvector identification steps respectively, and optimization of the speed of these algorithms can be obtained by refining the procedures used.

1. The (generalized) eigenvalue load:

   Recall that the (generalized) eigenvalue steps, for a given order, can be performed in parallel as they are independent of each other. The closed-form similarity of the search function $h(\lambda)$ and its derivative $h'(\lambda)$ can be used to decrease the computational requirement of each iteration step. In the white noise case, i.e. the RITE decomposition, the parameter β_n can be computed explicitly before the iterative search begins. Therefore the evaluation of the white noise eigenvalue search function and its first order derivative are of the order $O(p)$ per iteration for a matrix of order p. The generalized eigenvalue search function is more complex. The parameter β_n can no longer be computed before the iterations begin, and the

derivative is computationally more expensive. For each iteration, $O(p^2)$ flops are needed to compute the function or its derivative.

Recall that either the restricted Newton or the rational approximation method can be used to compute the updated eigenvalues. As mentioned earlier, the approximation method converges in fewer iterations to the updated eigenvalues, however its computational cost per step is higher. In addition to the evaluation of the eigenvalue search function and its derivative (which are the only computational requirements of the Newton step), the rational approximation requires computation of four additional coefficients and the closed form solution of a quadratic equation, the latter involving a square root computation. Therefore, considering the additional computational load required per step for the rational approximation, one can expect to have a crossover dimension n_c, below which the Newton scheme will be faster (i.e. the additional number of Newton steps will still end up being faster to compute) than the approximation based technique, while for larger dimensional problems the opposite will hold. Again, definite conclusions regarding the comparative speeds of these two possible iterative techniques are difficult to draw as they very much depend upon the type of hardware implementation chosen, a subject beyond the scope of this work.

2. The eigenvector computational load:

   The Zohar algorithm, presently used in the algorithm implementation, solves a Toeplitz system of order p in $O(p^2)$ time. Further optimization of this task could be obtained by implementing a Fast Toeplitz solver, such as the one presented by Kung and Hu [KU1] for instance, which requires only $O(p)$ time when using a linear array of $O(p)$ processors.

The RITE and C-RITE algorithms are well adapted for parallel implementations. A rough estimate of the number of operations needed in a parallel implementation of the recursive procedures, when using the restricted Newton search, is presented next. As mentioned earlier, the evaluation of the regular (white noise) eigenvalue search functions and its derivative are of the order $O(p)$ per Newton iteration for a matrix of order p. This leads to a total of $n_i O(n^2)$ operations for a parallel implementation of the search task, where n_i is the maximum number of Newton steps at a

given order. Due to parallelism, $O(n)$ processors are needed in this step. The evaluation of the generalized (colored noise) eigenvalue search function and its derivative are of the order $O(p^2)$ for a given p-dimensional problem. This leads to an order of $n_t O(n^3/6)$ flops for successive decompositions from order 3 to n, where n_t is the maximum number of steps.

Using the fast Toeplitz solver proposed by Kung and Hu [KU1], a parallel implementation of the eigenvector task can be performed in roughly $O(n^2)$. Thus, using $O(n^2)$ processors, a parallel implementation of the RITE procedure can be performed in roughly $O(n^2)$ time, where n represents the maximum dimension of the problem. Similarly a parallel implementation of the C-RITE procedure can be performed in roughly $O(n^3)$. Note that these are pessimistic estimates because no actual parallelism was taken into account in the computation of the eigenvalue search function, and further reduction in these time requirement estimates can be expected depending on the type of hardware chosen for the implementation.

Table 3. C-RITE algorithm implementation

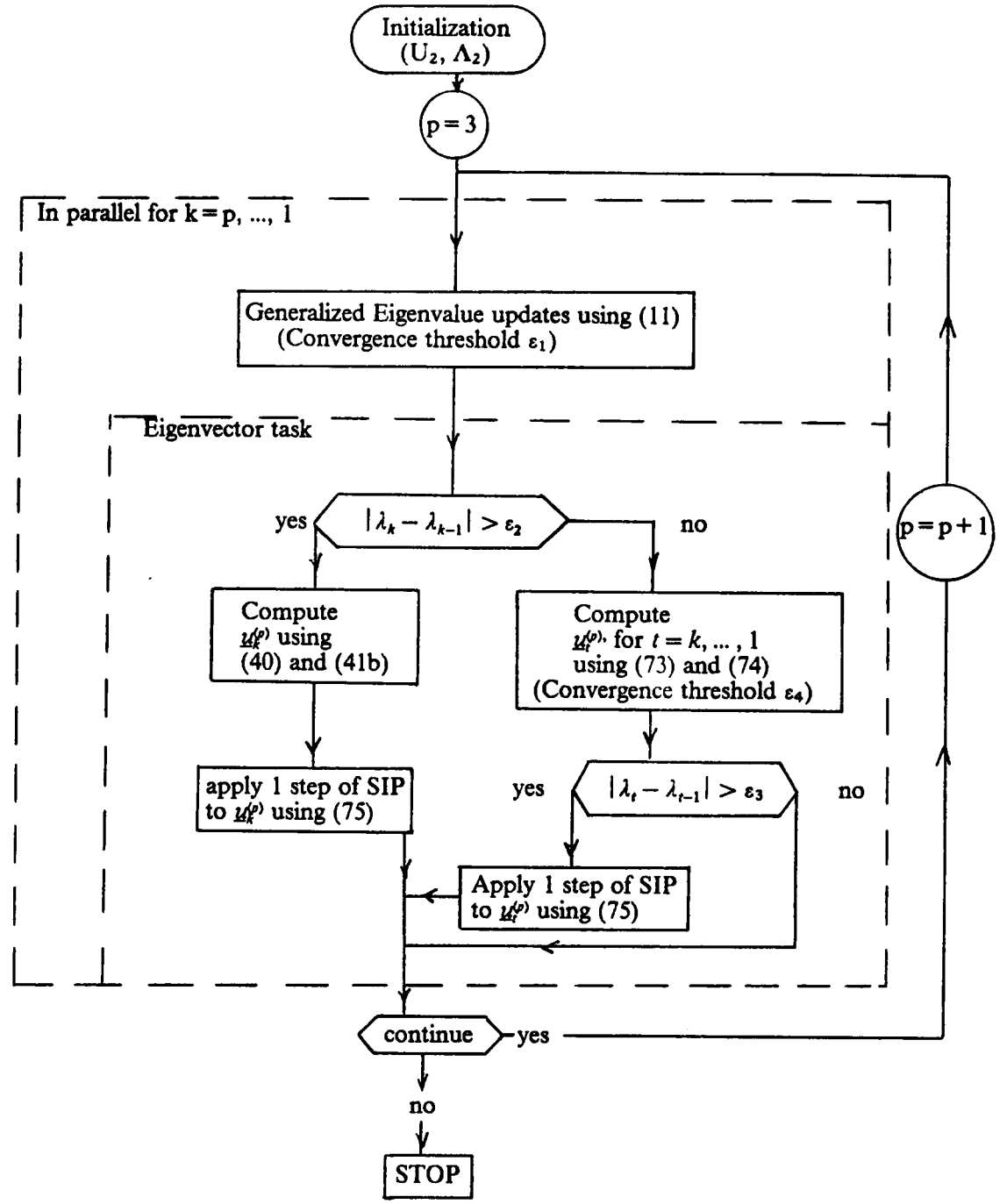

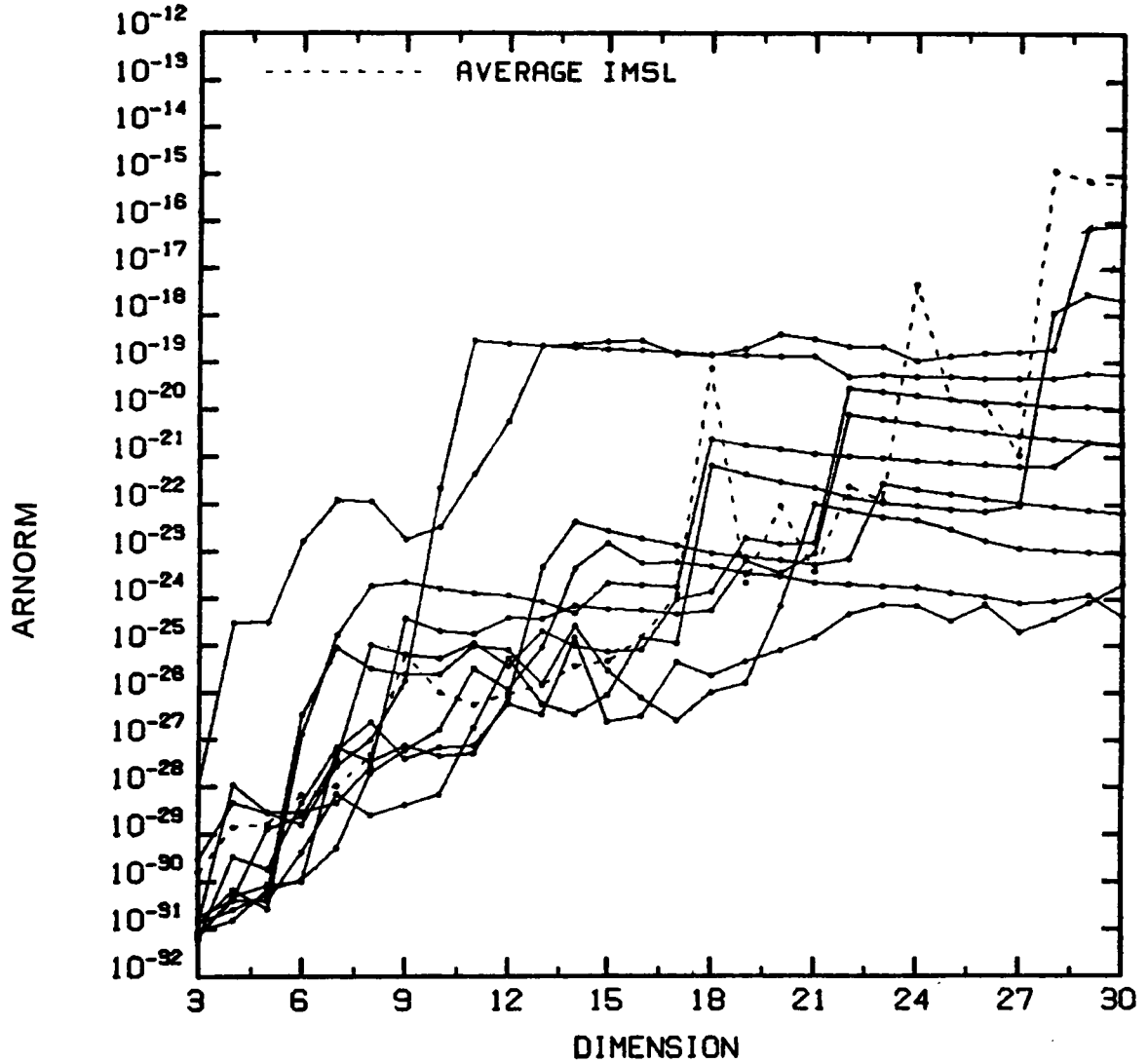

Trial Run Parameters										
θ_1 (Deg)	30	60	10	40	05	20	70	18	18	25
θ_2 (Deg)	50	65	50	50	30	40	75	24	60	50
SNR (dB)	00	00	-2	-10	-10	00	-2	02	00	-2
Nest	100	100	50	100	300	300	500	100	100	100
AR(2) Noise poles: (r,α°)										
Real	.7,45°	.7,0°	.8,70 °	.6,60°	.9,50°	.7,0°	.8,30°	.7,45°	.6,60°	.7,45°
Imaginary	.5,40°	.7,45°	.5,40°	.7,60°	.8,70°	.7,45°	.6,60°	.7,0°	.8,70°	.5,40°

Figure 8. Averaged residual norms squared for the C-RITE algorithm: 10 trial runs

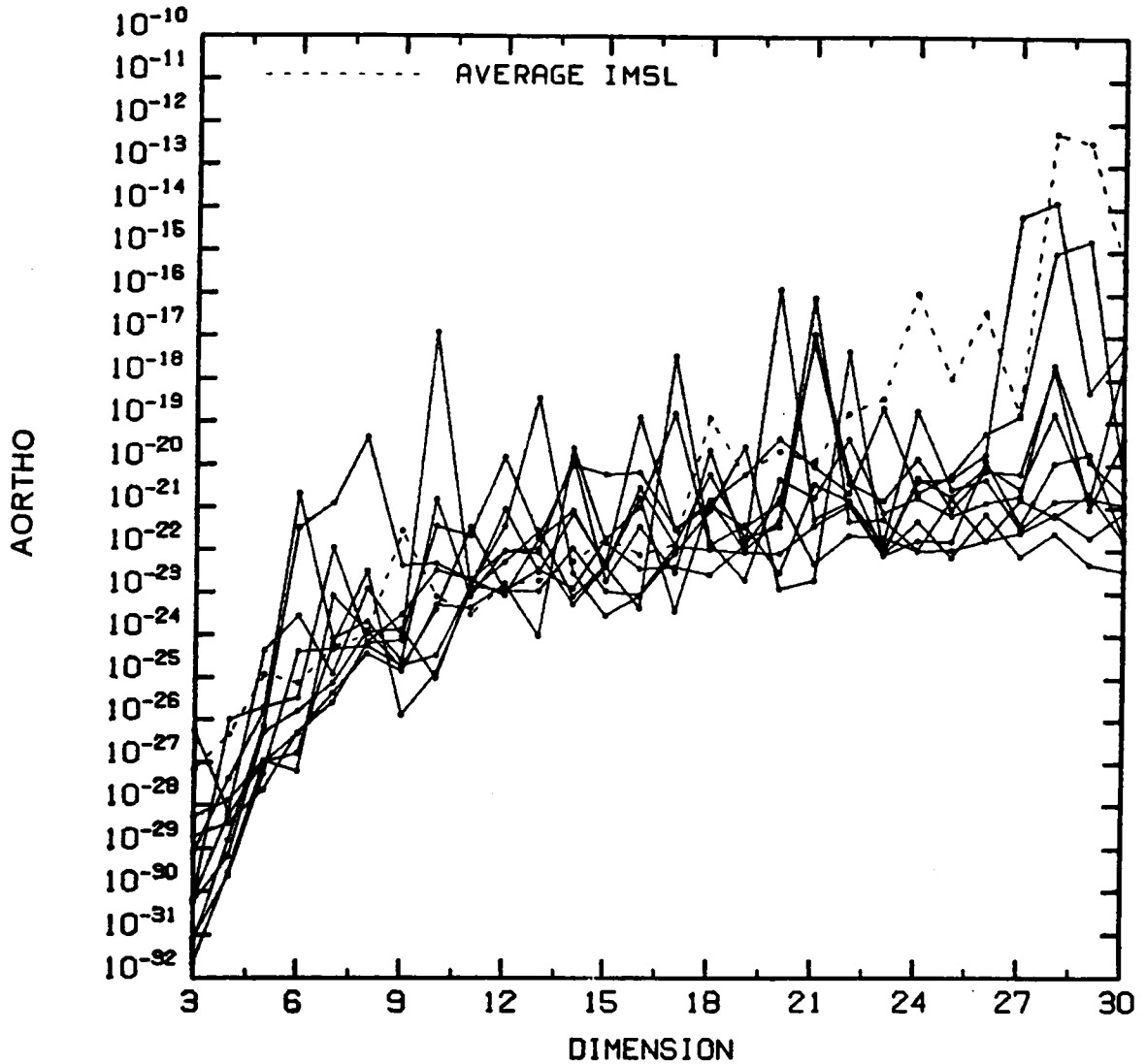

Figure 9. Averaged orthonormality norms squared for the C-RITE algorithm: 10 trial runs

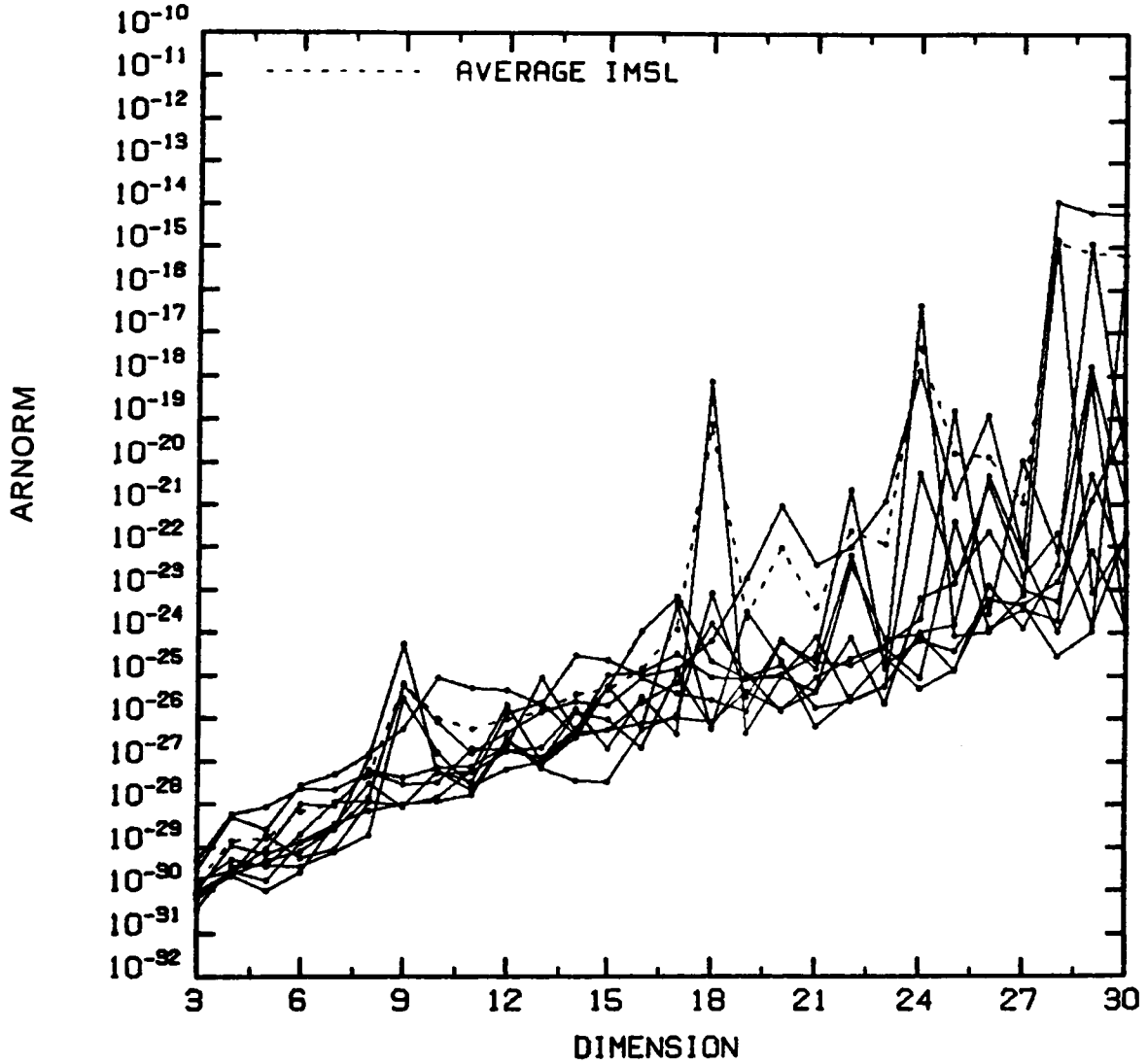

Figure 10. Averaged residual norms squared for the IMSL routine EIGZC: 10 trial runs

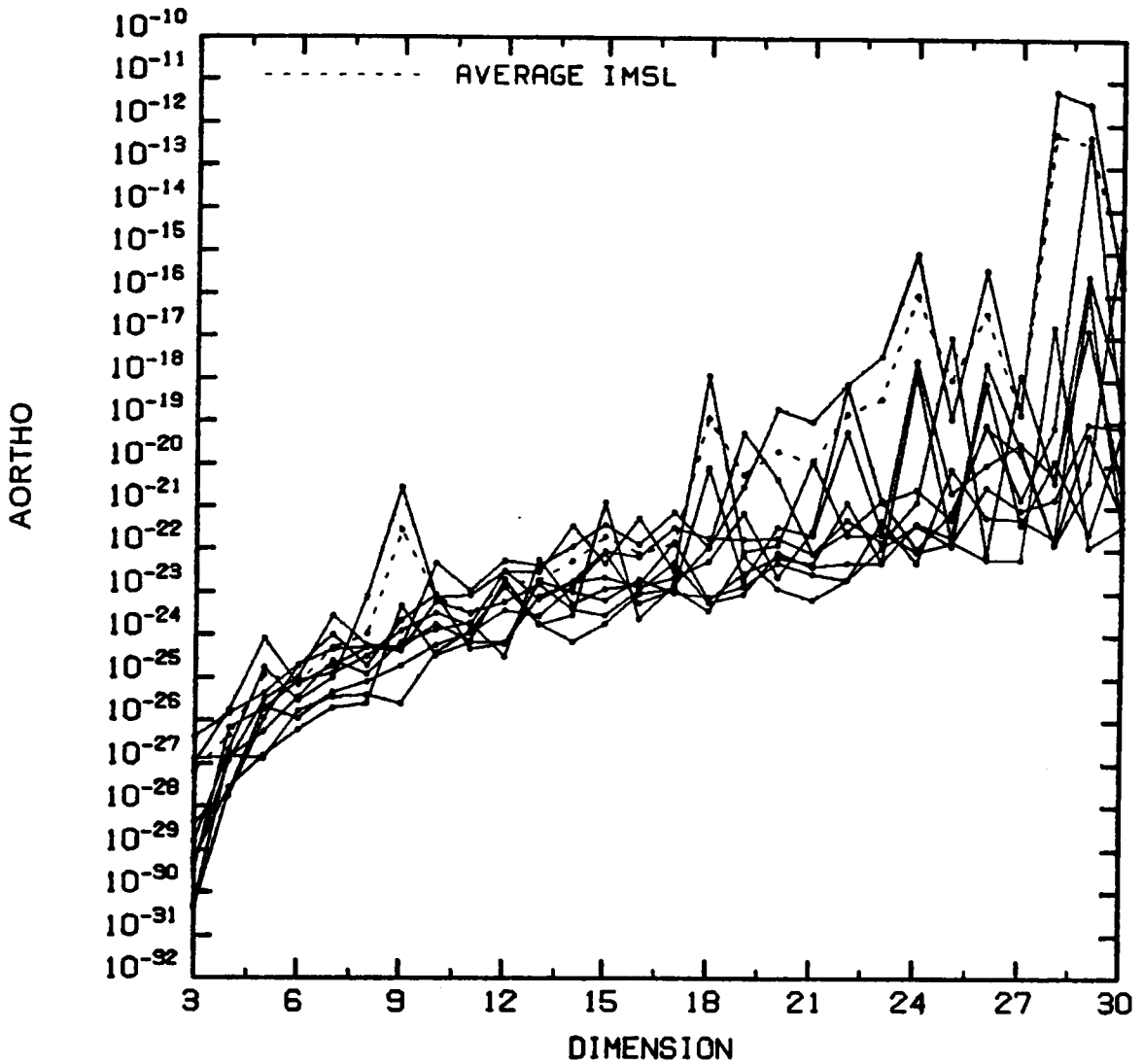

Figure 11. Averaged orthonormality norms squared for the IMSL routine EIGZC: 10 trial runs

4.0 Eigen-Techniques Applied to Passive Bearing Estimation

As mentioned in Chapter 1, numerous eigen-based techniques have been proposed in the literature. This chapter considers the application of the order recursive RITE and C-RITE procedures to the Direction Of Arrival (DOA) identification problem. A brief introduction to array processing is given next in Section 4.1. The application of eigenstructure methods to the DOA problem, in white and colored noise situations, is discussed in Section 4.2. Section 4.3 introduces the information criteria used to estimate the number of sources. Finally, Section 4.4 presents implementation results.

4.1 Introduction to Array Processing

Assume a linear equi-spaced array of sensors receiving narrowband signals. Under the assumption of nondispersive propagation, sensors without distortion, and envelope variations that

are slow relative to the carrier frequencies of the narrowband signals, the received signal from a passive array is

$$x_t = s_t + n_t \tag{76}$$

where s_t represents the narrowband signal, and n_t represents the noise. Consider a linear array of p sensor elements. The output at the q^{th} array element of the array, to m incoming sources arriving at angles θ_1 to θ_m is given by

$$y_{t,q} = \sum_{i=1}^{m} A_i \exp\left[j\left[\omega_c t - \frac{2\pi(q-1)d\sin(\theta_i)}{\Omega} + \psi_i \right] \right] + n_{t,q} \quad \text{for} \quad 1 \le q \le p \tag{77}$$

where θ_i represents the i^{th} signal arrival angle, ω_c represents the center frequency of the spatial sources, d is the array element spacing, A_i is the amplitude of each incoming signal, Ω is the wave-length, ψ_i represents the random phase of each incoming signal, assumed to be uniformly distributed over $[0, 2\pi]$, and $n_{q,t}$ is a zero mean random variable that represents the measurement noise.

Therefore, using a vector notation for (77), the output vector at time t can be expressed by the p-dimensional column vector

$$\underline{x}_t = [y_{t,1}, \cdots, y_{t,p}]^t \tag{78}$$

Let us define the mode vector $\underline{m}_\theta$ as follows

$$\underline{m}_\theta = [1, \exp(-2\pi j d \sin(\theta)/\Omega), \ldots, \exp(-2\pi j(p-1)\sin(\theta)/\Omega)]^t \tag{79}$$

and the noise vector as

$$\underline{n}_t = [n_{t,1}, \cdots, n_{t,p}]^t \tag{80}$$

Therefore, the received signal vector can be expressed as

$$\underline{x}_t = \sum_{l=1}^{m} A_l \exp[j[\omega_c t + \psi_l]] \cdot \begin{bmatrix} 1 \\ \exp(-2\pi j d \sin(\theta_l)/\Omega) \\ \cdot \\ \cdot \\ \exp(-2\pi j d(p-1)\sin(\theta_l)/\Omega) \end{bmatrix} + \underline{n}_t \tag{81}$$

For normalized angles defined as $z_i = d\sin(\theta_i)/\Omega$, (81) can be simplified and becomes:

$$\underline{x}_t = \sum_{l=1}^{m} A_l \exp[j[\omega_c t + \psi_l]] \cdot \begin{bmatrix} 1 \\ \exp(-2\pi j z_i) \\ \cdot \\ \cdot \\ \exp(-2\pi j(p-1)z_i) \end{bmatrix} + \underline{n}_t \tag{82}$$

Under the assumption that the signals and the zero mean noise are uncorrelated, and the noise is uncorrelated with the random phase shifts, the p-dimensional spatial correlation of the measured sensor signals takes on the form of the matrix equation

$$\begin{aligned} R_x &= \mathbf{E}\{\underline{x}_t \underline{x}_t^*\} \\ &= M R_s M^* + \sigma^2 B \end{aligned} \tag{83}$$

where R_s and $\sigma^2 B$ are respectively the signal and noise correlation matrices with σ^2 a normalization constant such that $\mathrm{tr}(B) = \mathrm{p}$; p being the dimension of the matrices under study. M has a Vandermonde structure and its column vectors are the mode vectors $\underline{m}_\theta$.

$$\begin{aligned} M &= [\, \underline{m}_{\theta 1} \mid \ldots \mid \underline{m}_{\theta m} \,] \\ &= \left[\begin{array}{c|c|c} 1 & & 1 \\ \exp(-2\pi j z_1) & \cdots & \exp(-2\pi j z_m) \\ \cdot & & \cdot \\ \cdot & & \cdot \\ \exp(-2\pi j(p-1)z_1) & & \exp(-2\pi j(p-1)z_m) \end{array}\right] \end{aligned} \tag{84}$$

The sources are assumed to be uncorrelated, so that the signal covariance matrix is given by

$$R_s = \mathbf{E}\{\underline{s}_t \underline{s}_t^*\} \tag{85}$$

where the narrowband vector signal $\underline{s}_t$ is defined as

$$\underline{s}_t = [s_{t,1}, \ldots, s_{t,m}]^t \tag{86}$$

with $s_{t,i}$ representing the i^{th} narrowband signal at time t. Therefore from (85)

$$R_S = \mathbf{E}\begin{bmatrix} s_{t,1} \\ \cdot \\ \cdot \\ s_{t,m} \end{bmatrix} \begin{bmatrix} s^*_{t,1} & \ldots & s^*_{t,m} \end{bmatrix} \tag{87}$$

$$= \mathrm{DIAG}(P_1, \ldots, P_m)$$

where DIAG(.) represents the diagonal matrix with diagonal elements as listed, and $P_i = A_i^2$ represents the power associated with each signal.

4.2 *Geometric Solution*

Projections of the mode vectors onto the signal and/or noise subspaces are used to identify the DOA parameters. Let us show how subspace projections lead to the determination of the DOA parameters. R_s has rank m equal to the number of incoming signals, B and M have each dimension p. From (83), we get

$$MR_sM^* = R_x - \sigma^2 B \tag{88}$$

Using the fact that MR_sM^* is non-negative definite (i.e., with non-negative eigenvalues only), and that it has less than full rank, then:

$$\lambda_i(MR_sM^*) = 0 \quad \text{for } i = 1, \ldots, p-m \tag{89}$$

Therefore,

$$|MR_sM^*| = |R_x - \sigma^2 B| = 0 \tag{90}$$

Since we restrict B to be positive definite, a full rank Choleski factorization can be used to express the matrix as

$$B = C^*C \tag{91}$$

Then, (90) becomes

$$|MR_sM^*| = |C^{-*}R_xC^{-1} - \sigma^2 I|\,|B| \tag{92}$$

Therefore,

$$\lambda(MR_sM^*) = \lambda(C^{-*}R_xC^{-1}) = \lambda(R_x,B) \tag{93}$$

Using the fact that MR_sM^* has rank m, the number of signals, we infer from (90) that $\lambda_{\min}(C^{-*}R_xC^{-1})$, i.e. $\lambda_{\min}(R_x,B)$, has multiplicity $q = p - m$. This yields

$$\lambda_{\min}(R_x,B) = \sigma^2 \quad \text{for } i = 1, \ldots, p-m \tag{94}$$

In general, from (88),

$$MR_sM^*\underline{u}_i^{(p)} = (R_x - \sigma^2 B)\underline{u}_i^{(p)} \text{ for all } i = 1, \ldots, p \tag{95}$$

Note that for the minimum generalized eigenvalue of the pencil (R_x,B), with $\underline{u}^{(p)}$ a corresponding eigenvector

$$R_x\underline{u}_i^{(p)} = \sigma^2 B\underline{u}_i^{(p)} \quad \text{for all } i = 1, \ldots, p-m \tag{96}$$

So that

$$MR_sM^*\underline{u}_i^{(p)} = \underline{0} \quad \text{for all } i = 1, \ldots, p-m \tag{97}$$

Hence, the generalized eigenvectors $\underline{u}_i^{(p)}$ for $i = 1, \ldots, p-m$ associated with the smallest generalized eigenvalue $\lambda_{\min}$ are orthonormal to the m mode vectors $\underline{m}_{\theta,i}$. The eigenvectors associated with the smallest eigenvalue span the $(p-m)$ dimensional *noise subspace* U_N, while the remaining p eigenvectors span the *signal subspace* U_S. These subspaces are B-orthonormal [PAR]. Projections onto the noise or signal subspaces can be used to recover the DOA information, as shown next.

4.2.1 Noise Subspace Projection

The DOA parameters can theoretically be found by finding the mode vectors which satisfy the property in (97). For estimated correlation matrices, (97) is not realized exactly. In such cases, the DOA parameters can be identified by mode vectors which minimize the projection of the mode vector $\underline{m}_\theta$ onto the noise subspace U_N:

$$\mathrm{MIN}_\theta(\underline{m}_\theta^* U_N U_N^* \underline{m}_\theta) \tag{98}$$

Equivalently

$$\mathrm{MIN}_\theta\left(\sum_{i=1}^{p-m} |\underline{m}_\theta^* \underline{u}_i^{(p)}|^2\right) \tag{99}$$

4.2.2 Signal Subspace Projection

When the noise is white, the eigenproblem reduces to a regular eigen-decomposition and the eigenvectors form an orthonormal basis. In such a case, minimization of mode vector projections onto the noise subspace is equivalent to maximizing the mode vector projections onto the signal

subspace. The latter method has poor resolution however, as a small change in direction hardly affects the shadow or projection. Much better resolution is obtained when looking at the norm minimization of the difference between the mode vector and its projection onto U_S:

$$\mathbf{MIN}_{\theta}\left(|\underline{m}_{\theta} - U_S(U_S^{*}\underline{m}_{\theta})|^2\right) \tag{100}$$

Equivalently

$$\mathbf{MIN}_{\theta}\left(|\underline{m}_{\theta}|^2 - \sum_{i=p-m+1}^{p} |\underline{m}_{\theta}^{*}\underline{u}_i^{(p)}|^2\right) \tag{101}$$

The above minimization procedure theoretically leads to the same result as that obtained with the earlier noise subspace projection.

When the noise is colored, the eigenvectors $\underline{u}_i$ are no longer orthonormal in the Euclidian norm. Instead, they are orthonormal using the generalized B-inner product (i.e. $U^{*}BU = I$). Signal projection expressions, similar to those using the noise subspace are derived next. The idea is to use the relationship between the pencil $(R,C^{*}C)$ and the matrix $C^{-*}RC^{-1}$ to derive the signal subspace projections. First recall that the B-normalized generalized eigenvector matrix U of the pencil $(R,C^{*}C)$ and the orthogonal eigenvector matrix V of $C^{-*}RC^{-1}$ are closely related, as shown in Appendix B:

$$V = CU \tag{102}$$

From (83) we have

$$\begin{aligned} R_x &= MR_sM^{*} + \sigma^2 B \\ &= MR_sM^{*} + \sigma^2 C^{*}C \end{aligned} \tag{103}$$

Using the fact that B is strongly regular, pre- and post- multiplying (103) by respectively C^{-*} and C^{-1} leads to:

$$\begin{aligned} C^{-*}R_xC^{-1} &= C^{-*}MR_sMC^{-1} + \sigma^2 I \\ &= \tilde{M}R_s\tilde{M}^* + \sigma^2 I \end{aligned} \tag{104}$$

where

$$\tilde{M} \triangleq C^{-*}M \tag{105}$$

Note that $S \triangleq C^{-*}R_xC^{-1}$ can be viewed as the matrix obtained after prewhitening of the received signal [BIE]. From (104), we have

$$\tilde{M}R_s\tilde{M}^* = C^{-*}R_xC^{-1} - \sigma^2 I \tag{106}$$

Using the fact that R_s has rank m, equal to the number of incoming signals, (106) yields:

$$\lambda_i(\tilde{M}R_s\tilde{M}^*) = 0 \quad \text{for all } i = 1, \ldots, p-m \tag{107}$$

and reasoning as before

$$\lambda_i(C^{-*}R_xC^{-1}) = \sigma^2 \quad \text{for all } i = 1, \ldots, p-m \tag{108}$$

Therefore, for the minimum eigenpair of S, we have:

$$(C^{-*}R_xC^{-1} - \sigma^2 I)\underline{v}_i^{(p)} = \tilde{M}R_s\tilde{M}^*\underline{v}_i^{(p)} = \underline{0} \quad \text{for all } i = 1, \ldots, p-m \tag{109}$$

so that

$$\tilde{M}^*\underline{v}_i^{(p)} = \underline{0} \text{ for all } i = 1, \ldots, p-m \tag{110}$$

Using a matrix form, (110) becomes

$$\tilde{M}^* V_N = O \tag{111}$$

where $V_N = \text{span}\{\underline{v}_1^{(p)}, \ldots, \underline{v}_{p-m}^{(p)}\}$ is the noise subspace associated with $C^{-*}RC^{-1}$. As mentioned earlier, for estimated correlation matrices (111) is not realized exactly, and the DOA parameters are identified by the mode vectors $\tilde{\underline{m}}_\theta$ which have minimal projection onto the noise subspace. Alternatively, we may again maximize the projection of the mode vector $\tilde{\underline{m}}_\theta$ onto the signal subspace (since $\underline{v}_i$ are I-orthonormal for all $i = 1, \ldots, p$). Consequently, this leads to expressions similar to those given in (99) and (101), where the mode vectors $\underline{m}_\theta$ are replaced by the transformed mode vectors $\tilde{\underline{m}}_\theta$ and the $\underline{u}_i^{(p)}$ are replaced by $\underline{v}_i^{(p)}$. Hence, the following minimization expressions are appropriate to recover the DOA parameters:

$$\text{MIN}_\theta\left(\sum_{i=1}^{p-m} |\tilde{\underline{m}}^* \underline{v}_i^{(p)}|^2\right) \tag{112}$$

and

$$\text{MIN}_\theta\left(|\tilde{\underline{m}}_\theta|^2 - \sum_{i=p-m}^{p} |\tilde{\underline{m}}_\theta^* \underline{v}_i^{(p)}|^2\right) \tag{113}$$

Substituting for $\tilde{\underline{m}}_\theta$ from (105), and for $\underline{v}$ from (102),

$$\text{MIN}_\theta\left(\sum_{i=1}^{p-m} |\underline{m}_\theta^* \underline{u}_i^{(p)}|^2\right) \tag{114}$$

and

$$\text{MIN}_\theta\left(\underline{m}_\theta^* B^{-1} \underline{m}_\theta - \sum_{i=p-m+1}^{p} |\underline{m}_\theta^* \underline{u}_i^{(p)}|^2\right) \tag{115}$$

Equation (115) shows that inverting the matrix B appears to be necessary to obtain good resolution in the DOA parameter identification process using signal subspace projections. This matrix inverse operation complicates the algorithmic procedure without bringing any new

information, as this information is already available by using the noise subspace projection. Furthermore, matrix inversion may potentially lead to numerical difficulties and is best avoided, when possible. Therefore, the results for the colored noise case use projections onto the estimated noise subspace only.

4.2.3 Fast Numerical Implementation

The specific linear sensor array assumptions yield a structure of the mode vector that can be used to efficiently evaluate the inner products contained in equations (99), (101) or (114). Note from (84), that the inner products can be written in the following form

$$\begin{aligned} \underline{u}_i^{(p)*}\underline{m}_\theta &= \sum_{n=1}^{p} u_{i,n}^{(p)*} e^{-jz_\theta(n-1)} \\ &= e^{jz_\theta}\sum_{n=1}^{p} u_{i,n}^{(p)*} e^{-jz_\theta n} \end{aligned} \tag{116}$$

The sum can be evaluated at all normalized angles $z_\theta = 2\pi i/N$ with the following Discrete Fourier Transform $\mathrm{DFT}_N\{u_{i,1}^{(p)}, \ldots, u_{i,p}^{(p)}, 0, \ldots, 0\}$, where p is the dimension of the problem, N is the FFT length chosen by the user, and $u_{i,k}^{(p)}$ represents the k^{th} component of the p-dimensional i^{th} eigenvector $\underline{u}_i^{(p)}$. Efficient FFT or Chirp Z-Transform algorithms can then be used, and the accuracy in resolving the maxima and/or minima of the projections onto the desired subspaces depends on the amount of zero padding (N-p).

4.3 *Estimation of the Number of Sources*

Theoretically, the number of incoming sources can be determined from the multiplicity of the smallest eigenvalue of the correlation matrix. In practice we do not have a smallest eigenvalue with high multiplicity but instead a set of clustered eigenvalues. Furthermore, for low SNRs these eigenvalues may be spread, and deciding on the multiplicity associated with the noise eigenvalues may become difficult. The technique introduced by Wax and Kailath [WAK] is based on applications of the information theoretic criteria for model selection introduced independently by Rissanen [RI1,RI2] and Schwartz [SWZ], and the Akaike Information Criterion (AIC) introduced by Akaike [AIK].

These criteria study the following problem:

Given a set of N observations X and a family of models, select the model that best fits the data.

The approach by Akaike leads to the selection of the model giving the minimum value of the criterion function defined as

$$\mathrm{AIC} = -2\log f(\mathrm{X}/\hat{\theta}) + 2k \tag{117}$$

where $\hat{\theta}$ is the maximum likelihood estimate of θ , $f(\mathrm{X}/\theta)$ a family of probability densities associated with the data, and k the number of free parameters in θ. The procedures by Schwartz and Rissanen are different. Schwartz assumes that each model can be assigned an a-priori probability, and his approach selects the model which gives the maximum a-posteriori probability. The method by Rissanen looks for the model that uses the minimum code length to model the data. However, the techniques by Schwartz and Rissanen techniques give the same asymptotical criterion defined by

$$\mathrm{MDL} = -\log f(\mathrm{X}/\hat{\theta}) + \frac{1}{2}k\log N \tag{118}$$

For the DOA problem, Wax and Kailath have redefined the estimation problem as a model identification problem. Using the model covariance matrix given by

$$R = \Psi + \sigma^2 I \tag{119}$$

where R, Ψ, I are p-dimensional matrices. The matrix $\Psi = ASA^*$, where S denotes the covariance matrix of the signal and A is the matrix defined from the parameter vectors associated with the signals. The following family of covariance matrices is then introduced

$$R^{(k)} = \Psi^{(k)} + \sigma^2 I \tag{120}$$

where $\Psi^{(k)}$ denotes a semi-positive definite matrix of rank k in the set $\{1, \ldots, p-1\}$ and σ is unknown. Note that k ranges over the set of the possible number of signals detectable for a p-dimensional matrix. The problem is reduced then to finding out for which k the model in (120) fits the data best. Eigenspace decomposition of the correlation matrix and the concept of maximum likelihood estimation are used to derive the criteria. The number of signals is then obtained by the value of k for which a criterion function is minimized. The form of the AIC applied to the DOA problem is:

$$\mathrm{AIC}(k) = -2\log\left[\frac{\prod_{i=k+1}^{p} \lambda_i^{1/(p-k)}}{\frac{1}{(p-k)}\sum_{i=k+1}^{p} \lambda_i}\right]^{(p-k)N} + 2k(2p-k) \tag{121}$$

The form of the MDL applied to the DOA problem is:

$$\mathrm{MDL}(k) = -\log\left[\frac{\prod_{i=k+1}^{p} \lambda_i^{1/(p-k)}}{\frac{1}{(p-k)}\sum_{i=k+1}^{p} \lambda_i}\right]^{(p-k)N} + \frac{1}{2}k(2p-k)\log(N) \tag{122}$$

where λ_i are the eigenvalues of the correlation matrix, N is the number of snapshots used to compute the sample-covariance matrix and, p is the dimension of R.

The performance of the above criteria depends on the quality of the correlation estimates [WAK]; overestimation or underestimation of the correct number of sources may occur when the

sample correlation matrix is estimated from a small number of snapshots. Note that the AIC and MDL criteria are derived for the DOA problem in white noise, i.e. for a regular eigenproblem. The colored noise case, with known colored noise sequence, can be solved by using the generalized eigenproblem (R,B), or by prewhitening the data and solving the regular eigenproblem $C^{-*}RC^{-1}$, with $B = C^*C$. Recall however that the eigenvalue distribution associated with the pencil (R,B) is identical to that of the matrix $C^{-*}RC^{-1}$. Therefore, the order criteria can still be used for the colored noise case solved as a generalized eigenproblem.

4.4 *DOA Implementation Results*

As stated in Chapter 2, the performance of eigen-based techniques for the DOA estimation problem depends upon the quality of the received signal and noise correlation sequence estimates. Theoretically, the eigenspace information contained in the m-dimensional correlation matrix, where m is the number of incoming signals, would be sufficient to recover the DOA information. However, in the estimated correlation case and in the presence of noise, the information contained in the correlation is incomplete and higher dimensional eigenspace decompositions are needed to recover the DOA information. The recursive RITE and C-RITE algorithms compute the decomposition of successive subproblems of increasing dimension imbedded in the original problem and this information can then be used for the DOA problem, as indicated in Table 4 on page 79. The following examples first illustrate the RITE algorithm operating in a white noise environment and the application of the MDL and AIC order determination criteria. Next, applications of the C-RITE algorithm to signals in colored noise are presented. Problems of bias and loss in resolution due to incorrect estimation of the sequences[17] are considered afterwards. *Recall that the novelty of these procedures resides in the recursive nature of the eigen-decomposition techniques and not in their*

[17] i.e. correlations estimated with too few snapshots and incorrect colored noise structure assumption.

specific utilization afterwards. They could be applied to different problems which require successive decompositions of strongly regular Toeplitz Hermitian pencils or Toeplitz Hermitian matrices in increasing order. For the DOA identification problem studied, simple projections of the mode vector onto noise and/or signal subspaces, as proposed initially for the **MUSIC** algorithm [SCH], are used. No approximations are made to derive the procedure, and as seen in Chapters 2 and 3, the propagation errors do not accumulate fast enough to deteriorate the performance of the algorithms. *Therefore, one may expect similar performance ranges as those obtained with the classical MUSIC algorithm.* Numerous other applications, as mentioned earlier in Chapter 2, of eigen-decompositions have been conducted to study the DOA problem. A MUSIC-type algorithm was chosen because it has been studied extensively and provides good performance. Numerous performance analyses can be found in the literature [SPK,SIB,JOM,KAB].

Correlation Sequence Generation

The **true correlation sequences** are generated according to the expressions given earlier in Section 4.1.

$$R_x = MR_sM^* + \sigma^2 B$$

where $R_s = \text{DIAG}(P_1, \ldots, P_m)$ and $M = [\, \underline{m}_{\theta_1} \mid \ldots \mid \underline{m}_{\theta_m} \,]$, with P_i defined as the power in an incoming source.

The **estimated correlation sequences** are generated by:

$$R_n = \frac{1}{nest} \sum_{k=1}^{nest} \underline{x}_k \underline{x}_k^*$$

where the measured vector is expressed as in (81)

$$x_t = \sum_{i=1}^{m} A_i \exp[j[\omega_c t + \psi_i]] \cdot \begin{bmatrix} 1 \\ \exp(-2\pi j z_i) \\ . \\ . \\ \exp(-2\pi j(p-1)z_i) \end{bmatrix} + n_t \qquad (123)$$

where

A_i is the amplitude of each incomimg signal,

ω_c is the center frequency of the spatial sources,

Ψ_i is the random phase of each incoming signal uniformly distributed over $[0, 2\pi]$,

z_i represents the normalized angle chosen between $[0, 2\pi]$,

n_t is the noise vector. The complex white noise vector is generated using the IMSL (version 9.2) routine GGNML. The complex colored noise sequence is generated by passing both real and imaginary components of the complex white noise sequence through different ARMA(p,q) type systems.

4.4.1 Simulation Results - White Noise Case

The following two examples are generated using two interference sources in white noise located at the normalized angles 30° and 39°, impinging on a linear array of 10 sensors. The temporal frequency is 3.5Hz and the phase variance 3 radians. The Signal-to-Noise Ratio (SNR) defined as $10\log_{10}(\frac{A^2}{2\sigma^2})$ is 20dB for each source in the first example, and 5dB in the second example. The following illustrates the use of the eigenvalue spread of the matrix and the information criteria for the estimation of the number of sources. Recall that theoretically, the number of sources can be found by examining the eigenvalue spread of the problem; the *signal* eigenvalues are large and distinct while the *noise* eigenvalues are smaller and clustered. Table 5 on page 80 and Table 6 on page 81 present the values of the information criteria and the eigenvalue spreads obtained for successive eigendecompositions from order 3 to 10 for example 1 (SNR = 20dB). Table 6 shows

a clear separation between the *signal* eigenvalue set (which has two components) and the *noise* eigenvalues. Thus, the number of sources can be found for subproblems of order 4 and higher. Note that the information criteria, shown in Table 5, yield correct and marked minima for subproblems of order 4 and higher. Next, Table 7 on page 81 and Table 8 on page 82 represent the eigenvalue spreads and values of the information criteria obtained for successive eigendecompositions from order 3 to 10 when the incoming sources have a SNR = 5dB. Using Table 7, we see that the gradual decrease in eigenvalues makes it more difficult to identify the correct number of incoming sources. However, the information criteria, given in Table 8, lead to correct identification of the number of sources for subproblems of order 8 and higher. Once the number of sources is estimated, the MUSIC algorithm is used to recover the DOA angles. The projections of the mode vector onto successive signal subspaces for increasing subproblems, as indicated in equation (101), are illustrated in Figure 12 on page 83 and Figure 13 on page 84 for examples 1 and 2 (the inverse of the argument of (101) is plotted). 1024 point FFT's are used, resulting in an angle resolution of .35°. Figure 12 shows that correct DOA angle identification is obtained from order 5 and higher (i.e. correct peak locations are obtained from order 5 and higher, as indicated in Figure 12). Thus, the algorithm could be stopped at order 5, long before the eigen-decomposition at the maximum order, thereby reducing the overall computational load of the procedure. Higher dimensional eigendecompositions are needed as expected from the remarks made for Table 7 and Table 8, for example 2 (when the sources have a SNR equal to 5dB); a correct identification is not obtained for subproblems of order 7 or less (see Figure 13). Note that the bias of the estimated angles decreases when using higher dimensional eigen-information; this is due to the fact that the information contained in the estimated correlation is incomplete, and higher dimensional subspace decomposition may be needed to compensate.

4.4.2 Simulation Results - Colored Noise Case

The examples are generated using either one or two closely spaced interference sources impinging on a linear array of 10 sensors. The known noise correlation matrix is either estimated for the estimated correlation case, or it is derived using true correlation information for the exact correlation case. For the estimated case, the noise correlation matrix is given as

$$B_p = \frac{1}{nest} \sum_{k=1}^{nest} \underline{n}_k \underline{n}_k^* \tag{124}$$

For the true correlation situation, the noise correlation matrix becomes

$$B_p = (R_r + R_i) + j(R_{r,i} - R_{i,r}) \tag{125}$$

where R_i and R_r represent the autocorrelation of the real and imaginary noises, while $R_{r,i}$ and $R_{i,r}$ represent the cross-correlation sequences. True autocorrelation and cross-correlation sequences are generated by using the method presented by Beex [BX2]. In the following, the noise structure is that of a complex AR(2) type with poles for the real part located at (.7, $\pm$ 45°) and for the imaginary part with double poles at (.7,0°). The use of 1024 point FFT's results in a DOA quantization interval of 0.35°. The n-dimensional noise matrix B is normalized such that tr(B) = n, this implies that the noise variance is taken equal to 1. The Signal-to-Noise (SNR) ratio is then defined as

$$SNR = 10\log\left(\frac{A_i^2}{2}\right)$$

where A_i is the signal (interference) amplitude.

The first example is generated using two closely spaced interference sources impinging on the array at the normalized angles of 18° and 24°. The Signal to Noise Ratio (SNR) is 12dB for each source and 600 snapshots are used to compute the correlation sequence estimates. Correct identification of the DOA angles is obtained for correlation matrices of order 5 by using the noise

subspace, as shown in Figure 14 on page 85. Note that the increase in order needed to identify the DOA angles is due to the quality of the estimated received signal and noise correlation estimates. Correct identification of the angles can be obtained for a pencil of order 3 when true noise and received signal correlation sequences are used, as shown in the same figure.

Figure 15 on page 86 and Figure 16 on page 87 show the bias in the identified angle due to incorrect noise estimation. This example has one incoming signal located at 40°. The SNR is 4dB and 600 snapshots are used for the estimated correlation case. The noise structure is first assumed to be white, and successive eigen-decompositions for matrices of order 3 to 9 are computed and used for the DOA identification procedure. The results obtained are labelled: IN-dim 3 to IN-dim 9 (Incorrect Noise (IN) dimension 3 to IN dimension 9). However, early and unbiased estimation of the DOA angle is obtained for a correct noise structure assumption, as shown by the curves labelled: Correct Noise (CN-dim 3) obtained for a system of order 3. Note that both estimated (shown in Figure 15), and true correlation situations (shown in Figure 16) lead to similar results.

Figure 17 on page 88 and Figure 18 on page 89 illustrate the loss in resolution in identifying the angles of arrival when the noise structure is assumed incorrectly. This example is generated using 2 sources at 18° and 24° with a SNR of 12dB. Figure 17 and Figure 18 present respectively the estimated and true correlation situations. The SNR is 12dB and 600 snapshots are used for the correlation sequence estimates. Assuming the noise to be white (curve labelled as: IN-dim 5 and IN-dim 8 respectively) does not lead to correct identification of the arrival angles. However, the assumption of a correct noise structure of high enough dimension facilitates the identification of both peaks, as shown by the curves labelled CN-dim 5 and CN-dim 3 respectively.

Table 4. Recursive algorithms applied to the DOA problem

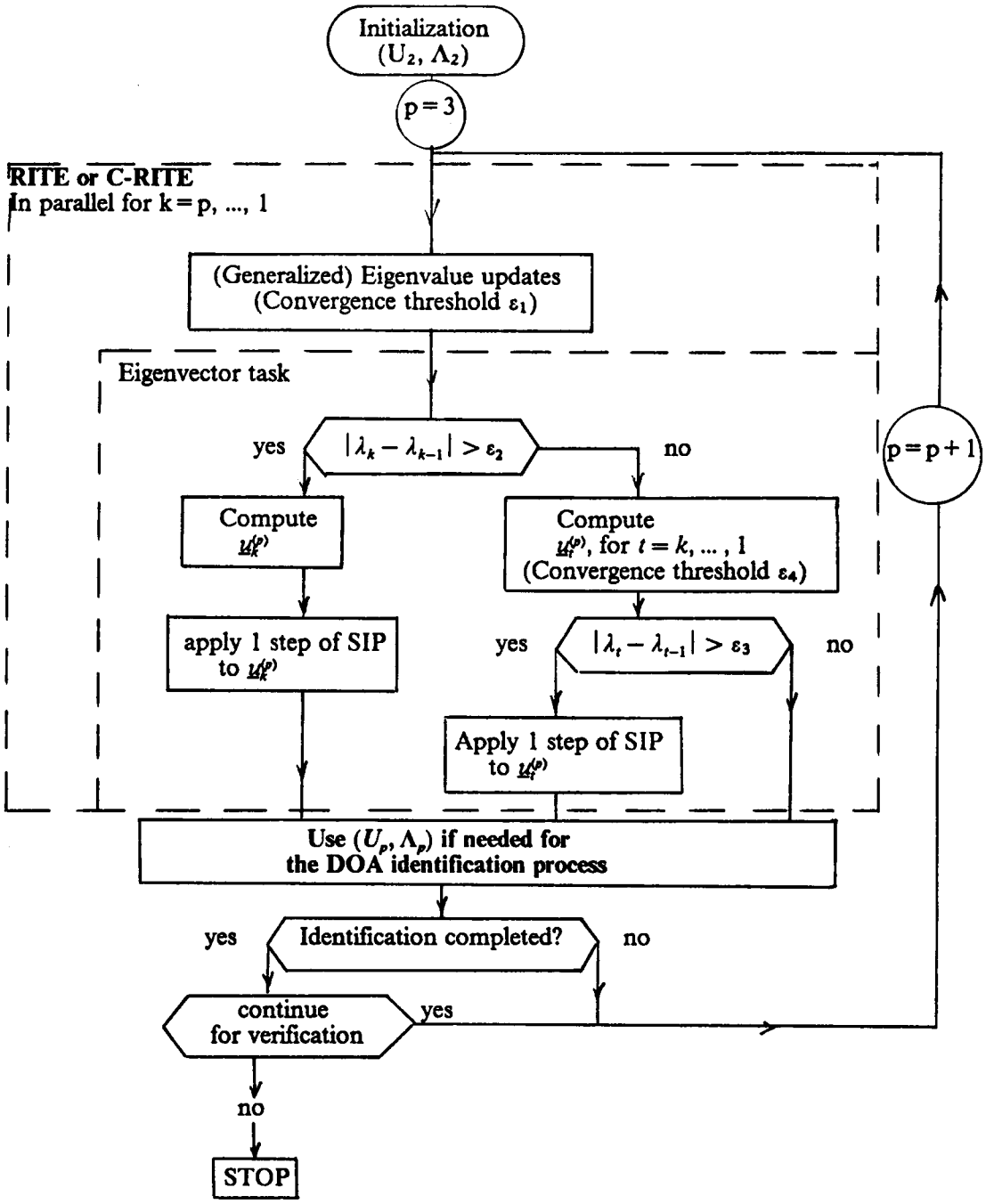

Table 5. MDL and AIC functions for decompositions from order 3 to 10 - Example 1

Matrix order p K = 0, ..., p-1	MDL	AIC
K = 0	0.33380E + 03	0.66761E + 03
K = 1	0.13788E + 02	0.27577E + 02
K = 2	0.80000E + 01*	0.16000E + 02*
K = 0	0.50320E + 03	0.10064E + 04
K = 1	0.42838E + 02	0.85676E + 02
K = 2	0.12047E + 02*	0.24093E + 02*
K = 3	0.15000E + 02	0.30000E + 02
K = 0	0.67944E + 03	0.13589E + 04
K = 1	0.96640E + 02	0.19328E + 03
K = 2	0.16283E + 02*	0.32565E + 02*
K = 3	0.21107E + 02	0.42213E + 02
K = 4	0.24000E + 02	0.48000E + 02
K = 0	0.85900E + 03	0.17180E + 04
K = 1	0.16944E + 03	0.33889E + 03
K = 2	0.20703E + 02*	0.41405E + 02*
K = 3	0.27419E + 02	0.54839E + 02
K = 4	0.32128E + 02	0.64256E + 02
K = 5	0.35000E + 02	0.70000E + 02
K = 0	0.10459E + 04	0.20919E + 04
K = 1	0.26439E + 03	0.52877E + 03
K = 2	0.25854E + 02*	0.51708E + 02*
K = 3	0.34163E + 02	0.68327E + 02
K = 4	0.40777E + 02	0.81553E + 02
K = 5	0.45435E + 02	0.90871E + 02
K = 6	0.48000E + 02	0.96000E + 02
K = 0	0.12370E + 04	0.24741E + 04
K = 1	0.37627E + 03	0.75253E + 03
K = 2	0.31068E + 02*	0.62135E + 02*
K = 3	0.41005E + 02	0.82009E + 02
K = 4	0.49351E + 02	0.98702E + 02
K = 5	0.55730E + 02	0.11146E + 03
K = 6	0.60308E + 02	0.12062E + 03
K = 7	0.63000E + 02	0.12600E + 03
K = 0	0.14427E + 04	0.28854E + 04
K = 1	0.51381E + 03	0.10276E + 04
K = 2	0.48435E + 02*	0.96869E + 02*
K = 3	0.56260E + 02	0.11252E + 03
K = 4	0.65687E + 02	0.13137E + 03
K = 5	0.73308E + 02	0.14662E + 03
K = 6	0.78598E + 02	0.15720E + 03
K = 7	0.80920E + 02	0.16184E + 03
K = 8	0.80000E + 02	0.16000E + 03
K = 0	0.16715E + 04	0.33429E + 04
K = 1	0.68434E + 03	0.13687E + 04
K = 2	0.85605E + 02*	0.17121E + 03*
K = 3	0.92401E + 02	0.18480E + 03
K = 4	0.98757E + 02	0.19751E + 03
K = 5	0.10719E + 03	0.21437E + 03
K = 6	0.11220E + 03	0.22441E + 03
K = 7	0.11435E + 03	0.22870E + 03
K = 8	0.10595E + 03	0.21191E + 03
K = 9	0.99000E + 02	0.19800E + 03

* indicates the position of the minimum obtained for the criteria for each order p

Table 6. Eigenvalue spread from order 3 to 10 - Example 1

Dimension	Eigenvalues		
3	0.662863227E-02	0.215050623E-01	0.297186631E+01
4	0.647941199E-02 0.394362596E+01	0.725826063E-02	0.426363675E-01
5	0.624947813E-02 0.764148693E-01	0.687499980E-02 0.490209392E+01	0.836673272E-02
6	0.591376931E-02 0.916291476E-02	0.677480820E-02 0.126574123E+00	0.751561749E-02 0.584405877E+01
7	0.559774041E-02 0.827415334E-02 0.676700028E+01	0.674011545E-02 0.101953507E-01	0.715885734E-02 0.195033503E+00
8	0.504578597E-02 0.807563567E-02 0.285210049E+00	0.671423908E-02 0.855610758E-02 0.766799461E+01	0.692502774E-02 0.114785432E-01
9	0.417652852E-02 0.774233825E-02 0.138229970E-01	0.655452259E-02 0.819311636E-02 0.398045863E+00	0.676471835E-02 0.961161917E-02 0.854508830E+01
10	0.353381210E-02 0.764597733E-02 0.974221786E-02 0.939619633E+01	0.613599774E-02 0.780170308E-02 0.175733137E-01	0.673476317E-02 0.909318199E-02 0.535542707E+00

Table 7. Eigenvalue spread from order 3 to 10 - Example 2

Dimension	Eigenvalues		
3	0.169627530E+00	0.195168758E+00	0.263520371E+01
4	0.166847411E+00 0.343755573E+01	0.179787281E+00	0.215809580E+00
5	0.164455498E+00 0.244315504E+00	0.175197635E+00 0.422901300E+01	0.187018365E+00
6	0.161977008E+00 0.187402593E+00	0.169341568E+00 0.290397731E+00	0.186304172E+00 0.500457693E+01
7	0.159582968E+00 0.187118283E+00 0.576449852E+01	0.168146853E+00 0.192278472E+00	0.178793703E+00 0.349581199E+00
8	0.156390458E+00 0.183554056E+00 0.426897235E+00	0.167702433E+00 0.190756235E+00 0.650559200E+01	0.173983556E+00 0.195124028E+00
9	0.149256574E+00 0.179791308E+00 0.210209504E+00	0.166753466E+00 0.190198414E+00 0.510539003E+00	0.169807876E+00 0.191505095E+00 0.723193876E+01
10	0.142296690E+00 0.176411699E+00 0.194352261E+00 0.794000921E+01	0.164906481E+00 0.188163607E+00 0.224355302E+00	0.168893153E+00 0.191211678E+00 0.609399920E+00

Table 8. MDL and AIC functions for decompositions from order 3 to 10 - Example 2

Matrix order p K = 0, ..., p-1	MDL	AIC
K = 0	0.10593E + 03	0.21186E + 03
K = 1	0.52134E + 01*	0.10427E + 02*
K = 2	0.80000E + 01	0.16000E + 02
K = 0	0.16526E + 03	0.33052E + 03
K = 1	0.77725E + 01*	0.15545E + 02*
K = 2	0.12061E + 02	0.24121E + 02
K = 3	0.15000E + 02	0.30000E + 02
K = 0	0.22543E + 03	0.45087E + 03
K = 1	0.11054E + 02*	0.22107E + 02*
K = 2	0.16179E + 02	0.32359E + 02
K = 3	0.21043E + 02	0.42087E + 02
K = 4	0.24000E + 02	0.48000E + 02
K = 0	0.28564E + 03	0.57128E + 03
K = 1	0.16098E + 02*	0.32196E + 02*
K = 2	0.20336E + 02	0.40673E + 02
K = 3	0.27224E + 02	0.54447E + 02
K = 4	0.32021E + 02	0.64043E + 02
K = 5	0.35000E + 02	0.70000E + 02
K = 0	0.34586E + 03	0.69172E + 03
K = 1	0.23153E + 02*	0.46306E + 02*
K = 2	0.24505E + 02	0.49010E + 02
K = 3	0.33316E + 02	0.66631E + 02
K = 4	0.40141E + 02	0.80281E + 02
K = 5	0.45030E + 02	0.90059E + 02
K = 6	0.48000E + 02	0.96000E + 02
K = 0	0.40626E + 03	0.81252E + 03
K = 1	0.33146E + 02	0.66293E + 02
K = 2	0.28751E + 02*	0.57503E + 02*
K = 3	0.39519E + 02	0.79039E + 02
K = 4	0.48293E + 02	0.96587E + 02
K = 5	0.55127E + 02	0.11025E + 03
K = 6	0.60053E + 02	0.12011E + 03
K = 7	0.63000E + 02	0.12600E + 03
K = 0	0.46679E + 03	0.93359E + 03
K = 1	0.45246E + 02	0.90491E + 02
K = 2	0.33615E + 02*	0.67230E + 02*
K = 3	0.45943E + 02	0.91886E + 02
K = 4	0.56709E + 02	0.11342E + 03
K = 5	0.65390E + 02	0.13078E + 03
K = 6	0.72209E + 02	0.14442E + 03
K = 7	0.77133E + 02	0.15427E + 03
K = 8	0.80000E + 02	0.16000E + 03
K = 0	0.52751E + 03	0.10550E + 04
K = 1	0.60155E + 02	0.12031E + 03
K = 2	0.38749E + 02*	0.77498E + 02*
K = 3	0.52512E + 02	0.10502E + 03
K = 4	0.65225E + 02	0.13045E + 03
K = 5	0.75917E + 02	0.15183E + 03
K = 6	0.84553E + 02	0.16911E + 03
K = 7	0.91368E + 02	0.18274E + 03
K = 8	0.96236E + 02	0.19247E + 03
K = 9	0.99000E + 02	0.19800E + 03

* indicates the position of the minimum obtained for the criteria for each order p

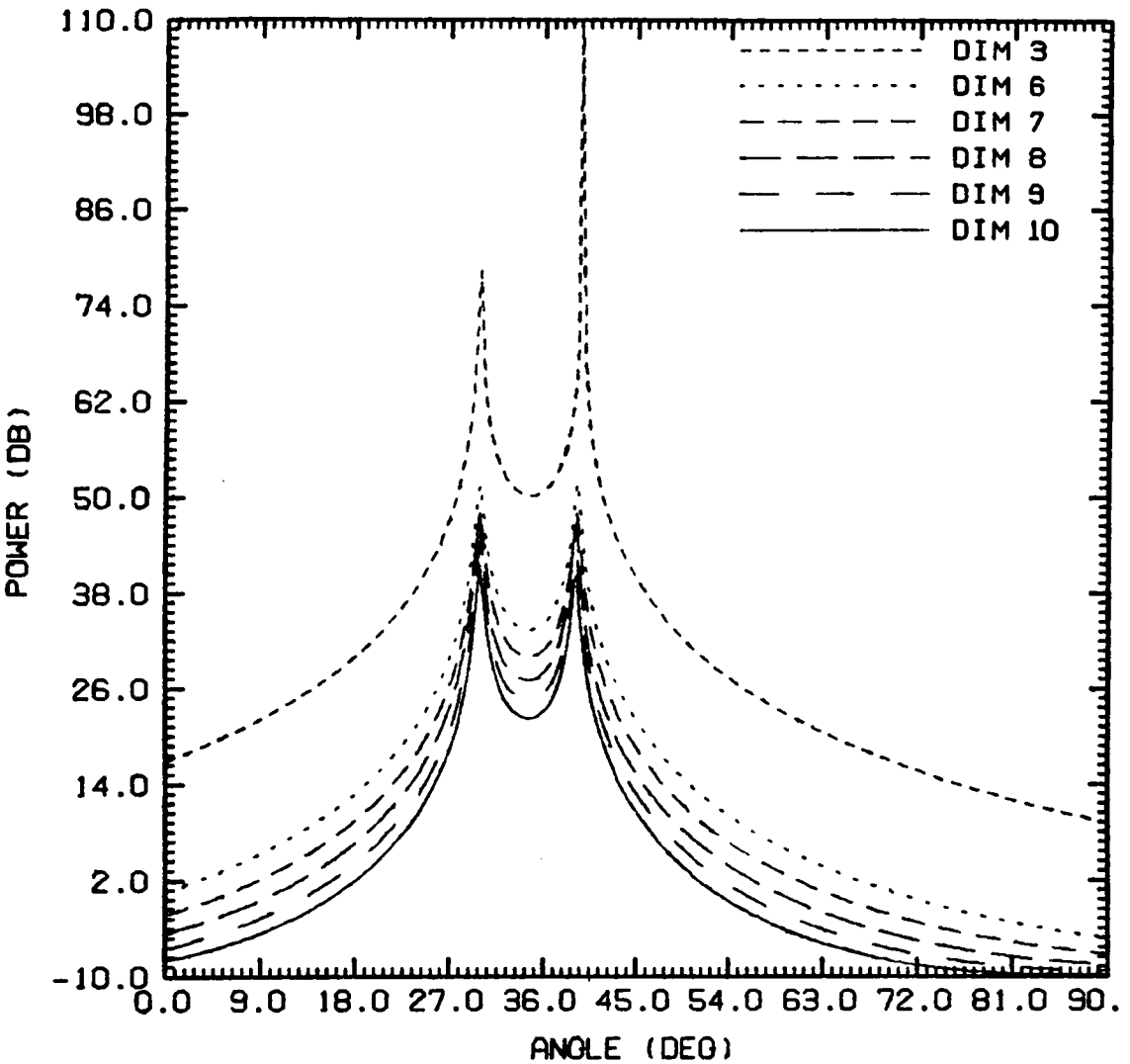

SNR = 20dB, Nest = 100								
Dimension	**3**	**4**	**5**	**6**	**7**	**8**	**9**	**10**
θ_1	29.88°	30.58°	30.23°	29,88°	29.88°	29.88°	29.88°	29.88°
θ_2	39.72°	40.43°	39.37°	39.37°	39.37°	39.37°	39.37°	39.37°

Figure 12. **Signal subspace projections for increasing orders - Example 1:** Incoming sources at 30° and 39°, Nest = 100pts, SNR = 20dB

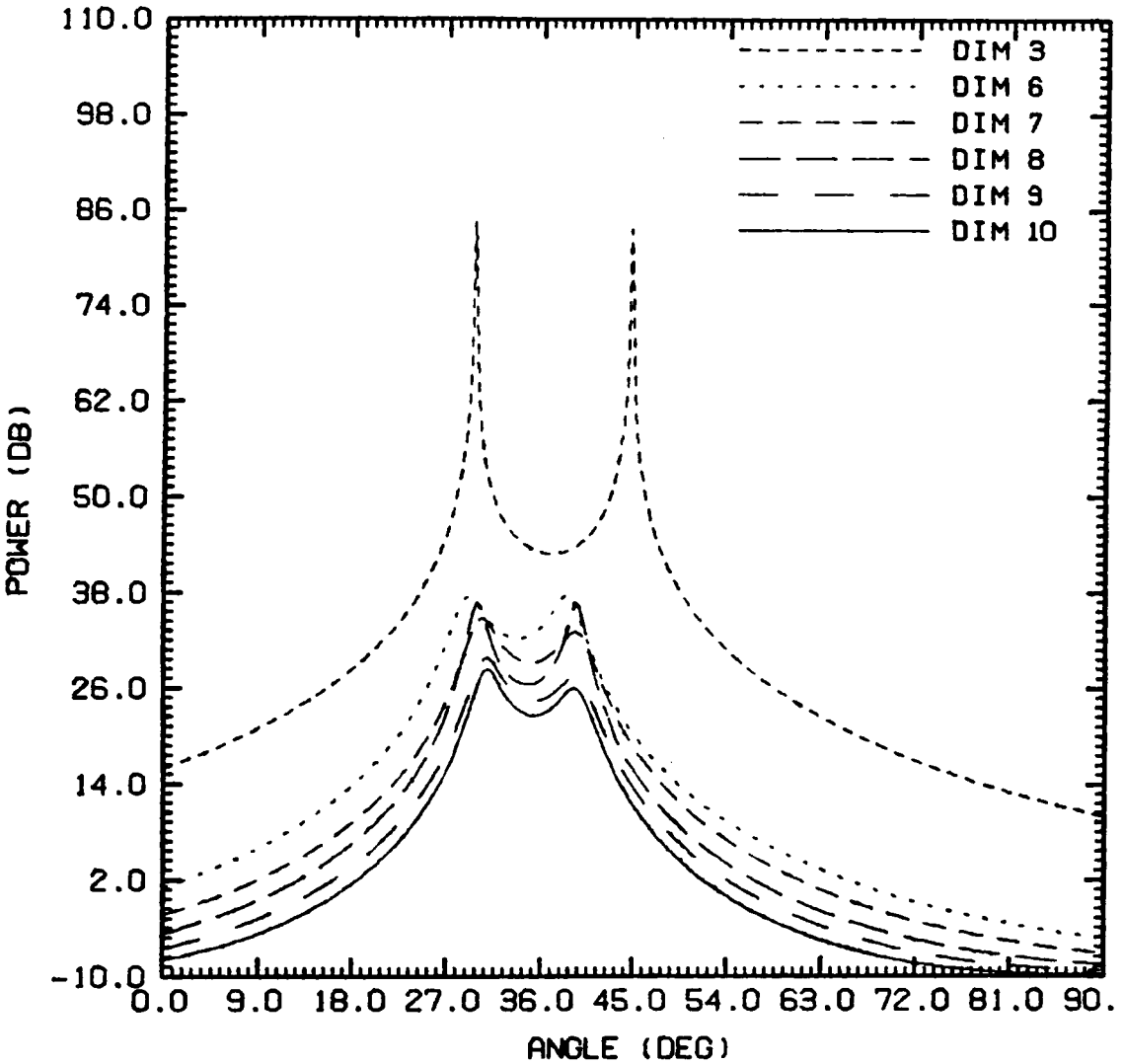

SNR = 5dB, Nest = 100								
Dimension	**3**	**4**	**5**	**6**	**7**	**8**	**9**	**10**
θ_1	29.53°	34.10°	34.45°	29.17°	30.23°	29.88°	30.93°	30.93°
θ_2	44.64°			38.67°	39.37°	39.72°	39.37°	39.37°

Figure 13. **Signal subspace projections for increasing orders - Example 2:** Incoming sources at 30° and 39°, Nest = 100pts, SNR = 5dB

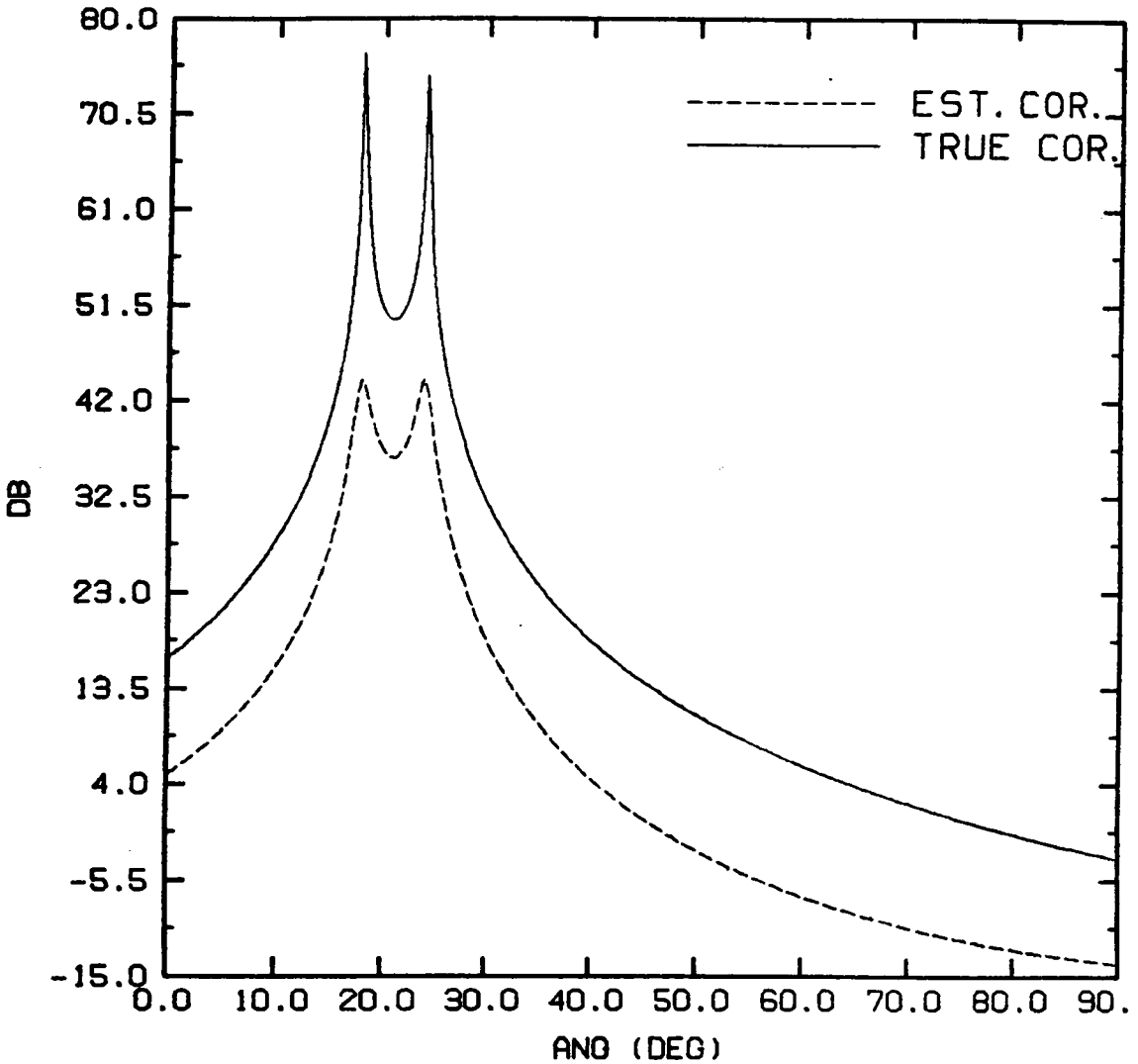

True cor.	Est. Cor.
17.59° & 23.92°	17.59° & 23.78°

Figure 14. **Estimated/True correlation - Projection of the mode vector onto the noise subspace:** the pencil has dimension 5 (estimated) and dimension 3 (true)

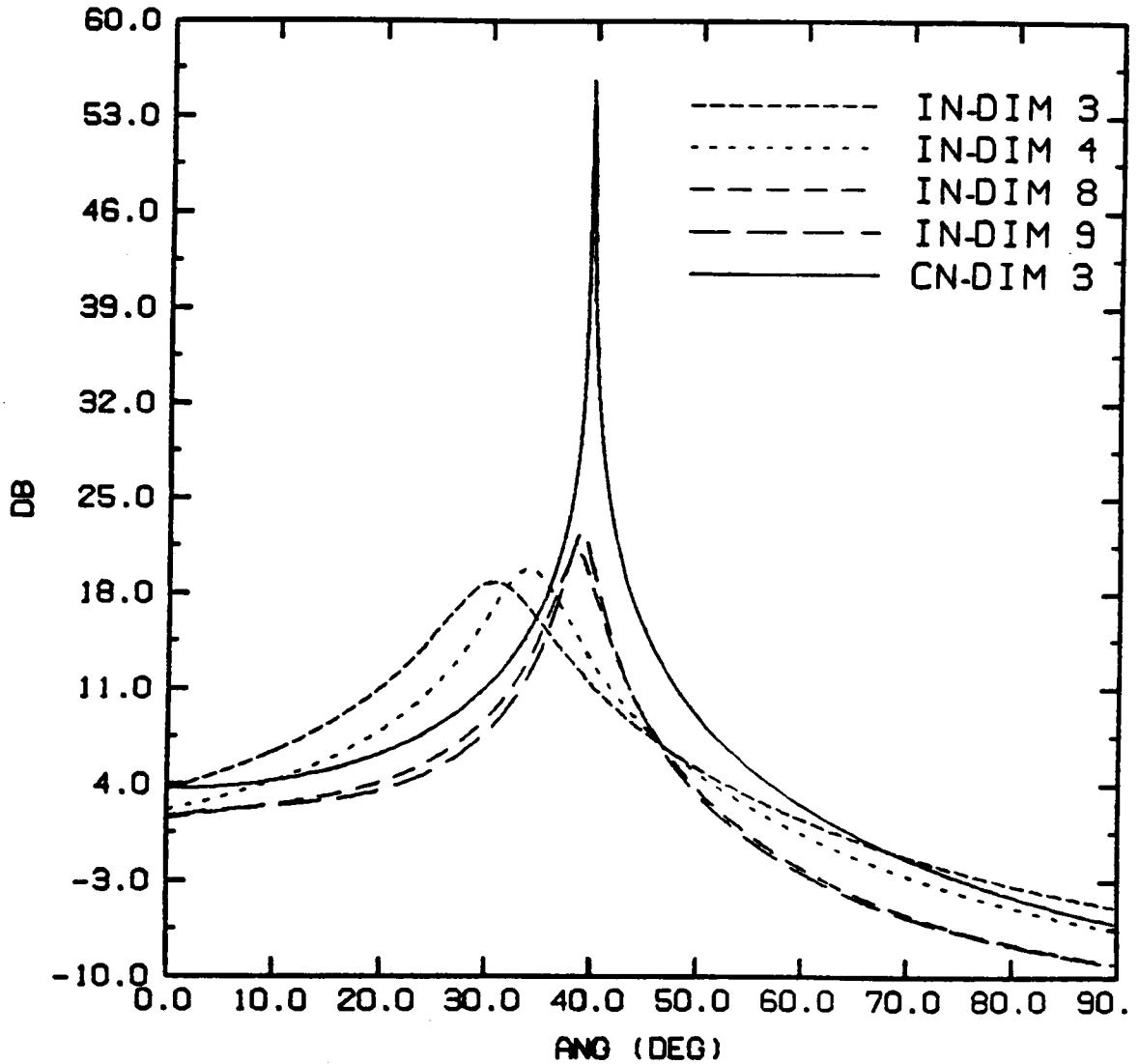

	Incorrect Noise (White)				Col. Noise
DIMENSION	3	4	8	9	3
peak	30.58°	33.75°	38.23°	38.67°	39.72°

Figure 15. **Estimated correlation - bias due to incorrect noise structure:** for successive decompositions from order 3 to 9, 1 signal at 40°

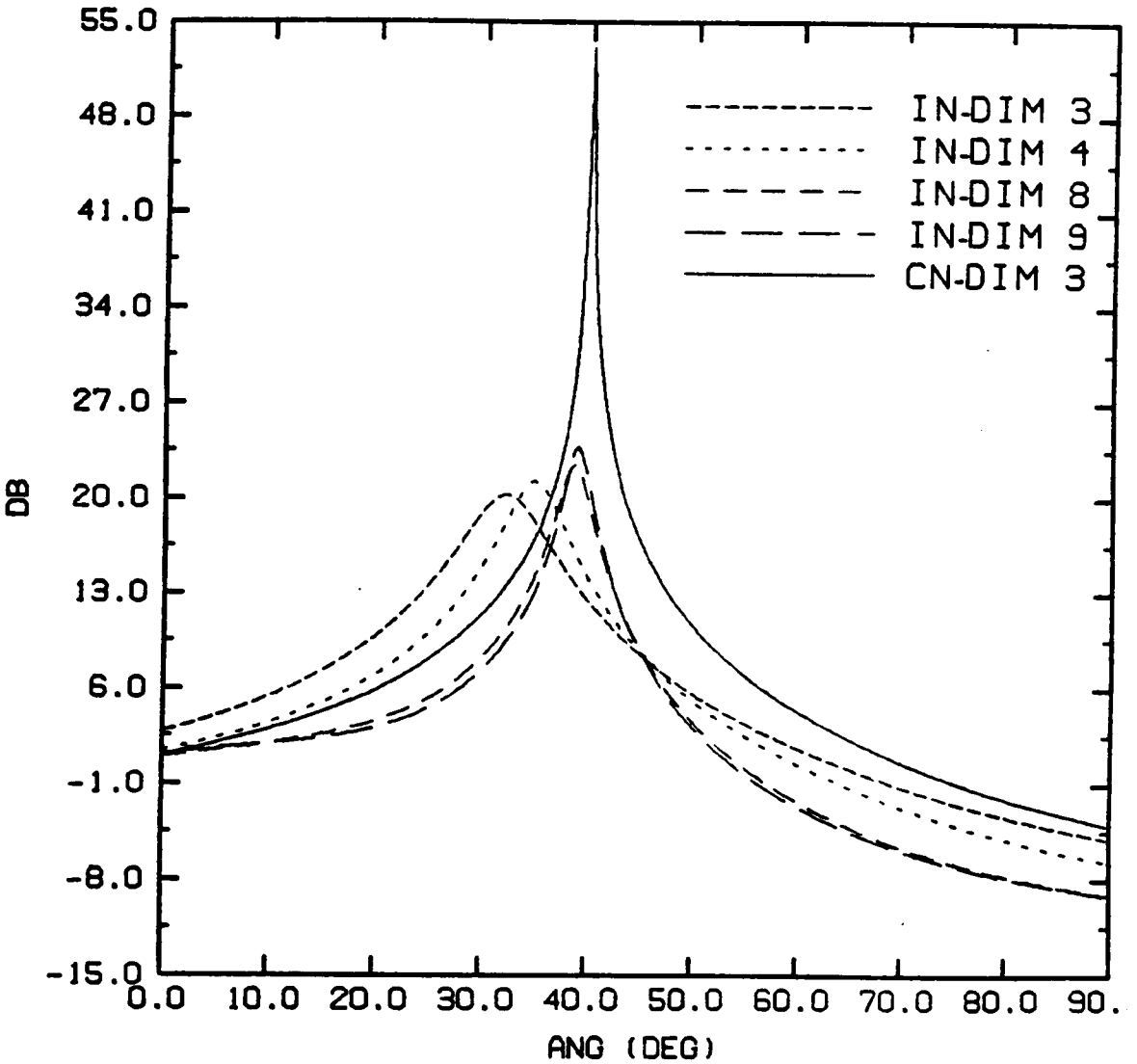

	Incorrect Noise (White)				Col. Noise
DIMENSION	3	4	8	9	3
peak	31.99°	34.80°	38.67°	39.02°	39.72°

Figure 16. **True correlation - bias due to incorrect noise structure:** for decompositions of orders 3 and 8, 1 signal at 40°

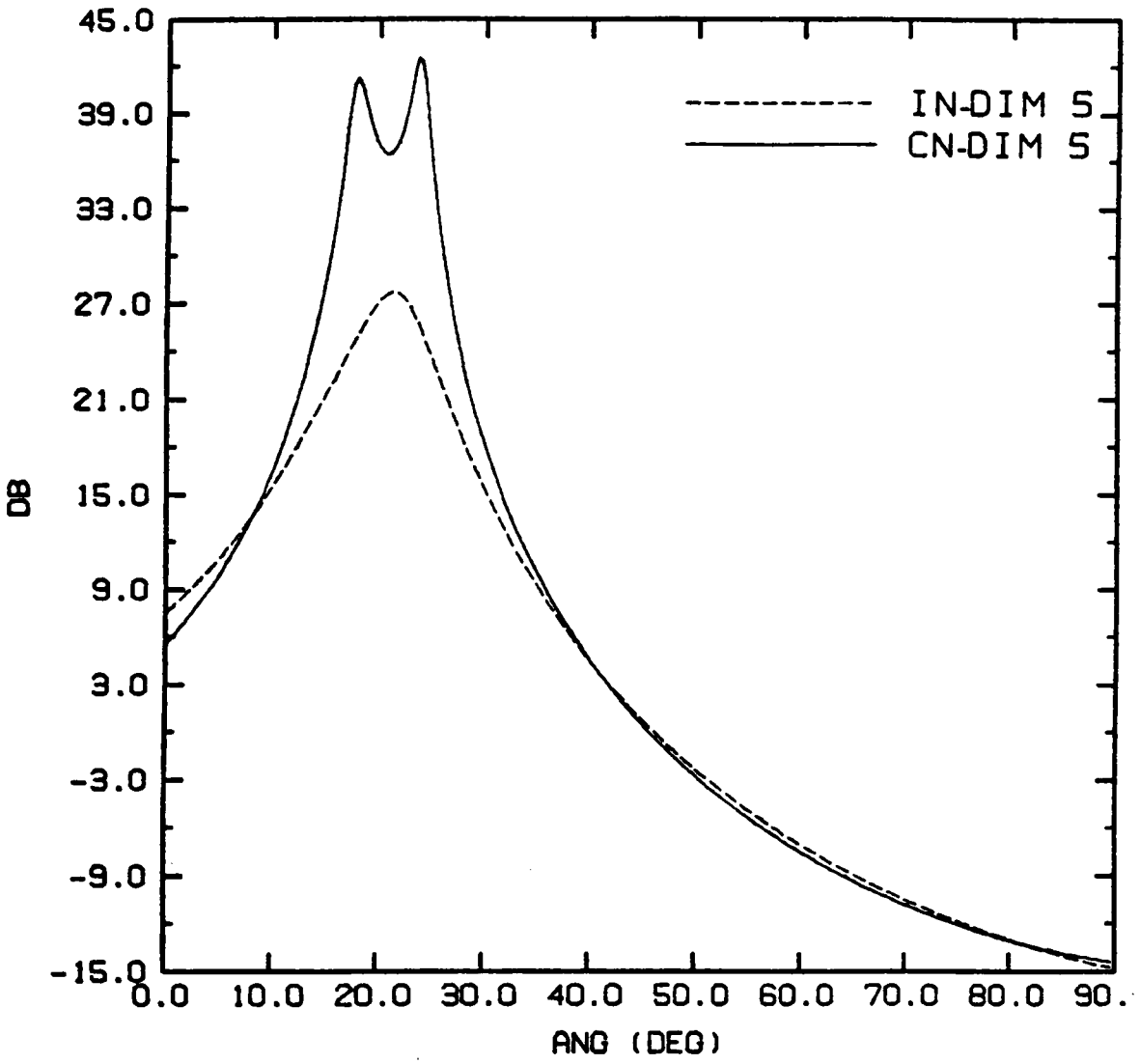

Incorrect Noise (White), dim 5	Col. Noise, dim 5
21.44°	17.92° & 23.55°

Figure 17. **Estimated correlation - resolution loss due to incorrect noise structure:** for decompositions of order 5, 2 signals at 18° and 24°

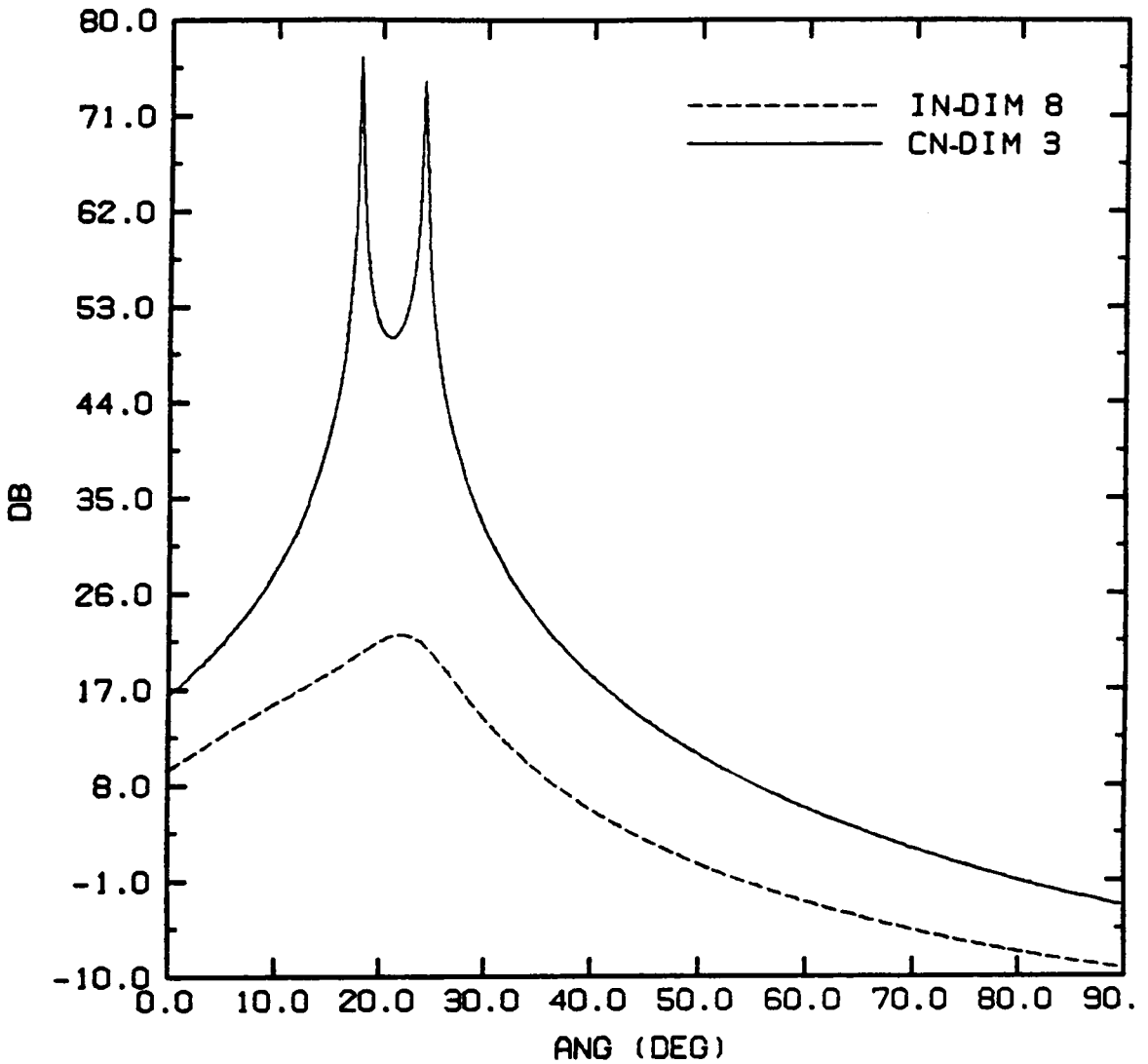

Incorrect Noise (White), dim 8	Col. Noise, dim 5
21.79°	17.92° & 23.90°

Figure 18. True correlation - resolution loss due to incorrect noise structure: for successive decompositions of order 3 and 8, 2 signals at 18° and 24°

5.0 Using RITE in the Non-Stationary Environment

5.1 Introduction

As stated in Chapter 2, the RITE technique is designed for Toeplitz matrices. Its application to the DOA problem is thus restricted to incoming signals with stationary characteristics in white noise. However, there are situations where this assumption is not satisfactory. In such cases, correlation matrices are still Hermitian, but they have lost their Toeplitz structure, as is the case for example with correlation matrices for exponentially damped (interference) signals in white noise. Nevertheless, for nearly stationary processes, the underlying stationary behavior may be of some use. Note that the analysis presented here is restricted to the RITE procedure, i.e. the eigen-decomposition of the pencil (R,I). The idea behind this extension is to take advantage of the fast RITE decomposition eigenpair information and to apply it to the non-Toeplitz Hermitian environment. Two different approaches are investigated here. The first one considers the non-stationary case as a perturbation problem. The averaged Toeplitz matrix R_t is extracted from the non-stationary correlation matrix R_h and is used to analyze the underlying stationary

characteristics of the process. The perturbation matrix $P = R_h - R_t$ is then used to correct the Toeplitz eigenpairs. The above approach characterizes the perturbation of individual eigenvectors. However, only the concept of signal and/or noise subspace is important, as the needed information (such as DOA angles) is invariant to a change of basis in the correctly identified subspace. Therefore, the second method investigated uses the concept of Subspace Iteration (SI) [GVL,PAR], and builds on previous work by Kirsteins and Tufts [KIT] and Vaccaro and Kot [VAK]. Here, the Toeplitz eigenspace decomposition is used as the initial starting point leading to an approximation of the eigenspace decomposition for the Hermitian correlation.

5.2 *Perturbation Approach*

The perturbation approach used for the non-stationary extension is similar to the eigenpair perturbation analysis proposed by Wilkinson [WIL]. Let us define the Hermitian correlation matrix R_h as

$$R_h = R_t + \varepsilon P \tag{126}$$

where R_t and εP are respectively the Toeplitz approximation and the perturbation matrix, and ε is a small real constant scaling the perturbation matrix. Let us define $(\underline{u}(\varepsilon), \lambda(\varepsilon))$ and $(\underline{u}, \lambda)$ to be the eigenpairs of the n-dimensional matrices R_h and R_t respectively. Then, the "Hermitian" eigenpairs[18] $(\underline{u}_i(\varepsilon), \lambda_i(\varepsilon))$ can be expressed in terms of the "Toeplitz" eigenpairs[19] $(\underline{u}_i, \lambda_i)$ for all $i = 1, \ldots, p$

$$\underline{u}_j(\varepsilon) = \underline{u}_j + \varepsilon \underline{z}_1^{(j)} + \varepsilon^2 \underline{z}_2^{(j)} + \cdots \tag{127a}$$

[18] i.e. the eigenpairs associated with the Hermitian matrix.

[19] i.e. the eigenpairs associated with the Toeplitz matrix.

$$\lambda_j(\varepsilon) = \lambda_j + \varepsilon\alpha_1^{(j)} + \varepsilon^2\alpha_2^{(j)} + \cdots \tag{127b}$$

where $z^{(j)}$ can be expressed in terms of the orthonormal basis of eigenvectors of R_t. Therefore,

$$z_i^{(j)} = \sum_{k \neq j} s_{ki}^{(j)} u_k \tag{128}$$

For a first order (linear) perturbation approach, only those terms which are constant or linear in ε are taken into account. Therefore, (127a) and (127b) become

$$u_j(\varepsilon) = u_j + \varepsilon z_1^{(j)} \tag{129a}$$

$$\lambda_j(\varepsilon) = \lambda_j + \varepsilon\alpha_1^{(j)} \tag{129b}$$

Thus, the identification procedure of $(u_j(\varepsilon), \lambda_j(\varepsilon))$ is performed by the following 2 steps:

1. identify the eigenpairs (u_j, λ_j) using RITE,

2. identify the (linear) perturbation terms $\alpha^{(j)}$ and $z^{(j)}$ (i.e. all coefficients $s_{k,1}^{(j)}$ for all $k \neq j$).

For convenience, as the analysis is restricted to a first-order perturbation, the subscripts on z_1 and α_1 will be dropped in the following.

5.2.1 Eigenvalue perturbation

The first order (linear) perturbation scheme leads to the following equality:

$$(R_t + \varepsilon P)(u_j + \varepsilon z^{(j)}) = (\lambda_j + \varepsilon\alpha^{(j)})(u_j + \varepsilon z^{(j)}) \tag{130}$$

For all small ε then, (130) can be decomposed as follows

$$R_t \underline{u}_j = \lambda_j \underline{u}_j \tag{131a}$$

$$P\underline{u}_j + R_t \underline{z}^{(j)} = \alpha^{(j)} \underline{u}_j + \lambda_j \underline{z}^{(j)} \tag{131b}$$

Note that (131a) is always true by our definition of the "Toeplitz" eigenpair. Substituting in (131b) for $\underline{z}^{(j)}$ its expression in terms of the eigenvector basis $(\underline{u}_1, \ldots, \underline{u}_n)$, from (128) leads to

$$P\underline{u}_j + R_t\left[\sum_{k \neq j} s_k^{(j)} \underline{u}_k\right] = \alpha^{(j)} \underline{u}_j + \lambda_j \sum_{k \neq j} s_k^{(j)} \underline{u}_k \tag{132}$$

Using the fact that $R_t \underline{u}_k = \lambda_k \underline{u}_k$, (132) becomes:

$$P\underline{u}_j + \sum_{k \neq j} (\lambda_k - \lambda_j) s_k^{(j)} \underline{u}_k = \alpha^{(j)} \underline{u}_j \tag{133}$$

Pre-multiplying (133) by $\underline{u}_j^*$ leads to

$$\underline{u}_j^* P\underline{u}_j + \sum_{k \neq j} (\lambda_k - \lambda_j) s_k^{(j)} \underline{u}_j^* \underline{u}_k = \alpha^{(j)} \underline{u}_j^* \underline{u}_j \tag{134}$$

R_t is Toeplitz Hermitian, and therefore, $(\underline{u}_1, \ldots, \underline{u}_n)$ form an orthonormal basis. From (134) then

$$\alpha^{(j)} = \underline{u}_j^* P\underline{u}_j \quad \text{for all } j = 1, \ldots, p \tag{135}$$

Therefore, from (129b) and (134), the first order perturbation eigenvalues associated with the Hermitian matrix R_t are given by

$$\lambda_j(\varepsilon) = \lambda_j + \underline{u}_j^* \varepsilon P \underline{u}_j \quad \text{for all } j = 1, \ldots, p \tag{136}$$

Note that, from (131a), we can write this as

$$\lambda_j(\varepsilon) = \underline{u}_j^* R_l \underline{u}_j + \underline{u}_j^* \varepsilon P \underline{u}_j$$
$$= \underline{u}_j^* R_h \underline{u}_j \tag{137}$$

5.2.2 Eigenvector perturbation

The perturbation term $z^{(j)}$ is uniquely identified once its coefficients $s_k^{(j)}$ are known for all $k \neq j$. Pre-multiplying (133) by $\underline{u}_m^*$ for $m \neq j$, leads to

$$\underline{u}_m^* P \underline{u}_j + \sum_{k \neq j} (\lambda_k - \lambda_j) s_k^{(j)} \underline{u}_m^* \underline{u}_k = \alpha^{(j)} \underline{u}_m^* \underline{u}_j \tag{138}$$

Due to the orthonormality of $\underline{u}_i$, we have $\underline{u}_i^* \underline{u}_j = 0$ for all $i \neq j$ and therefore,

$$\underline{u}_m^* P \underline{u}_j + (\lambda_m - \lambda_j) s_m^{(j)} = 0 \tag{139}$$

which leads to

$$s_m^{(j)} = -\frac{\underline{u}_m^* P \underline{u}_j}{\lambda_m - \lambda_j} \quad \text{for all } m \neq j \text{ and } \lambda_m \neq \lambda_j \tag{140}$$

Therefore, from (129a), the k first order perturbation eigenvectors $\underline{u}_j(\varepsilon)$, associated with the signal subspace of the Hermitian matrix R_h, are given by

$$\underline{u}_j(\varepsilon) = \underline{u}_j + \varepsilon \sum_{k \neq j} s_k^{(j)} \underline{u}_k$$
$$= \underline{u}_j - \sum_{k \neq j} \frac{\underline{u}_k^* \varepsilon P \underline{u}_j}{\lambda_k - \lambda_j} \underline{u}_k \tag{141}$$

Note that this approach is restricted to the identification of the signal subspace eigenvectors, i.e. those with distinct eigenvalues. Equation (140) is ill-conditioned when $\lambda_m - \lambda_j \simeq 0$. This approach cannot be used to identify the first order perturbation noise subspace eigenvectors due to the clustering of the noise eigenvalues. However, for nearly stationary processes (i.e. small εP matrix), the number of incoming signals can be extracted from the Toeplitz eigen-decomposition. The above computation can then safely be restricted to the signal subspace eigenvectors. Next, the DOA information is obtained by using projections of the mode vector onto the signal subspace, as was presented for the Toeplitz case in Section 4.2. Performance results for the estimated eigenpairs are presented at the end of the section.

An alternative, and updated, estimate of a first order perturbation eigenvalue can be obtained using the Rayleigh quotient of the estimated Hermitian eigenvector. Recall that the Rayleigh quotient associated with the Hermitian eigenvector $\underline{u}_j^h$ is given by [PAR]

$$\rho_j(\varepsilon) = \underline{u}_j^{h*} R_h \underline{u}_j^h \tag{142}$$

5.3 *Subspace Iteration Approaches*

As stated in Section 5.1, the advantage of the SI method is that concepts of signal and noise subspaces are used to compute the eigen-decomposition of the Toeplitz matrix associated with diagonally averaging of the Hermitian matrix. The important difference with the first order (linear) perturbation approach introduced in the preceding section is that the eigenvectors are not considered individually for this computation. As a result, the method is less sensitive to problems due to clustered eigenvalues. Furthermore, it leads to complete identification of signal and noise subspace estimates, if so desired. Subspace iteration methods have been extensively studied in the literature. Performance analyses and convergence behaviors can be found elsewhere [GVL,PAR]. Note that the performance of these techniques depends upon the number of iterations used, the

eigenvalue spread and the starting point. The purpose of this section is to first introduce the concept of SI and to present its potential application to the non-stationary situation. A modified SI which uses the modified GS procedure is presented next. Finally, performance comparisons with the perturbation approach are presented at the end of the section.

5.3.1 Introduction to Subspace Iteration

Subspace iteration is a generalization of the Power and Inverse Power method (PM and IPM) [PAR]. The straight PM leads to identification of the leading eigenvector[20] $\underline{u}_{max}$ of a p-dimensional Hermitian matrix R by computing successive iterations of $R^k\underline{x}$, where $\underline{x}$ is an initial starting vector. This result is easily understood by expanding R in terms of its spectral decomposition.

$$R = \sum_{i=1}^{p} \lambda_i \underline{u}_i \underline{u}_i^* \tag{143}$$

If $\underline{x} = \sum_{i=1}^{p} a_i \underline{u}_i$, then

$$R^k\underline{x} = a_1 \lambda_1^k \left[\underline{u}_1 + \sum_{j=2}^{p} \frac{a_j}{a_1} \left(\frac{\lambda_j}{\lambda_1} \right)^k \underline{u}_j \right] \tag{144}$$

Therefore, $R^k\underline{x}$ converges to a scaled version of $\underline{u}_{max} = \underline{u}_1$ for large enough k if $\lambda_1 > \lambda_j$ for all $j \neq 1$. The SI method generalizes the idea to the concept of iterating on a subspace $(\underline{x}_1, \ldots, \underline{x}_m)$. Then $R^k U_m$ is spanned by $S = (R^k\underline{x}_1, \ldots, R^k\underline{x}_m)$. This expression shows that the SI method can be viewed as k individual PM iterations, each of which converges to the leading eigenvector. Therefore, S is becoming a poor basis for the potentially good approximation of the subspace spanned by $R^k U_m$. However, convergence to the correct subspace is insured if the iterated subspace is orthogonalized

[20] i.e. the eigenvector associated with the maximum eigenvalue.

after each iteration of the procedure. The improvement is drastic especially when the matrix has clustered eigenvalues [PAR].

5.3.2 Subspace iteration and the perturbation problem

The idea behind this approach is to obtain an approximation to the signal eigenspace span($U_{s,h}$) of the Hermitian matrix R_h by using the Toeplitz signal eigenspace information span($U_{s,t}$). Thus $U_{s,t}$ is used to find a basis which approximately spans the same subspace as $U_{s,h}$. Using the first order small perturbation, R_h may be rewritten as $R_h = R_t + \varepsilon P$. Let us apply one step of the SI method to the matrix $U_{s,t}$, using the non-stationary Hermitian correlation matrix R_h. We get

$$R_h U_{s,t} = R_t U_{s,t} + \varepsilon P U_{s,t} \tag{145}$$

Equation (145) depends linearly on the perturbation matrix. Using the properties of the SI method introduced above, it can be viewed as a first-order approximation of the subspace spanned by $U_{s,h}$, as iterating several times on $U_{s,t}$ will produce a set of vectors which will converge to the subspace spanned by $U_{s,h}$. Recall that the rate of convergence actually depends upon the gap between the eigenvalue set $\lambda(U_{s,h})$ and $\lambda(U_{s,h}^{\perp})$, where $U_{s,h}^{\perp}$ represents the orthogonal complement to $U_{s,h}$. Hence, a slower rate of convergence to the true eigenvectors is to be expected when dealing with closely spaced sources, or incoming signals with low SNR, as this generates an eigenvalue distribution with a smaller gap between $\lambda(U_{s,h})$ and $\lambda(U_{s,h}^{\perp})$ (see examples presented in Section 4.4, Table 6 and Table 7). Furthermore, note that the dimension of the subspace to be approximated is numerically limited if accurate orthogonalization of the vectors cannot be performed after each iteration. Therefore, a Gram-Schmidt orthogonalization of the iterated subspace is performed after each iteration to insure orthogonality of the eigenvectors.

5.3.3 Modified subspace iteration

A Modified SI (MSI) method is investigated next. It uses the modified Gram-Schmidt (GS) procedure [PAR] to estimate the same dominant Hermitian subspace as before. This method was studied because the modified GS has better numerical properties [GVL], which might lead to a better approximation of the Hermitian subspace $U_{s,h}$. Let us assume that we want to recover the k dominant eigenvectors of the Hermitian matrix R_h. At each step the MSI transforms an orthonormal basis Q_i into an orthonormal basis Q_{i+1} by the following algorithm

a) Compute $D_{i+1} = R_h Q_i$,

b) Use the modified GS procedure to orthonormalize D_{i+1}, which gives Q_{i+1}.

The iterative procedure stops when the vectors have converged to the desired direction [PAR], and the resulting orthonormal matrix Q forms an orthonormal basis for the eigenvector space. The eigenvectors must then be recomputed by means of a change of basis, thereby increasing the computational load of the procedure compared to the regular SI method.

If one is interested in only a subset of the eigenvectors contained in Q, then the computational load to recover the eigenvectors can be reduced, as shown next. Let $Q = [Q_s, Q_n]$ be the p-dimensional orthogonal matrix obtained after applying the MSI procedure to a p-dimensional set of starting vectors, where Q_s contains the k column vectors of interest. Then pre- and post-multiplying R_h by Q^* and Q leads to

$$Q^* R_h Q = \begin{bmatrix} Q_s^* \\ Q_n^* \end{bmatrix} R_h [Q_s, Q_n] = \begin{bmatrix} Q_s^* R_h Q_s & Q_s^* R_h Q_n \\ Q_n^* R_h Q_s & Q_n^* R_h Q_n \end{bmatrix} \tag{146}$$

R_h is Hermitian, therefore Q is orthogonal, and Q_s and Q_n have orthonormal column vectors. Hence, $U_s = \text{span}(Q_s)$ and $U_n = \text{span}(Q_n)$ are invariant, and $Q_s^* R_h Q_n = Q_n^* R_h Q_s = O$. Therefore, (146) becomes

$$Q^* R_h Q = \begin{bmatrix} Q_s^* R_h Q_s & O \\ O & Q_n^* R_h Q_n \end{bmatrix} \tag{147}$$

and

$$\lambda(Q^* R_h Q) = \lambda(Q_s^* R_h Q_s) \cup \lambda(Q_n^* R_h Q_n) = \lambda(R_h) \tag{148}$$

Thus, the eigenvalues associated with the subspace $U_{s,h}$ can be recovered from those of $Q_s^* R_h Q_s$. Now let us assume (θ_i, x_i) to be the eigenpairs of the k-dimensional matrix $Q_s^* R_h Q_s$. Then, using (147) leads to

$$\begin{bmatrix} Q_s^* R_h Q_s & O \\ O & Q_n^* R_h Q_n \end{bmatrix} \begin{bmatrix} x_i \\ 0 \end{bmatrix} = \theta_i \begin{bmatrix} x_i \\ 0 \end{bmatrix} \quad \text{for all } i = 1, \ldots, k \tag{148}$$

Therefore, with (147), (148) leads to

$$Q^* R_h Q \begin{bmatrix} x_i \\ 0 \end{bmatrix} = \theta_i \begin{bmatrix} x_i \\ 0 \end{bmatrix} \text{ for all } i = 1, \ldots, k \tag{149}$$

Using the fact that Q is orthogonal, (149) becomes

$$R_h \left(Q \begin{bmatrix} x_i \\ 0 \end{bmatrix} \right) = \theta_i Q \begin{bmatrix} x_i \\ 0 \end{bmatrix} \text{ for all } i = 1, \ldots, k \tag{150}$$

Hence, (150) shows that $Q[x_i^t, 0^t]^t$, for all $i = 1, \ldots, k$, are eigenvectors of R_h. Therefore, $(\theta_i, Q[x_i^t, 0^t]^t)$, for $i = 1, \ldots, k$ are the eigenpairs of R_h spanning the subspace $U_{s,h}$.

Closed form expressions for the eigenpairs of $Q_s^* R_h Q_s$ exist when the matrix is of dimension $k \leq 3$. For $k > 3$, iterative methods have to be used to recover the eigenpairs (θ_i, x_i) of $Q_s^* R_h Q_s$, thereby increasing the computational load of the algorithm. For some applications however, one may expect the dimension k for $U_{s,h}$ to be small because it represents the number of DOA angles to be identified. Performance comparisons of the different non-stationary extensions are presented next.

5.4 *Performance Comparisons*

The quality of the different extensions is first compared in terms of residual norms and angle difference between Hermitian (true) and estimated (using the extension techniques) eigenvectors. A summary of the performance checks is given in Figure 19 on page 103. Next, the extensions are compared in terms of DOA performance results using the MUSIC algorithm as before.

Implementation Comments

The different non-stationary extensions are tested on Hermitian correlation matrices generated from exponentially damped sinusoids in white noise. The Hermitian correlation matrices are generated by:

$$R_h = \frac{1}{nest} \sum_{k=1}^{nest} x_k x_k^* \tag{151}$$

where the measured vector is expressed as

$$x_t = \sum_{i=1}^{m} A_i \exp[(j\omega_c t + \psi_i)] \cdot \begin{bmatrix} 1 \\ \exp(-2\pi(jz_i + \alpha_i)) \\ \vdots \\ \exp(-2\pi(jz_i + \alpha_i)(p-1)) \end{bmatrix} + n_t \tag{152}$$

where z_i represents the normalized angle chosen between $[0, 2\pi]$, α_i is the damping factor, A_i is the peak amplitude of each incoming source, ω_c is the center frequency of the spatial sources, and ψ_i is the random phase of each incoming signal uniformly distributed over $[0, 2\pi]$. The complex white noise vector is generated using the IMSL (version 9.2) routine GGNML. We saw in (99), (101), and (114), that evaluation of inner products is required to estimate the location of the radiating sources. As indicated in Section 4.2.3, equation (116), the inner products can be efficiently evaluated with FFT algorithms. Similar comments still hold when dealing with damped spatial

frequencies when the damping factors α_i are assumed to be known. Therefore, we consider the damping factors to be known, and restrict the considered DOA application to estimation of the angles of arrival[21]. In such a case, projections onto noise or signal subspaces still yield the same expressions as those given in (99), (101), and (114). The only difference lies in the definition of the mode vector $\underline{m}_\theta$. The associated mode matrix, with mode vectors $\underline{m}_\theta$ as column vectors, is now given by

$$M = \left[\underline{m}_{\theta 1} \mid \ldots \mid \underline{m}_{\theta m} \right] = \left[\begin{array}{c|c|c} 1 & & 1 \\ \exp(-2\pi(jz_1 + \alpha_1)) & \cdots & \exp(-2\pi(jz_m + \alpha_m)) \\ \vdots & & \vdots \\ \exp(-2\pi(p-1)(jz_1 + \alpha_1)) & & \exp(-2\pi(p-1)(jz_m + \alpha_m)) \end{array}\right] \tag{153}$$

Therefore, the new inner products to be evaluated become

$$\begin{aligned} \underline{u}_i^{(p)*} \underline{m}_\theta &= \sum_{n=1}^{p} u_{i,n}^{(p)*} e^{-(n-1)(jz_\theta + \alpha_i)} \\ &= \sum_{n=1}^{p} \left(u_{i,n}^{(p)*} e^{-(n-1)\alpha_i}\right) e^{-jz_\theta(n-1)} \end{aligned} \tag{154}$$

The sum can be evaluated at all normalized angles $z_\theta = 2\pi k/N$ with the following Discrete Fourier Transform $\mathrm{DFT}_N\{u_{i,1}^{(p)}, u_{i,2}^{(p)} e^{-\alpha_i}, \ldots, u_{i,p}^{(p)} e^{-(p-1)\alpha_i}, 0, \ldots, 0\}$, where p is the dimension of the problem, N is the FFT length chosen by the user, $u_{i,k}^{(p)}$ represents the k^{th} component of the p-dimensional i^{th} eigenvector $\underline{u}_i^{(p)}$, and α_i is the i^{th} damping factor. As for the Toeplitz case studied in Chapter 4, efficient FFT algorithms can then be used, and the accuracy in resolving the maxima and/or minima of the projections onto the different subspaces depends on the amount of zero padding (N-p).

---

[21] This problem is equivalent to estimating the pole frequencies of exponentially damped sinusoids in noise, assuming the damping factors to be known.

Eigenstructure Performance

The eigenstructure quality of the extensions is first compared by the residual norms r^x defined as $r^x = |(R_h - \lambda^x I)\underline{u}^x|$, where $(\lambda^x, \underline{u}^x)$ represent the eigenpairs of the original Hermitian matrix, the averaged Toeplitz matrix, or those resulting from the extensions. Note that eigen-based techniques applied to the DOA problem usually use only either the signal or the noise eigenvectors (not the eigenvalues) to recover the desired information (in the sequel, the number of incoming sources is assumed to be known and the comparisons are conducted on the signal subspace portion only of the eigendecomposition). Therefore, a more application oriented comparison of the extensions involving only the estimated eigenvectors is considered next. Assuming the eigenvalues of the Hermitian matrix to be known, the following residual norms are compared: $s^x = |(R_h - \lambda^h I)\underline{u}^x|$, where λ^h is a known eigenvalue of R_h. In the latter s^x characterizes the quality of the estimated eigenvectors only, as no additional error comes from the eigenvalues. Finally, the angle difference between Hermitian (true) and approximated (by the extension techniques) eigenvectors is evaluated also. This measure is defined as

$$\begin{aligned}\theta_i &= \text{ang}(\underline{u}_{i,PERT}, \underline{u}_{i,IMSL}) \\ &= \cos^{-1}\left(|\underline{u}^*_{i,PERT}\underline{u}_{i,IMSL}|\right)180/\pi\end{aligned} \tag{154}$$

where $\underline{u}_{i,IMSL}$ and $\underline{u}_{i,PERT}$ respectively represent the i^{th} Hermitian eigenvector and its estimate obtained by one of the extension techniques studied. Direct eigen-decomposition information of the Hermitian matrix is obtained with the IMSL (version 9.2) routine EIGCH.

Correlation sequences created from two exponentially damped signals impinging on a 10 sensor linear array are used to build the Hermitian matrices. The location and SNR of the sources are variables used to study the effects of the eigenvalue distribution and the convergence behavior of the Subspace Iteration techniques. The first example considers two exponentially damped signals at 18° and 30° with SNR equal to 5dB. The Hermitian correlation matrix is estimated from using 500 snaphots. A damping factor of -0.1 is chosen and 10 iterations are used for the SI and MSI techniques. This correlation sequence is used to build the matrices of order 3, 6 and 10 generated for Table 9, Table 10 and Table 11. The different extension techniques are compared in terms

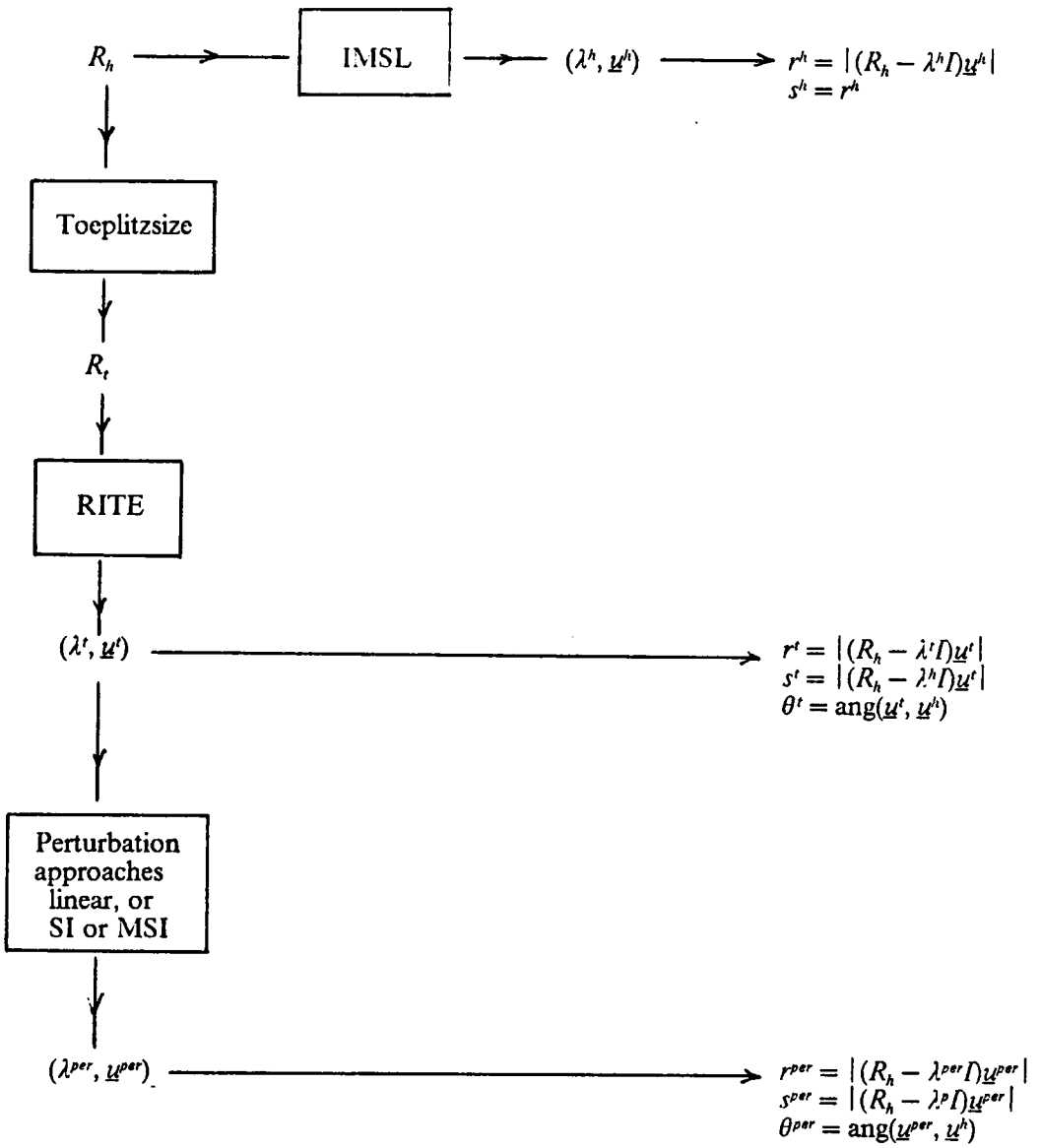

Figure 19. Performance comparisons for perturbation approaches

of the eigenvalue estimates, the residual norms and the angle differences for the set of signal eigenvectors, i.e. the eigenvectors associated with the two largest eigenvalues denoted λ_1 and λ_2 in this section. The measures of angle difference between the corresponding estimated and true signal eigenvectors are defined by $\theta_1 = \text{ang}(\underline{u}_{p,PERT}, \underline{u}_{p,IMSL})$ and $\theta_2 = \text{ang}(\underline{u}_{p-1,PERT}, \underline{u}_{p-1,IMSL})$. The Rayleigh quotient, as defined in (142) is used to estimate the eigenvalues obtained for the SI technique, even if they are not needed to estimate the eigenvectors. Finally, eigenvalues and residual norms are included for the original Hermitian matrix so as to give a point of comparison between approximated and direct eigenspace decompositions.

Several observations can be made from Table 9 to Table 11. The averaged Toeplitz matrix does not of itself lead to a good approximation of either the eigenvalue set or the eigenvector set (the residual norms r^t and s^t are large). This seems to contradict the previous finding that "Toeplitzsizing" leads to improvement [MOB]. The latter was the result of making the correct assumption about the underlying data. In the present context the underlying data is known to lead to a Hermitian, non-Toeplitz, correlation and therefore Toeplitzsizing imposes the wrong constraint.

The first order (linear) perturbation introduces some improvement on the eigenvalue set but the corresponding residual norms appear to be still large. The Hermitian matrix in this example is probably too far from its averaged Toeplitz structure to justify such a first order linear approximation. The direct effect of the damping factor on the Toeplitz and first order linear perturbation techniques can be viewed by comparing the performance on examples 1 and 2 given respectively in Table 9 to Table 11 and Table 12 to Table 14. Identical parameters, except for a damping of -0.01, are used to generate the matrices for example 2. The Toeplitz and linear perturbation methods lead to better results for smaller damping. Recall that the eigenvectors associated with Hermitian matrices are ill-conditioned, i.e. they are very sensitive to perturbations. This may explain the lack of more improvement in s^{per}. The results show that the SI and MSI techniques have produced similar performances, and have the smaller residual norms s^{per} and angle differences of the extension techniques. This is due to the fact that eigenspaces are much less sensitive to perturbations than individual eigenvectors. Note that convergence to the Hermitian

eigenvectors is faster (i.e. fewer iterations are required) when using the Toeplitzsized (diagonally averaged) matrix than when using an arbitrary (in this case identity) matrix to start the iterative SI technique. The improvement can be seen in Table 15 which compares the angle differences between true and estimated angles, when either the Toeplitzsized matrix (denoted SI_T in Table 15) or the identity matrix (denoted SI_I in Table 15) are used to start the iterative procedure for example 1. Similar comments could be drawn from example 2. The number of iterations used in each of the trial runs is shown in Table 15. The difference in performance decreases when the number of iterations is allowed to increase, as both iterative procedures will tend to converge to the same eigenvector space. The decrease in iterations needed to get estimates of the Hermitian eigenvectors, when using the Toeplitzsized matrix however, is very interesting for real-time applications where one wants to minimize the computational load.

Further comments can be made on the SI and MSI techniques. Note that a degradation of the performance is visible for the second signal eigenvector. This was expected because the leading eigenvector converges faster towards the true direction, and the number of iterations was fixed rather than determined by a residual based stopping criteria. The relationship between the convergence rate of the signal subspace iteration technique and the gap between the signal and noise eigenvalue sets is illustrated in Table 9 and Table 12, which show that the SI techniques converge faster for larger gaps (i.e. for smaller ratio λ_2/λ_3).

Table 10 and Table 13 show that good eigenvalue estimates are obtained by any of the extension techniques. This was to be expected as the Hermitian eigenvalue problem is well conditioned (while the corresponding eigenvector problem is not). Finally, Table 11 and Table 14 give a better interpretation of the actual direction difference between estimated and true eigenvector directions for all the different extension techniques investigated. As expected from our previous comments, the smaller angle differences are obtained using the SI techniques.

DOA Performance Comparisons

The performance of the extension techniques is compared next in terms of the DOA identification results. Projections of the mode vector onto the signal subspace, obtained for the 10-dimensional correlation matrix, using the Toeplitzsized matrix, the linear perturbation approximation, the SI technique, and the true Hermitian decomposition are given in Figure 20 and Figure 21 for examples 1 and 2. Several observations can be made from these examples. First, note that the incoming angles estimated using the Toeplitsized matrix or the linear perturbation approach exhibit a higher bias than those from the SI technique. Again we see that Toeplitzsizing is not a good idea if the Toeplitz assumption is erroneous. Next, note that the linear perturbation approach leads to correct DOA identification for very small damping only. Therefore, its range of application is extremely limited. Much better results are obtained using the SI technique, which for both examples exhibits the same performance as that obtained with the Hermitian decomposition.

In conclusion, the simple subspace iteration techniques studied here appear to be a good alternative to directly computing the Hermitian signal subspace as they lead to accurate and fast approximations. However, the rate of convergence will depend upon the gap between signal and noise eigenvalue sets, i.e. convergence to the Hermitian signal subspace will be faster when the incoming sources are not too closely spaced or the SNR is not too low. Finally, note that the non-stationary extension does not actually need to be performed for every order of the RITE decompositions. The alternative is to use RITE up to a high enough order to then apply an "extension" to get an improved approximation to the Hermitian signal subspace.

Table 9. Performance comparisons of extensions - Example 1

DIMENSION 3 ($\lambda_2/\lambda_3 = 0.857$)					
	IMSL	Toeplitz	Lin. Pert.	SI (10it)	MSI (10it)
$r(\lambda_1)$		0.471E01	0.727	0.479E-08	0.209E-06
$s(\lambda_1)$	0.285E-28	0.814	0.728	0.206E-06	0.139E-03
$r(\lambda_2)$		0.804	0.700	0.139E-02	0.139E-02
$s(\lambda_2)$	0.553E-27	0.806	0.700	0.139E-02	0.139E-02

DIMENSION 6 ($\lambda_2/\lambda_3 = 0.657$)					
	IMSL	Toeplitz	Lin. Pert.	SI (10it)	MSI (10it)
$r(\lambda_1)$		0.2642E01	0.664	0.556E-08	0.563E-08
$s(\lambda_1)$	0.387E-27	0.131E01	0.585	0.246E-06	0.246E-06
$r(\lambda_2)$		0.128E01	0.585	0.397E-03	0.397E-03
$s(\lambda_2)$	0.136E-26	0.129E01	0.572	0.397E-03	0.397E-03

DIMENSION 10 ($\lambda_2/\lambda_3 = 0.406$)					
	IMSL	Toeplitz	Lin. Pert.	SI (10it)	MSI (10it)
$r(\lambda_1)$		0.149E01	0.504	0.557E-08	0.829E-05
$s(\lambda_1)$	0.698E-28	0.153E01	0.209	0.250E-06	0.829E-05
$r(\lambda_2)$		0.149E01	0.1028	0.829E-05	0.829E-05
$s(\lambda_2)$	0.386E-26	0.152E01	6.94831	0.829E-05	0.829E-05

Table 10. Comparison of estimated eigenvalues - Example 1

DIMENSION 3					
	IMSL	Toeplitz	Lin. Pert.	SI (10it)	MSI (10it)
λ_1	32.47291	18.36350	32.31153	32.47291	32.47291
λ_2	2.842257	2.816618	2.98768	2.84214	2.84214

DIMENSION 6					
	IMSL	Toeplitz	Lin. Pert.	SI (10it)	MSI (10it)
λ_1	47.86343	32.61854	47.52143	47.86344	47.86344
λ_2	4.109717	4.492380	4.35553	4.10971	4.10971

DIMENSION 10					
	IMSL	Toeplitz	Lin. Pert.	SI (10it)	MSI (10it)
λ_1	56.81421	48.56268	56.72791	56.81421	56.81421
λ_2	6.97541	8.99168	6.94831	6.97541	6.97541

Table 11. Comparison of angle differences - Example 1

DIMENSION 3				
	Toeplitz	Lin. Pert.	SI (10it)	MSI (10it)
θ_1 (in deg.)	4.729	4.232	0.141E-05	0.1415E-05
θ_2 (in deg.)	5.452	6.668	0.592	0.592

DIMENSION 6				
	Toeplitz	Lin. Pert.	SI (10it)	MSI (10it)
θ_1 (in deg.)	10.351	5.037	0.193E-05	0.193E-05
θ_2 (in deg.)	17.008	8.2382	0.904E-01	0.904E-01

DIMENSION 10				
	Toeplitz	Lin. Pert.	SI (10it)	MSI (10it)
θ_1 (in deg.)	17.820	2.367	0.330E-05	0.330E-05
θ_2 (in deg.)	24.913	6.1365	0.113E-01	0.113E-01

Table 12. Performance comparisons of extensions - Example 2

DIMENSION 3 ($\lambda_2/\lambda_3 = 0.834$)					
	IMSL	Toeplitz	Lin. Pert.	SI (10it)	MSI (10it)
$r(\lambda_1)$		0.755E-01	0.123E-01	0.167E-06	0.167E-06
$s(\lambda_1)$	0.864E-28	0.191	0.119E-01	0.258E-06	0.258E-06
$r(\lambda_2)$		0.192	0.98E-01	0.110E-02	0.110E-02
$s(\lambda_2)$	0.726E-27	0.185	0.964E-02	0.110E-02	0.110E-02

DIMENSION 6 ($\lambda_2/\lambda_3 = 0.542$)					
	IMSL	Toeplitz	Lin. Pert.	SI (10it)	MSI (10it)
$r(\lambda_1)$		0.465	0.129E-01	0.594E-07	0.594E-07
$s(\lambda_1)$	0.160E-26	0.295	0.103E-01	0.269E-06	0.269E-06
$r(\lambda_2)$		0.230	0.582E-01	0.313E-04	0.313E-04
$s(\lambda_2)$	0.114E-28	0.228	0.117E-01	0.313E-04	0.313E-04

DIMENSION 10 ($\lambda_2/\lambda_3 = 0.221$)					
	IMSL	Toeplitz	Lin. Pert.	SI (10it)	MSI (10it)
$r(\lambda_1)$		0.336	0.111E-01	0.363E-07	0.381E-07
$s(\lambda_1)$	0.604E-28	0.315	0.415E-02	0.269E-06	0.269E-06
$r(\lambda_2)$		0.236	0.819E-02	0.358E-06	0.364E-06
$s(\lambda_2)$	0.400E-26	0.236	0.792E-02	0.358E-06	0.365E-06

Table 13. Comparison of estimated eigenvalues - Example 2

DIMENSION 3					
	IMSL	Toeplitz	Lin. Pert.	SI (10it)	MSI (10it)
λ_1	32.47291	35.66505	37.85878	37.86682	37.86682
λ_2	2.89845	2.755292	2.60411	2.89839	2.89839

DIMENSION 6					
	IMSL	Toeplitz	Lin. Pert.	SI (10it)	MSI (10it)
λ_1	69.92986	67.09294	69.25076	69.29860	69.29860
λ_2	4.97046	4.80342	4.63745	4.97046	4.97046

DIMENSION 10					
	IMSL	Toeplitz	Lin. Pert.	SI (10it)	MSI (10it)
λ_1	104.88771	103.62096	104.78490	104.88771	104.88771
λ_2	12.89462	12.88180	12.87351	12.89462	12.89462

Table 14. Comparison of angle differences - Example 2

DIMENSION 3				
	Toeplitz	Lin. Pert.	SI (10it)	MSI (10it)
θ_1 (in deg.)	0.940	0.586	0.905E-06	0.522E-06
θ_2 (in deg.)	2.507	1.754	0.408	0.408

DIMENSION 6				
	Toeplitz	Lin. Pert.	SI (10it)	MSI (10it)
θ_1 (in deg.)	1.548	0.537	0.108E-05	0.112E-05
θ_2 (in deg.)	6.105	1.548	0.451E-02	4514E-02

DIMENSION 10				
	Toeplitz	Lin. Pert.	SI (10it)	MSI (10it)
θ_1 (in deg.)	1.869	0.244	0.108E-05	0.116E-05
θ_2 (in deg.)	4.516	0.348	0.674E-05	0.113E-05

Table 15. Comparison of angle differences with different initial matrices - Example 1

DIMENSION 3						
	SI_T(1it)	SI_I(1it)	SI_T(5it)	SI_I(5it)	SI_T(10it)	SI_I(10it)
θ_1 (in deg.)	0.629	7.392	0.158E-4	0.319E-3	0.141E-5	0.113E-5
θ_2 (in deg.)	6.102	56.579	5.864	39.032	0.592	20.918

DIMENSION 6						
	SI_T(1it)	SI_I(1it)	SI_T(5it)	SI_I(5it)	SI_T(10it)	SI_I(10it)
θ_1 (in deg.)	0.835	11.466	0.406E-4	0.437E-3	0.193E-5	0.202E-5
θ_2 (in deg.)	7.569	76.654	0.901	30.550	0.904E-1	3.537

DIMENSION 10						
	SI_T(1it)	SI_I(1it)	SI_T(5it)	SI_I(5it)	SI_T(10it)	SI_I(10it)
θ_1 (in deg.)	1.732	18.415	0.201E-3	0.171E-2	0.33E-5	0.284E-5
θ_2 (in deg.)	7.893	78.744	0.308	7.051	0.113E-1	0.106

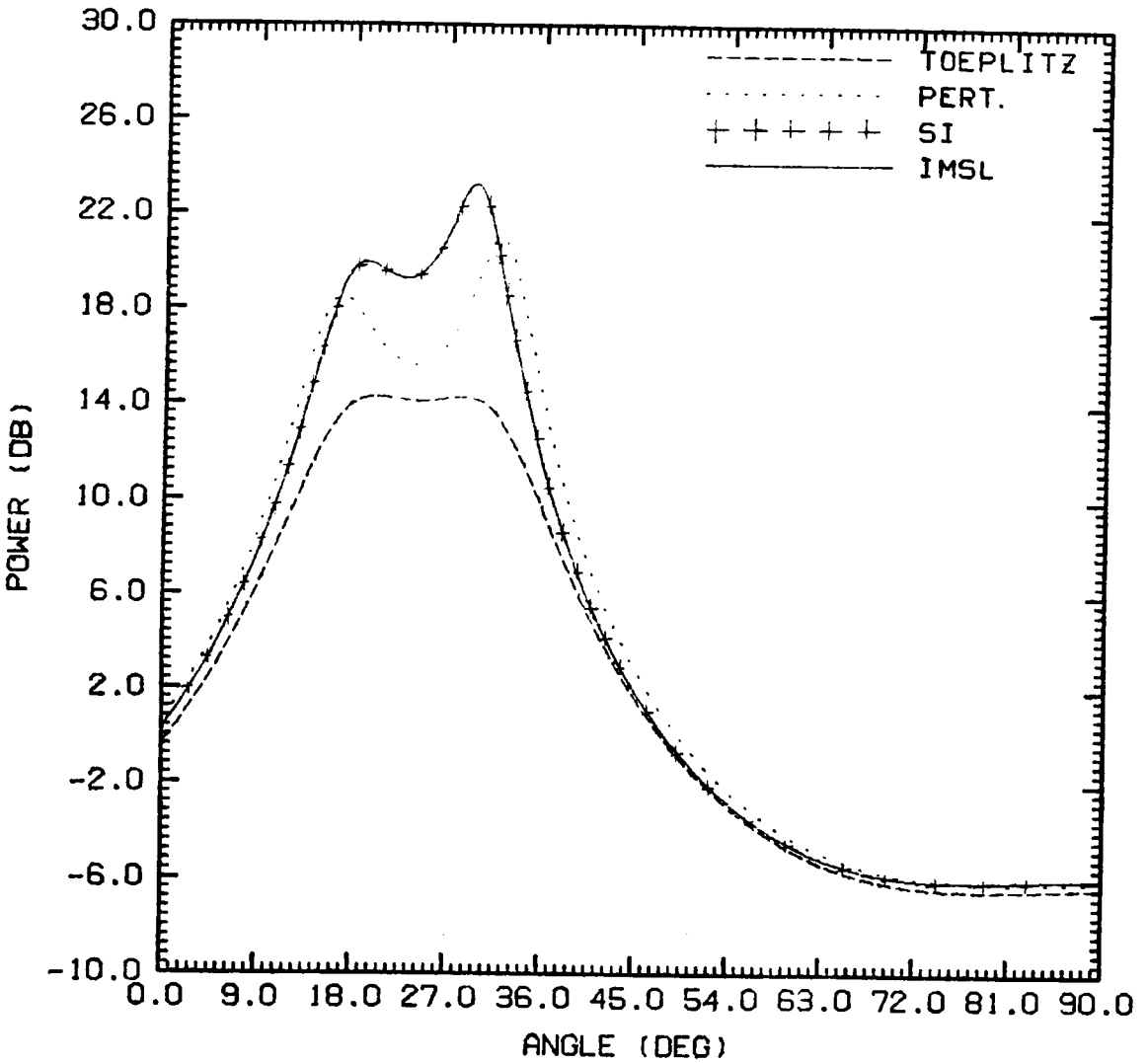

	Toeplitz	Lin. Pert.	SI	IMSL
θ_1	20.039°	16.875°	18.984°	18.984°
θ_2	28.125°	31.992°	29.531°	29.531°

Figure 20. **Estimated Hermitian signal subspace projections - Example 1:** 2 signals at 18° and 30°, SNR = 5dB, 500 snapshots, damping = -0.1, dimension 10

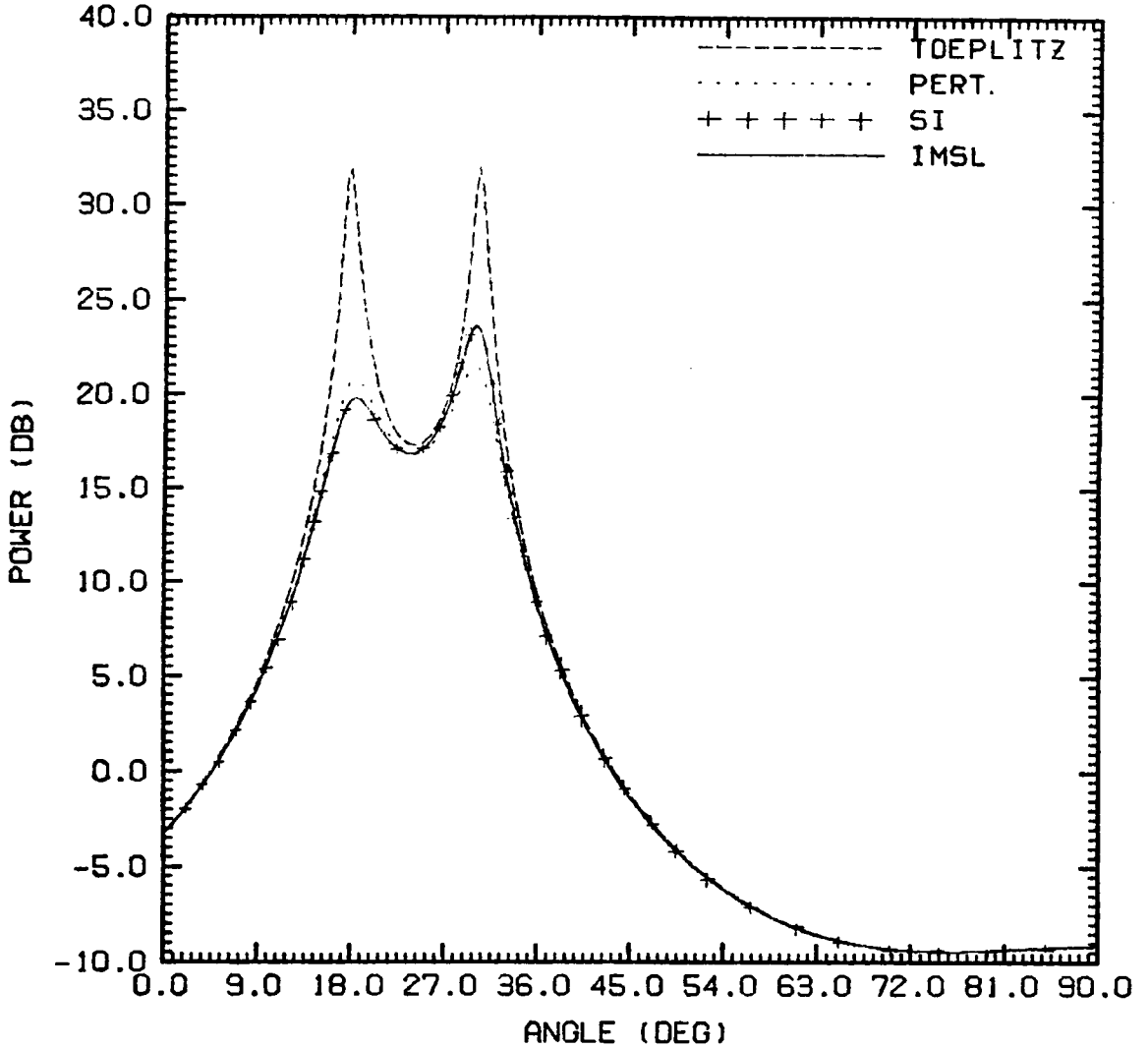

	Toeplitz	Lin. Pert.	SI	IMSL
θ_1	18.631°	18.281°	18.281°	18.281°
θ_2	31.289°	29.883°	29.883°	29.883°

Figure 21. **Estimated Hermitian signal subspace projections - Example 2:** 2 signals at 18° and 30°, SNR = 5dB, 500 snapshots, damping = -0.01, dimension 10

6.0 Conclusions and Recommendations

We have presented a new recursive/iterative Toeplitz Hermitian eigenspace (**RITE**) procedure and its extension to the generalized eigenspace (**C-RITE**) problem. Both procedures exhibit highly parallel computational features, and have been applied here to passive array processing. The derivation of the RITE algorithm has been presented in Chapter 2. RITE uses the Toeplitz Hermitian structure of the matrix to recursively compute in increasing order, successive eigendecompositions of the submatrices imbedded in the original problem. At each order, a number of independent, structurally identical, non-linear problems is solved in parallel. The eigenvalues can be found by quadratically convergent iterative search techniques. Two different eigenvalue search methods, a restricted Newton approach and a rational approximation based search technique, have been investigated. The restricted Newton approach is computationally cheap, performs well, and is more suitable for problems of small dimension. The rational approximation based search technique seems more competitive for large dimensional ones. The eigenvectors can be found efficiently by solving Toeplitz systems. The minimal multiple eigenvalue case and the case of a clustered set of small eigenvalues are also treated. Both use information already available from the decomposition at the previous rank to directly identify all but one of the eigenvectors associated with the multiple eigenvalue or the set of clustered eigenvalues. The case of a clustered set of small eigenvalues is solved by first assuming the eigenvalues to be identical to

get estimates of the corresponding eigenvectors, followed by correcting this assumption by using one iteration of the shifted inverse power method.

The modifications needed for the generalized eigendecomposition problem (R,B) presented in Chapter 3, C-RITE, turn out to be easy to implement. It is of practical importance that no factorization of the noise matrix B is required for this procedure. The main differences with RITE lie in the definition of the generalized eigenvalue functions, and the generalized inner products needed for the multiple eigenvalue case or the case of a set of clustered generalized eigenvalues. Residual norm and orthonormality norm performance checks, when compared with those for the IMSL library (version 9.2) routines EIGCH and EIGZC, indicate good stability behavior of RITE and C-RITE for increasing dimensions.

Applications of our procedures to the Direction of Arrival identification problem, using the MUSIC algorithm, were presented in Chapter 4. The order-recursive properties of RITE and C-RITE permit estimation of angles for intermediate orders imbedded in the original problems, facilitating the earliest possible estimation of the number of sources. The detection algorithm based on RITE or C-RITE can then stop, thereby minimizing the overall computational load to that corresponding to the smallest order for which angle of arrival estimation is indicated to be reliable.

Extensions of the RITE procedure to Hermitian non-Toeplitz matrices have been considered in Chapter 5. In the array processing context, this corresponds for instance to correlation matrices estimated from non-linear arrays or incoming signals with non-stationary characteristics. Two different procedures have been considered; a first-order perturbation approach and a Subspace Iteration (SI) based method. These techniques take advantage of the fast RITE eigen-information by using the Toeplitz eigendecomposition as an initial approximation of the desired Hermitian eigen-information. Results show that the SI based techniques lead to a good approximation of the Hermitian eigen-information, with the rate of convergence depending upon the SNR and the angle difference between incoming sources.

Recommendations

Two different iterative search techniques have been proposed for the (generalized) eigenvalue search portion of the procedures. Additional study would be needed to define the optimal range of application for each of these methods. Furthermore, additional analyses of the eigenvalue interpolants in a finite-precision environment would be of practical interest. Note that among the interpolants that produce efficient and stable calculation, only upper bounding interpolants were available. This produced an upper quadrant approximation of the root, as opposed to the left quadrant approximation resulting from the approach by Bunch et al. The upper quadrant approximation, as defined, is not insured to converge monotically to the root, yet we saw that the approximations are quite good. Nevertheless, the absence of monotone convergence to the root could potentially introduce accumulation errors in the evaluation of the (generalized) eigenvalue search function, which then could accumulate from step to step. Although, this has not appeared on any of the runs performed to date, strict guarantees of stability are desired prior to detailed consideration of implementation issues for high performance applications, such as occur in VLSI design.

The RITE and C-RITE algorithms have been designed for Hermitian Toeplitz structures, and eigenvectors are presently found using fast Toeplitz solvers and a vector iteration, if needed. For non-Toeplitz Hermitian matrices or pencils, the corresponding eigenvectors may still be recovered with a vector iteration. However, a potentially preferable approach, more conducive to high performance implementation, would involve a non-iterative process. After many conversations with Dr. C.A. Beattie (VPI&SU, Department of Mathematics) [BFB], it appears that such an approach, based on an idea presented earlier by Bunch et al [BNS], would be possible. The non-iterative eigenvector task would involve direct computation of eigenvectors associated with distinct eigenvalues, and a process of deflation to compute eigenvectors associated with multiple eigenvalues. A careful study and analysis of eigenvector accuracy when round-off errors are introduced would have to be conducted.

Finally, adding adaptive capability to RITE, C-RITE, and their Hermitian upgrade would be very useful. Adaptive algorithms which can update (in time) and forget (exponentially) the

eigen-information by using new data samples are very useful to track moving sources. Such an extension will give the procedures the ability of tracking moving sources during the course of repeated extension in subproblem dimensions, thereby taking full advantage of the latest information available. A first potential adaptive extension would be to consider the tracking of time-varying signals in a stationary noise environment. For tracking of time-varying narrow-band signals, windowing of the received signal before estimating the correlation matrix is usually introduced to emphasize the most recent data available. Recall that the p-dimensional correlation matrix $R_p^{(k)}$ estimated from k snapshots can be expressed as

$$R_p^{(k)} = X_p X_p^* = \underline{x}^{(1)}\underline{x}^{(1)*} + \cdots + \underline{x}^{(k)}\underline{x}^{(k)*} \tag{155}$$

The addition of new information to the data matrix X_p, in the form of data vector $\underline{x}^{(k+1)}$, results in the rank-one modified matrix

$$R_p^{(k+1)} = R_p^{(k)} + \underline{x}^{(k+1)}\underline{x}^{(k+1)*} \tag{156}$$

A time varying correlation matrix $\tilde{R}_p^{(k+1)}$ can then be recursively defined as

$$\tilde{R}_p^{(k+1)} = \alpha \tilde{R}_p^{(k)} + (1-\alpha)\underline{x}^{(k+1)}\underline{x}^{(k+1)*} \tag{157}$$

where $\tilde{R}_p^{(1)} \triangleq \underline{x}^{(1)}\underline{x}^{(1)*}$, and α is an exponential forgetting memory factor defined in [0, 1]. Note that the forms of (156) and (157) are both rank-one modifications.

With the introduction of adaptive capability to the order recursive technique, a new problem formulation would result. Now, assuming the (p-1)-dimensional eigendecomposition of (R_{p-1}, B_{p-1}) to be known, the problem is to compute efficiently the eigendecomposition of the pencil $(\dot{R}_p, B_p)$, where

$$\dot{R}_p = \begin{bmatrix} R_{p-1} + \rho \underline{z}\underline{z}^* & \underline{r} \\ \underline{r}^* & r_0 \end{bmatrix} \quad \text{and} \quad B_p = \begin{bmatrix} B_{p-1} & \underline{b} \\ \underline{b}^* & b_0 \end{bmatrix} \tag{158}$$

where $\rho \underline{z}\underline{z}^*$ represents the additional rank-one correlation information. Thus, the above is equivalent to simultaneously performing a rank-one modification and a rank-one extension of the original problem. The associated generalized eigenvalue search function can be defined using [BEA,BE2] but is more complex. Note that we are actually performing a rank-two perturbation of the original pencil (R_{p-1}, B_{p-1}) [PAR]. In such a case, the Cauchy interlace theorem no longer guarantees the updated eigenvalues of $(\dot{R}_p, B_p)$ to be between adjacent eigenvalues of (R_p, B_p). Spectrum slicing formulas developed in [BEA,BE2] could then be used to regain the finer level of a-priori localization we used for parallel computation advantage.

The next logical step would be to study the potential extension of the adaptive upgrade discussed above to signals in the time-varying colored noise situation. Following the framework discussed earlier, the problem would then be to compute efficiently the eigenstructure of the matrix pencil $(\dot{R}_p, \dot{B}_p)$, where $\dot{R}_p$ and $\dot{B}_p$ are both time-varying, and given by

$$\dot{R}_p = \begin{bmatrix} R_{p-1} + \rho_1 \underline{z}\underline{z}^* & \underline{r} \\ \underline{r}^* & r_0 \end{bmatrix} \quad \text{and} \quad \dot{B}_p = \begin{bmatrix} B_{p-1} - \rho_2 \underline{y}\underline{y}^* & \underline{b} \\ \underline{b}^* & b_0 \end{bmatrix} \tag{159}$$

where the eigen-information of (R_{p-1}, B_{p-1}) is assumed to be known. It is expected that methods that can be applied for the rank-one extension or the rank-one modification problem would prove effective for this problem setting. Feasibility of deflation and numerical stability of the eigenvector computations would have to be carefully investigated also.

References

[AIK]: H. Akaike, "A New Look at the Statistical Model Identification," IEEE Trans. Autom. Contr., Vol. AC-19, 1974, pp. 716-723.

[AN1]: A.L. Andrew, "Eigenvectors of Certain Matrices," Linear Algebra and its Applications, Vol. 7, 1973, pp. 151-162.

[AN2]: ----------, "Further Comments on: On the Eigenvectors of Symmetric Toeplitz Matrices," IEEE Trans. Acoust., Speech, Signal Processing, Vol. ASSP-33, No. 4, Aug. 1985, p. 1013.

[BAE]: E.H. Bareiss, "Numerical Solutions of Linear Equations with Toeplitz and Vector Toeplitz Matrices," Num. Math., Vol. 13, 1969, pp. 404-424.

[BAR]: A.J. Barabell, "Improving the Resolution Performance of Eigenstructure-Based Direction-Finding Algorithms," ICASSP-83, pp. 336-339.

[BEA]: C.A. Beattie and D. Fox, "Schur Complements and the Weinstein-Aronszajn Theory for Modified Matrix Eigenvalue Problems," UMSI Report, Nov. 1987.

[BE1]: C.A. Beattie, "An Extension of Aronszajn's Rule: Slicing the Spectrum for Intermediate Problems," SIAM J. Num. Anal., Vol. 24, No. 4, 1987, pp. 828-843.

[BE2]: ----------, Private Communications, VPI&SU, 1988.

[BFB]: C.A. Beattie, M.P. Fargues, A.A. (Louis) Beex, "Rank-One Extensions of the Generalized Hermitian Eigenvalue Problem for High Resolution Array Processing," submitted to NATO/ASI on Numerical Linear Algebra, Digital Signal Processing and Parallel Algorithms, Leuven, Belgium, August 1-12, 1988.

[BF1]: A.A. Beex, M.P. Fargues and V.E. DeBrunner, "Fast Recursive/Iterative Eigenspace Decomposition," *Final Report,* Center for Innovative Technology grant number INF-85-020 and SPERRY Corporation grant number V120483, June 1987.

[BF2] : ----------,"Fast High-Resolution Non-Linear Array Processing," *Final Report*, Center for Innovative Technology Grant# INF-86-018 and UNISYS (SPERRY) Corporation Grant# V120483, November 1987.

[BF3] : ----------,"Fast Recursive/Iterative Toeplitz Eigenspace Decomposition," submitted to IEEE Trans. Acoust., Speech, Signal Processing (in review process).

[BGY] : R.P. Brent, F.G. Gustavson and D.Y. Yun, "Fast Solutions of Toeplitz Systems of Equations and Computation of Pade Approximants," J. of Algorithms, Vol. 1, 1980, pp. 259-295.

[BIA] : R.R. Bitmead and B.D.O. Anderson, "Asymptotically Fast Solution of Toeplitz Systems of Equations and Computations of Pade Approximants," J. of Algorithms, Vol. 1, 1980, pp. 259-295.

[BIE] : G. Bienvenu, "Underwater Passive Detection and Spatial Coherence Testing," JASA 1979, pp. 425-437.

[BNS] : J.R. Bunch, C.P. Nielsen and D.C. Sorensen, "Rank-One Modification of the Symmetric Eigenproblem," Numer. Math., Vol. 31, No. 31, 1978, pp. 31-48.

[BRK] : Y. Bresler, V.U. Reddi and T. Kailath, "A Polynomial Approach to Optimum Beamforming for Correlated or Coherent Signals and Interferences," Proc. IEEE ICASSP-87, pp. 53.9.1-4.

[BRL] : R.P. Brent and F.T. Luk, "A Systolic Array for the Linear-Time Solution of Toeplitz Systems of Equations," J. of VLSI and Comp. Syst., Vol. 1, No. 1, 1983, pp. 1-22.

[BRO] : T.P. Bronez and J.A. Cadzow, "An Algebraic Approach to Superresolution Array Processing," IEEE Trans. on Aerosp. Electron. Syst., Vol. AES-19, No. 1, 1983, pp. 123-133.

[BU1] : J.R. Bunch, "Stability of Methods for Solving Toeplitz Systems of Equations," SIAM J. Sci. Stat. Comp., Vol. 6, No. 2, April 1985, pp. 349-364.

[BU2] : ----------, "The Weak and Strong Stability of Algorithms in Numerical Linear Algebra," Linear Algebra and its Applications, Vol. 88, No. 89, 1987, pp. 49-66.

[BU3] : ---------, "Stability, strong stability, and weak stability of algorithms for solving linear equations," Proc. of SPIE, Vol. 696, Aug. 1986, San Diego, CA, pp.19-22.

[BX1] : A.A. Beex, "Fast Recursive/Iterative Toeplitz Eigenspace Decomposition," European Signal Processing Conference (EUSIPCO-86), The Hague, The Netherlands, Sept. 2-5 1986, pp. 1001-1004.

[BX2] : ---------, "Efficient Generation of ARMA Cross-Covariance Sequences," Proc. IEEE ICASSP-85, pp. 9.7.1-4.

[CAB] : A. Cantoni and P. Butler, "Eigenvalues and Eigenvectors of Symmetric CentroSymmetric Matrices," Linear Algebra and its Applications, Vol. 13, 1976, pp. 275-288.

[CAD] : J.A. Cadzow, "SVD Representation of Unitarily Invariant Matrices," IEEE Trans. Acoust., Speech, Signal Processing, Vol. ASSP-32, No. 3, June. 1984, pp. 512-516.

[CYV] : G. Cybenko and C. Van Loan, "Computing the Minimum Eigenvalue of a Symmetric Positive Definite Toeplitz Matrix," SIAM J. Sci. Stat. Comput., Vol. 7, No. 1, Jan. 1986, pp. 123-131.

[CY1] : G. Cybenko, "The Numerical Stability of the Levinson-Durbin Algorithm for Toeplitz Systems of Equations," SIAM J. Sci. Stat. Comput., Vol. 1, No. 3, Sept. 1980, pp. 303-319.

[CY2] : G. Cybenko, "The Sensitivity of Beamforming Problems," 3rd. ASSP Workshop on Spectrum Estimation and Modelling, Nov. 17-18, 1986, pp. 176-177.

[DEG] : P. Delsarte and Y. Genin, "Spectral Properties of Finite Toeplitz matrices," Proc. Int. Symp. Math. Theory of Networks and Syst., Israel, 1983.

[DEK] : P. Delsarte, Y.V. Genin and Y.G. Kamp, "A Generalization of the Levinson Algorithm for Hermitian Toeplitz Matrices with any Rank Profile," IEEE Trans. Acoust., Speech, Signal Processing, Vol. ASSP-33, No. 4, Aug. 1985, pp. 964-971.

[DEM] : A. Dembo, "Bounds on the Extreme Eigenvalues of Positive-Definite Toeplitz Matrices," IEEE Trans. on Inf. Th., Vol. IT-34, No. 2, March 1988, pp. 352-355.

[DER] : R.D. DeGroat and R.A. Roberts, "Highly Parallel Eigenvector Update Methods with Applications to Signal Processing," Proc. of SPIE, Vol. 696, 1986, pp. 62-70.

[DGK] : J.W. Daniel, W.B. Gragg, L. Kaufman and G.W. Stewart, "Reorthogonalization and Stable Algorithms for Updating the Gram-Schmidt QR Factorization," Math. Comput., Vol. 30, No. 136, Oct. 1976, pp. 772-795.

[DOS] : J.J. Dongarra and D.C. Sorensen, "A Fully Parallel Algorithm for the Symmetric Eigenvalue Problem," SIAM J. Sci. Stat. Comput., Vol. 8, No. 2, March 1987, pp. 139-154.

[DUR] : J. Durbin, "The fitting of Time-Series Models," Rev. Inst. Internat. Statist., No. 28, 1960, pp. 233-244.

[FA1] : M.P. Fargues and A.A. Beex, "Efficient Generalized Toeplitz Eigenspace Decomposition," Proc. 21st Asilomar Conference on Signals, Systems, and Computers, Pacific Grove, CA, Nov. 2-4, 1987.

[FA2] : ----------, "Fast Order-Recursive Generalized Hermitian Toeplitz Eigenspace Decomposition," Submitted to Mathematics of Control, Signals, and Systems.

[FOK] : R. Foka, "Properties of Toeplitz Approximation Method (TAM) for Direction Finding Problems," Proc. IEEE ICASSP-87, pp. 2233-2236.

[FUL] : D.R. Fuhrmann and B. Liu, "A Perturbation Approach to Improving Pisarenko Harmonic Retrieval," Proc. 22nd Annual Allerton Conference on Communication, Control, and Computing, Monticello, Il., Oct. 1984, pp. 891-900.

[GAT] : F.R. Gantmacher, *The Theory of Matrices,* Chelsea Publishing Company, New York, NY, 1974

[GOL] : G.H. Golub, "Some Modified Matrix Eigenvalue Problems," SIAM Review, Vol. 15, No. 2, April 1973, pp. 318-334.

[GUE] : C. Gueguen and F. Gianella, "Extractions des Vecteurs Propres de Matrices de Toeplitz," GRETSI, Nice, France, June 1981.

[GUS] : C. Gueguen and M. Sidahmed, "The Singular Case and Robust Linear Prediction," IEEE Proc. ICASSP-82, Paris, France, 1982, pp. 1371-1374.

[GVL] : G.H. Golub and C.F. Van Loan, *Matrix Computations*, Johns Hopkins Univ. Press, 1983.

[HAC] : M.H. Hayes and M.A. Clements, "An Efficient Algorithm for Computing Pisarenko's Harmonic Decomposition using Levinson's Recursion," IEEE Trans. Acoust., Speech, Signal Processing, Vol. ASSP-34, No. 3, June 1986, pp. 485-491.

[HOO] : F. de Hoog, "A New Algorithm for Solving Toeplitz Systems of Equations," Linear Algebra and its Applications, Vol. 88, No. 89, 1987, pp. 123-138.

[HWK] : H. Hung, H. Wang and M. Kaveh, "Further Results on Coherent Signal-Subspace Processing," Proc. IEEE ICASSP-86, pp. 97-100.

[IMS] : IMSL (Version 9.2) User's Guide.

[JAI] : J.R. Jain, "An Efficient Algorithm for a Large Toeplitz Set of Linear Equations," IEEE Trans. Acoust., Speech, Signal Processing, Vol. ASSP-27, No. 6, Dec. 1979, pp. 612-615.

[JD1] : D.H. Johnson and S.R. DeGraaf, "Improving the Resolution of Bearing in Passive Sonar Arrays by Eigenvalue Analysis," IEEE Trans. Acoust., Speech, Signal Processing, Vol. ASSP-29, Aug. 1982, pp. 401-413.

[JD2] : ----------, "Capability of Array Processing Algorithms to Estimate Source Bearings," IEEE Trans. Acoust., Speech, Signal Processing, Vol. ASSP-33, No. 6, Dec. 1985, pp. 1368-1379.

[JNF] : J. N. Franklin, *Matrix Theory*, Prentice-Hall, Inc., Englewood Cliffs, New Jersey, 1968.

[JOH] : D.H. Johnson and S.R. DeGraaf, "Improving the Resolution of Bearing in Passive Sonar Arrays by Eigenvalue Analysis," IEEE Trans. Acoust., Speech, Signal Processing, Vol. ASSP-29, Aug. 1982, pp. 401-413.

[JOM] : R.L. Johnson and G.E. Miner, "Comparison of Superresolution Algorithms for Radio Direction Finding," IEEE Trans. on Aerosp. Electron. Syst., Vol. AES-22, No. 4, July 1986, pp. 432-441.

[KAB] : M. Kaveh and A. Barabell, "The Statistical Performance of the MUSIC and the Minimum-Norm Algorithms in Resolving Plane Waves in Noise," IEEE Trans. Acoust., Speech, Signal Processing, Vol. ASSP-34, April 1986, pp. 331-340.

[KAR] : J. Karhunen, "Adaptive Algorithms for Estimating Eigenvectors of Correlation Matrices," Proc. IEEE ICASSP-84, pp. 14.6.1-4.

[KAY] : S. Kay and S.L. Marple, "Spectrum Analysis - A Modern Perspective," Proc. IEEE, Vol. 69, No. 11, Nov. 1981, pp. 1380-1419.

[KIT] : I.P. Kirsteins and D.W. Tufts, "On the Probability Density of Signal-to-Noise Ratio in an Improved Adaptive Detector," Proc. IEEE ICASSP-85, pp. 15.6.1-4.

[KKM] : T. Kailath, S-Y. Kung and M. Morf, "Displacement Ranks of Matrices and Linear Equations," Journal of Math. Anal. and Appl., Vol. 68, 1979, pp. 395-407.

[KLF] : S.Y. Kung, C.K. Lo and R. Foka, "A Toeplitz Approximation Approach to Coherent Direction Finding," Proc. IEEE ICASSP-86, pp. 5.1.1-4.

[KUA] : R. Kumar, "A Fast Algorithm for Solving a Toeplitz System of Equations," IEEE Trans. Acoust., Speech, Signal Processing, Vol. ASSP-33, No. 1, Feb. 1985, pp. 254-267.

[KU1] : S-Y. Kung and Y. Hu, "A Highly Concurrent Algorithm and Pipelined Architecture for Solving Toeplitz Systems," IEEE Trans. Acoust., Speech, Signal Processing, Vol. ASSP-31, No. 1, Feb. 82, pp. 66-75.

[KU2] : ----------, "Toeplitz Eigensystem Solver," IEEE Trans. Acoust., Speech, Signal Processing, Vol. ASSP-33, No. 5, Oct. 1985, pp. 1264-1271.

[KUM] : R. Kumaresan, "Estimating the Parameters of Exponentially Damped or Undamped Sinusoidal Signals in Noise," Ph.D. Dissertation, University of Rhode Island, Kingston, RI, 1982.

[KUN] : S.Y. Kung, H.J. Whitehouse and T. Kailath, *VLSI and Modern Signal Processing*, Prentice Hall, 1985, pp. 53-56.

[KUT] : R. Kumaresan and D.W. Tufts, "Improved Spectral Resolution 3: Efficient Realization," Proc. of the IEEE, Vol. 68, No. 10, Oct. 1980, pp. 1354-1355.

[LAU] : D.P. Laurie, "A Numerical Approach to the Inverse Toeplitz Eigenproblem," SIAM J. Sci. Stat. Comput., Vol. 9, No. 2, March 1988, pp. 401-405.

[LAW] : D.N. Lawley, "Tests of Significance of the Latent Roots of the Covariance and Correlation Matrices," Biometrica, Vol. 43, 1956.

[LEV] : N. Levinson, "The Wiener RMS Error Criterion in Filter Design and Prediction," J. Math. Phy. 25, 1947, pp. 261-278.

[MAK] : J. Makhoul, "On the Eigenvectors of Symmetric Toeplitz Matrices," IEEE Trans. Acoust., Speech, Signal Processing, Vol. ASSP-29, No. 4, Aug. 1981, pp. 868-872.

[MAR] : K.V. Mardia, J.T. Kent and J.M. Bibby, *Multivariate Analysis*, Academic Press, 1979.

[MAT] : G.E. Martin, "Degradation of Angular Resolution for Eigenvector-Eigenvalue (EVEV) High-Resolution Processors with Inadequate Estimation of Noise Coherence," Proc. IEEE ICASSP-84, pp. 33.13.1-4.

[MOB] : R.L. Moses and A.A. (Louis) Beex, "Instrumental Variable Array Processing," IEEE Trans. on Aerosp. Electron. Syst., Vol. AES-24, No. 2, 1988, pp. 192-202.

[MOR] : M. Morf, "Doubling Algorithms for Toeplitz and Related Equations," IEEE Proc. ICASSP-80, pp. 954-959.

[OR1] : S.J. Orfanidis, "A Reduced MUSIC Algorithm," 3rd ASSP workshop on Spectrum Estimation and Modelling, Nov. 1986, Boston, Ma, pp. 165-167.

[OR2] : ----------, "Pole Retrieval by Eigenvector Methods," Proc. IEEE ICASSP-87, pp. 35.8.1-4.

[ORF] : ----------, *Optimum Signal Processing: An Introduction*, Macmillan Publishers, New York, 1985.

[PAK] : A. Paulraj and T. Kailath, "Eigenstructure Methods for Direction of Arrival Estimation in the Presence of Unknown Noise Fields," IEEE Trans. Acoust., Speech, Signal Processing, Vol. ASSP-34, No. 1, Feb. 1986, pp. 13-20.

[PAR] : B.N. Parlett, *The Symmetric Eigenvalue Problem*, Prentice-Hall, Inc., 1980.

[PIS] : V.F. Pisarenko, "The Retrieval of Harmonics from a Covariance Function," Geophys. J. Roy. Astron. Soc., Vol. 33, pp. 247-266, 1973.

[POF] : B. Porat and B. Friedlander, "On the Accuracy of the Kumaresan-Tufts Method for Estimating Complex Damped Exponentials," IEEE Trans. Acoust., Speech, Signal Processing, Vol. ASSP-35, No. 2, Feb. 1987, pp. 231-235.

[PWM] : S. Prasad, R.T. Williams, A.K. Mahalanobis and L.H. Sibul, "A Transform Based Covariance Differencing Approach to Bearing Estimation," Proc. IEEE ICASSP-87, pp. 26.10.1-4.

[RED] : S.S. Reddi, "Multiple Source Location - A Digital Approach," IEEE Trans. on Aerosp. Electron. Syst., Vol. AES-15, pp. 95-105.

[REI] : ----------, "Eigenvector Properties of Toeplitz Matrices and their Application to Spectral Analysis of Time Series," Signal Processing, Vol. 7, 1984, pp.45-56.

[ROK] : R. Roy and T. Kailath, "Total Least-Squares ESPRIT," Proc. 21st Asilomar Conference on Signals, Circuits, and Systems, Pacific Grove, CA, Nov. 2-4, 1987.

[RPK] : R. Roy, A. Paulraj and T. Kailath, "ESPRIT - A Subspace Rotation Approach to Estimation of Parameters of Cisoids in Noise," IEEE Trans. Acoust., Speech, Signal Processing, Vol. ASSP-34, No. 5, Oct. 1986, pp. 1340-1342.

[RI1] : J. Rissanen, "Modelling by Shortest Data Description," Automatica, Vol. 14, 1978, pp.465-471.

[RI2] : ----------, "A Universal Prior for Integers and Estimation by Minimum Description Length," Ann. Stat., Vol. 11, No. 2, 1983, pp. 416-431.

[SAK] : H. Sakai, "Estimation of Frequencies of Sinusoids in Colored Noise," Proc. IEEE ICASSP-86, pp. 177-180.

[SCH] : R.O. Schmidt, "A Signal Subspace Approach to Multiple Emitter Location and Spectral Estimation," Ph.D. Dissertation, Stanford University, Stanford, CA, Nov. 1981.

[SHA] : K.C. Sharman, "Adaptive Algorithms for Estimating the Complete Covariance Eigenstructure," Proc. IEEE ICASSP-86, pp. 27.15.1-4.

[SHK] : T.J. Shan and T. Kailath, "Directional Signal Separation by Adaptive Arrays with a Root-Tracking Algorithm," Proc. IEEE ICASSP-86, pp. 53.8.1-4.

[SWK] : T.J. Shan, M. Wax and T. Kailath, "On Spatial Smoothing for Direction-of-Arrival Estimation of Coherent Signals," IEEE Trans. Acoust., Speech, Signal Processing, Vol. ASSP-33, No. 4, Aug. 1985, pp. 806-811.

[SWZ] : G. Schwartz, "Estimating the Dimension of a Model," Ann. Stat., Vol. 6, 1978, pp. 461-464.

[SIB] : L.H. Sibul and S.E. Burke, "Error Analysis on Eigenvector Preprocessors used in Adaptive Beamforming," Proc. IEEE ICASSP-85, pp. 46.9.1-4.

[SPK] : D. Spielman, A. Paulraj and T. Kailath, "Performance Analysis of the MUSIC Algorithm," Proc. IEEE ICASSP-86, pp. 35.24.1-4.

[TUM] : D.W. Tufts and C.D. Melissinos, "Simple, Effective Computation of Principal Eigenvectors and their Eigenvalues and Application to High-Resolution Estimation of Frequencies," IEEE Trans. Acoust., Speech, Signal Processing, Vol. ASSP-34, No. 5, Oct. 1986, pp. 1046-1053.

[TR1] : F.B. Tuteur and Y. Rockah, "A New Method for Signal Detection and Estimation using the Eigenstructure of the Covariance Difference," Proc. IEEE ICASSP-86, pp. 52.5.1-4.

[TR2] : ----------, "The Covariance Difference Method in Signal Detection," 3rd. ASSP Workshop on Spectrum Estimation and Modelling, Nov. 17-18, Boston, 1986, pp. 120-122.

[VAC] : R.J. Vaccaro, "On Adaptive Implementations of Pisarenko's Harmonic Retrieval Method," Proc. IEEE ICASSP-84, pp. 6.1.1-4.

[VAK] : R.J. Vaccaro and A.C. Kot, "A Perturbation Theory for the Analysis of SVD-Based Algorithms," Proc. ICASSP-87, pp. 37.8.1-4.

[WAK] : M. Wax and T. Kailath,"Detection of Signals by Information Theoretic Criteria," IEEE Trans. Acoust., Speech, Signal Processing, Vol. ASSP-33, Apr. 1985, pp. 387-392.

[WAL] : R.S. Walker, "Bearing Accuracy and Resolution Bounds of High-Resolution Beamformers," Proc. ICASSP-85, pp. 46.3.1-4.

[WA1] : ----------,"Extending the Threshold of the Eigenstructure Methods," Proc. IEEE ICASSP-85, pp. 556-559.

[WIH] : D.M. Wilkes and M.H. Hayes, "An Eigenvalue Recursion for Toeplitz Matrices," IEEE Trans. Acoust., Speech, Signal Processing, Vol. ASSP-35, No. 6, June 1987, pp. 907-909.

[WIL] : J.H. Wilkinson, *The Algebraic Eigenvalue Problem* , Clarendon Press, Oxford, 1965.

[WKV] : H. Wang and M. Kaveh, "Performance of NarrowbSignal-Subspace Processing," Proc. ICASSP-86, pp. 12.6.1-4.

[WK1] : ----------, "Sensitivity and Performance Analysis of Coherent Signal-Subspace Processing for Multiple Wideband Sources," Proc. ICASSP-85, pp. 17.6.1-4.

[WK2] : ----------, "Coherent Signal Subspace Processing for the Detection and Estimation of Angles of Arrival of Multiple Wide-Band Sources," IEEE Trans. Acoust., Speech, Signal Processing, Vol. ASSP-33, No. 4, Aug. 1985, pp.823-831.

[ZDB] : L-C. Zhao, P.R. Krishnaiah and Z-D. Bai, "Remarks on Certain Criteria for Detection of Number of Signals," IEEE Trans. Acoust., Speech, Signal Processing, Vol. ASSP-35, No. 2, Feb. 1987, pp. 129-132.

[ZO1] : S. Zohar, "Fortran Subroutines for the Solution of Toeplitz Sets of Linear Equations," IEEE Trans. Acoust., Speech, Signal Processing, Vol. ASSP-27, No. 6, Dec. 1979, pp. 656-658.

[ZO2] : ---------, "Corrections to - Fortran Subroutines for the Solution of Toeplitz Sets of Linear Equations," IEEE Trans. Acoust., Speech, Signal Processing, Vol. ASSP-28, No. 5, Oct. 1980, p. 601.

[ZO3] : ---------, "Toeplitz Matrix Inversion: The Algorithm of W.F. Trench," ACM, Vol. 16, No. 4, Oct. 1969, pp. 592-601.

[ZO4] : ---------, "The Solution of a Toeplitz Set of Linear Equations," ACM, Vol. 21, No. 2, Apr. 1974, pp. 272-276.

[ZOL] : M.D. Zoltowski, "Solving the Semi-Definite Generalized Eigenvalue Problem with Application to ESPRIT," Proc. ICASSP-87, pp. 54.5.1-4.

Appendix A. Complex Version of the Zohar Algorithm.

```
C*************************************************************************
C       SUBROUTINE -TPLIZ6-
C       The algorithm presented by Zohar (for real Toeplitz matrices)
C       is extended here to the
C       case of a complex Hermitian Toeplitz system of equations.
C
C   ---------------------------------------------------------------------
C
C              R*X = SD   (ORDER M)
C
C     Reference : S. ZOHAR, Fortran Subroutines for the Solution
C                 OF Toeplitz Sets of Linear Equations.
C                 ASSP-27, NB. 6, DEC. 79
C                + Correction to the article : S. ZOHAR
C                 ASSP-28, NB. 5, OCT. 80
C
C         RESTRICTION : Strongly Regular Square Matrix.
C
C       INPUT PARAMETERS :
C       M     : dimension of the system,
C       R0    : main diagonal element of the matrix,
C       RT(.) : contains the remainder of the first column of the
C               matrix,
C       AT(.) : contains the remainder of the first row of the
C               matrix,
C       SDT(.): contains the right-hand side vector in input,
C               on return it contains the solution vector,
C       ET(.), GT(.) :  work arrays.
C
C*************************************************************************
C
C
        SUBROUTINE TPLIZ6(M,R0,RT,AT,SDT,ET,GT)
        IMPLICIT COMPLEX (A-H,O-Z)
```

```
      COMPLEX RT(M),SDT(M),ET(M),AT(M),GT(M)
      REAL RO
C
      N=M-1
      T=1./RO
      DO 14 I=1,N
      RT(I)=T*RT(I)
      AT(I)=T*AT(I)
   14 SDT(I)=T*SDT(I)
      SDT(M)=T*SDT(M)
C
      ET(1)=-AT(1)
      GT(1)=-RT(1)
      FLAMDA=1.-AT(1)*RT(1)
C
      DO 02 I=1,N
      IP=I+1
      TETLAM=SDT(IP)
      ETALAM=-AT(IP)
      GAMLAM=-RT(IP)
C
      DO 03 J=1,I
      IMJ=IP-J
      TETLAM=TETLAM - RT(J)*SDT(IMJ)
      GAMLAM=GAMLAM - RT(J)*GT(IMJ)
      ETALAM=ETALAM - AT(J)*ET(IMJ)
   03 CONTINUE
C
      TETLAM = TETLAM/FLAMDA
C
      DO 09 J=1,I
      IMJ=IP-J
      SDT(J)= SDT(J) +TETLAM*ET(IMJ)
   09 CONTINUE
C
      SDT(IP)=TETLAM
      IF(I-N) 11,2,2
   11 GAMLAM=GAMLAM/FLAMDA
      T=ETALAM
      ETALAM=ETALAM/FLAMDA
      FLAMDA=FLAMDA - T*GAMLAM
C
      DO 06 J=1,I
      IMJ=IP-J
      T=ET(J)
      ET(J) = ET(J) + ETALAM*GT(IMJ)
      GT(IMJ) = GT(IMJ) + GAMLAM*T
   06 CONTINUE
C
      ET(IP) = ETALAM
      GT(IP) = GAMLAM
   02 CONTINUE
      RETURN
      END
C
```

Appendix B. Relations between Eigenvectors and Generalized Eigenvectors

This appendix gives proof of the relation between eigenvectors and generalized eigenvectors used in Chapter 3.

Lemma:

For R and $B = C^*C$ Hermitian matrices and B nonsingular, the generalized B-normalized (i.e. such that $U^*BU = I$) eigenvector matrix U of the pencil (R,B) and the orthogonal (i.e. such that $V^*V = I$) eigenvector matrix V of the matrix $C^{-*}RC^{-1}$ satisfy the following relation:

$$V = CU$$

Proof:

The matrix $C^{-*}RC^{-1}$ is Hermitian and therefore has the following eigendecomposition, with orthogonal V,

$$C^{-*}RC^{-1} = V\Lambda V^* \tag{B.1}$$

Consequently, for any eigenpair $(\lambda, \underline{v})$

$$C^{-*}RC^{-1}\underline{v} = \lambda\underline{v}$$
$$C^{-*}[\,R - \lambda B\,]C^{-1}\underline{v} = \underline{0} \tag{B.2}$$

For B a full rank matrix, i.e. C nonsingular, (B.2) is equivalent to

$$[\,R - \lambda B\,]C^{-1}\underline{v} = \underline{0} \tag{B.3}$$

This implies that $C^{-1}\underline{v}$ is a generalized eigenvector associated with the pencil (R,B). Writing this in matrix form yields

$$U = C^{-1}V \text{ equivalently } V = CU \tag{B.4}$$

Note that

$$U^*BU = (C^{-1}V)^*B(C^{-1}V) = V^*V = I \tag{B.5}$$

Therefore, the generalized eigenvector matrix U is automatically B-normalized when the eigenvector matrix V is chosen to be unitary.

■

Appendix C. Rational approximation based approach of the regular eigenvalue search function

This appendix derives the relationships between the rational approximation and the regular (white noise) eigenvalue search function defined in Chapter 2.

Lemma 2 Suppose that λ is given. Let t, q, r, s be defined by equation (20). Then $v(\lambda) \triangleq t + q/(\lambda - d_k) \geq \phi(\lambda)$ and $u(\lambda) \triangleq r + s/(d_{k+1} - \lambda) \geq \psi(\lambda)$ $\forall \lambda \in [d_k, d_{k+1}]$, where $d_k \triangleq \lambda_k^{(p-1)}$ for all k.

Proof:

Part a: $v \geq \phi$

Define

$$h(\lambda) = v(\lambda) - \phi(\lambda) \tag{C.1}$$

Let us show that $h(\lambda) \geq 0$ for all $\lambda \in I_k^{\ell} = [d_k, d_{k+1}]$. Define

$$y(\lambda) = h(\lambda)\prod_{i=1}^{k}(\lambda - d_i) \tag{C.2}$$

Note that $\prod_{i=1}^{k}(\lambda - d_i) \geq 0 \quad \forall \lambda \in I_k^p$. Thus from (C.2), proving

$$h(\lambda) \geq 0 \quad \forall \lambda \in I_k^p \tag{C.3}$$

is equivalent to proving

$$y(\lambda) \geq 0 \quad \forall \lambda \in I_k^p \tag{C.4}$$

Substituting $h(\lambda)$ by its expression in terms of $v(\lambda)$ and $\phi(\lambda)$, given in (16), in (C.2), yields

$$\begin{aligned} y(\lambda) &= \left(t + \frac{q}{\lambda - d_k} - r_0 - \sum_{i=1}^{k} \frac{|\beta_i|^2}{\lambda - d_i} \right) \prod_{i=1}^{k}(\lambda - d_i) \\ &= (t - r_0)\prod_{i=1}^{k}(\lambda - d_i) + q\prod_{i=1}^{k-1}(\lambda - d_i) - \sum_{i=1}^{k}|\beta_i|^2 \prod_{j \neq i,\, j=1}^{k} (\lambda - d_j) \end{aligned} \tag{C.5}$$

where $\beta_i = \underline{r}^* \mathrm{col}_i(U_{p-1})$. Note that $y(\lambda)$ is a polynomial of order k. The idea behind the derivation is to show that y has a double zero, but does not change sign in the interval I_k^p.

First, recall from (19) that the coefficients r and s are defined such that $v(\lambda_1) = \phi_1$ and $v'(\lambda_1) = \phi'_1$. This implies that $y(\lambda_1) = y'(\lambda_1) = 0$. Therefore, y has a double zero located at λ_1. Next, from (C.5) follows, for $m = 1, \ldots, k-1$

$$y(d_m) = -\sum_{i=1}^{k}|\beta_i|^2 \prod_{j \neq i,\, j=1}^{k} (d_m - d_j) \tag{C.6}$$

Hence, $\mathrm{sign}(y(d_m)) = (-1)^{k-m+1}$, which shows that the sign of y changes between each root d_m for $m = 1, \ldots, k-1$. Therefore, $y(\lambda)$ has $k-2$ zeroes located between d_1 and d_{k-1}.

Thus, the k^{th} order polynomial $y(\lambda)$ has k-2 zeroes located between d_1 and d_{k-1}, and a double zero at λ_1. Therefore, y does not change sign in I_k^ℓ. Furthermore, $\text{sign}(y(d_{k-1})) = 1$ implies that $y(\lambda) \geq 0$ for all $\lambda \in I_k^\ell$. Using (C.2), this implies $h(\lambda) \geq 0$, and therefore from (C.1), $v(\lambda) \geq \phi(\lambda)$ for all $\lambda \in I_k^\ell$.

Part b: $u \geq \psi$

Similarly to part a, let us define

$$h(\lambda) = u(\lambda) - \psi(\lambda) \tag{C.7}$$

and

$$y(\lambda) = h(\lambda) \prod_{j=k+1}^{p-1} (d_j - \lambda) \tag{C.8}$$

Note that

$$\prod_{j=k+1}^{p-1} (d_j - \lambda) \geq 0 \quad \forall \lambda \in I_k^p \tag{C.9}$$

Thus $y(\lambda)$ and $h(\lambda)$ have the same sign in I_k^ℓ. Let us show that

$$y(\lambda) \geq 0 \quad \forall \lambda \in I_k^p \tag{C.10}$$

Substituting $h(\lambda)$ by its expression in terms of $u(\lambda)$ and $\psi(\lambda)$, given in (15), in (C.8) leads to

$$\begin{aligned} y(\lambda) &= \left(r + \frac{s}{d_{k+1} - \lambda} - \lambda - \sum_{i=k+1}^{p-1} \frac{|\beta_i|^2}{d_i - \lambda} \right) \prod_{j=k+1}^{p-1} (d_j - \lambda) \\ &= (r - \lambda) \prod_{j=k+1}^{p-1} (d_j - \lambda) + s \prod_{j=k+2}^{p-1} (d_j - \lambda) - \sum_{i=k+1}^{p-1} |\beta_i|^2 \prod_{j \neq i, j=k+1}^{p-1} (d_j - \lambda) \end{aligned} \tag{C.11}$$

Note that $y(\lambda)$ is a polynomial of order $p-k$. Recall that r and s were defined in (19) such that $u(\lambda_1)=\psi_1$ and $u'(\lambda_1)=\psi'_1$, which leads to $y(\lambda_1)=y'(\lambda_1)=0$. Thus, y has a double zero at λ_1. From (C.11) follows, for $m=k+2,\ldots,p-1$

$$y(d_m)=-\sum_{l=k+1}^{p-1}|\beta_l|^2\prod_{j\neq i,j=k+1}^{p-1}(d_j-d_m) \tag{C.12}$$

Hence, $\text{sign}(y(d_m))=(-1)^{m-k}$, which indicates that $y(\lambda)$ has $p-k-3$ zeroes located between d_{k+2} and d_{p-1}, and a double zero located at λ_1. Next, let us show that the last zero is located to the right of d_{p-1}.

Using (C.12), we have

$$\text{sign}[y(d_{p-1})]=(-1)^{p-1-k} \tag{C.13}$$

Note that

$$\lim_{\lambda\to\infty}y(\lambda)=\lim_{\lambda\to\infty}-\lambda\prod_{j=k+1}^{p-1}(d_j-\lambda) \tag{C.14}$$

Using the fact that $d_j-\lambda<0$ for all $j=k+1,\ldots,p-1$ since $\lambda>d_{p-1}$, then

$$\text{sign}[\lim_{\lambda\to\infty}y(\lambda)]=-(-1)^{p-1-k} \tag{C.15}$$

Equations (C.13) and (C.15) show that $y(\lambda)$ changes sign, i.e. it has a zero located in the interval $[d_p,\infty)$. Thus from (C.12), y has a double zero, but does not change sign in I_k^p. Furthermore, equation (C.12) yields that $\text{sign}[y(d_{k+2})]=1$. Therefore,

$$y(\lambda)\geq 0 \quad \forall\lambda\in I_k^p \tag{C.16}$$

and from (C.8)

$$h(\lambda) \geq 0 \quad \forall \lambda \in I_k^p \tag{C.17}$$

and from (C.7)

$$u(\lambda) \geq \psi(\lambda) \quad \forall \lambda \in I_k^p \tag{C.18}$$

■

Appendix D. Proof of Local quadratic convergence for the rational approximation based approach

Theorem: Given $\lambda_1 \in I_k^{\ell} = [d_k, d_{k+1}]$, where $d_k \triangleq \lambda_k^{(\ell)}$, let λ_k be the solution of $r + \frac{s}{d_{k+1} - \lambda_k} - t - \frac{q}{\lambda_k - d_k} = 0$. Then for k sufficiently large, we have:
$|\lambda_{k-1} - \mu| \leq C|\lambda_k - \mu|^2$ where μ represents the updated eigenvalue in I_k^{ℓ} and C is a constant value.

Proof: We shall show that $|\lambda_2 - \mu| = O(|\lambda_1 - \mu|^2)$.

Let ε_1 and ε_2 be defined as

$$\varepsilon_1 = \lambda_1 - \mu \tag{D.1}$$

and

$$\varepsilon_2 = \lambda_2 - \mu \tag{D.2}$$

Then it is sufficient to show that

$$|\varepsilon_2| = O(\varepsilon_1^2) \tag{D.3}$$

Following the approach by Bunch et al [BNS], Taylor series expansions about μ of the functions ϕ and ψ are used. The expressions $\phi(\lambda_1)$, $\psi(\lambda_1)$, $\phi(\mu)$ and, $\psi(\mu)$ are written as ϕ_1, ψ_1, $\hat{\phi}$, and $\hat{\psi}$ in the following.

The new iterate λ_2 is found by solving

$$r+\frac{s}{d_{k+1}-\lambda_2}-\left(t+\frac{q}{\lambda_2-d_k}\right)=0 \tag{D.4}$$

with, from (19),

$$\begin{aligned} r &= \psi_1 - \psi'_1(d_{k+1}-\lambda_1) \\ s &= \psi'_1(d_{k+1}-\lambda_1)^2 \\ t &= \phi_1 + \phi'_1(\lambda_1 - d_k) \\ q &= -\phi'_1(\lambda_1 - d_k)^2 \end{aligned} \tag{D.5}$$

Substituting (D.5) in (D.4) yields

$$\psi_1 - \psi'_1(d_{k+1}-\lambda_1) + \psi'_1\frac{(d_{k+1}-\lambda_1)^2}{d_{k+1}-\lambda_2} = \phi_1 + \phi'_1(\lambda_1 - d_k) - \phi'_1\frac{(\lambda_1-d_k)^2}{\lambda_2-d_k} \tag{D.6}$$

which leads to

$$\psi_1 + \psi'_1\frac{\alpha_1}{\alpha_2}(\lambda_2-\lambda_1) = \phi_1 + \phi'_1\frac{\delta_1}{\delta_2}(\lambda_2-\lambda_1) \tag{D.7}$$

where

$$\begin{aligned} \alpha_1 &= d_{k+1}-\lambda_1, \;\; \alpha_2 = d_{k+1}-\lambda_2 \\ \delta_1 &= \lambda_1 - d_k, \;\; \delta_2 = \lambda_2 - d_k \end{aligned} \tag{D.8}$$

Using a Taylor series expansion of ϕ_1 and ϕ'_1 about μ leads to

$$\begin{aligned} \phi_1 &= \hat{\phi} + \varepsilon_1\hat{\phi}' + \frac{\varepsilon_1^2}{2}\hat{\phi}^{(2)} + \cdots \\ \phi'_1 &= \hat{\phi}' + \varepsilon_1\hat{\phi}^{(2)} + \cdots \end{aligned} \tag{D.9}$$

Substituting (D.9) in the right-hand side R of (D.7), we get

$$R = \varepsilon_1 \hat{\phi}' + \frac{\varepsilon_1^2}{2} \hat{\phi}^{(2)} + \left[\hat{\phi}' + \varepsilon_1 \hat{\phi}^{(2)} + \frac{\varepsilon_1^2}{2} \hat{\phi}^{(3)} \right] \frac{\delta_1}{\delta_2} (\lambda_2 - \lambda_1) + O(\varepsilon_1^3) \tag{D.10}$$

Using the fact from (D.1), (D.2), and (D.8), that $1 - \frac{\delta_1}{\delta_2} = \frac{\varepsilon_2 - \varepsilon_1}{\delta_2}$ in (D.10), and rearranging the terms in the equation leads to

$$R = \hat{\phi}' \frac{\varepsilon_1(\varepsilon_2 - \varepsilon_1)}{\delta_2} + \frac{\varepsilon_1^2}{2} \hat{\phi}^{(2)} + \frac{\delta_1 \varepsilon_2}{\delta_2} \left[\hat{\phi}' + \varepsilon_1 \hat{\phi}^{(2)} \right] + O(\varepsilon_1^2) \tag{D.11}$$

Thus from (D.11),

$$R = \phi'_1 \left(\frac{\varepsilon_1 + \delta_1}{\delta_2} \right) \varepsilon_2 + O(\varepsilon_1^2) \tag{D.12}$$

A similar expansion about μ of ψ_1 and ψ'_1, in the left-hand side L of (D.7), leads to

$$L = \psi'_1 \left(\frac{\alpha_1 - \varepsilon_1}{\alpha_2} \right) \varepsilon_2 + O(\varepsilon_1^2) \tag{D.13}$$

Equating (D.12) and (D.13) yields

$$\frac{\varepsilon_2}{\delta_2} (\varepsilon_1 + \delta_1) \phi'_1 = \frac{\varepsilon_2}{\alpha_2} (\alpha_1 - \varepsilon_1) \psi'_1 + O(\varepsilon_1^2) \tag{D.14}$$

Hence,

$$O(\varepsilon_1^2) = -\varepsilon_2 \left[\psi'_1 \left(\frac{\alpha_1 - \varepsilon_1}{\alpha_2} \right) - \phi'_1 \left(\frac{\delta_1 + \varepsilon_1}{\delta_2} \right) \right] \tag{D.15}$$

Note that

$$\lim_{\lambda_1, \lambda_2 \to \mu} \frac{\alpha_1 - \varepsilon_1}{\alpha_2} = 1 \quad \text{and} \quad \lim_{\lambda_1, \lambda_2 \to \mu} \frac{\delta_1 + \varepsilon_1}{\delta_2} = 1 \tag{D.16}$$

Therefore, from (D.16) and (10),

$$\lim_{\lambda_1, \lambda_2 \to \mu} \psi'_1\left(\frac{\alpha_1 - \varepsilon_1}{\alpha_2}\right) - \phi'_1\left(\frac{\delta_1 + \varepsilon_1}{\delta_2}\right) = \hat{\psi}' - \hat{\phi}' \geq 1 \tag{D.17}$$

which implies from (D.15)

$$|\varepsilon_2| = O(\varepsilon_1^2) \tag{D.18}$$

■

The vita has been removed from the scanned document